Quantification and Prediction of Substituent Effects in Aromatic Molecules and Cation-π Complexes Using Molecular Electrostatic Potential

Thesis submitted to the
UNIVERSITY OF KERALA
for the award of Degree of

DOCTOR OF PHILOSOPHY

in Chemistry under the Faculty of Science

By

FAREED BHASHA SAYYED MEERASAHEB

Chemical Sciences and Technology Division
National Institute for Interdisciplinary Science and Technology (CSIR)
Thiruvananthapuram – 695 019
Kerala, India

2012

DECLARATION

I hereby declare that the Ph.D. thesis entitled "**Quantification and Prediction of Substituent Effects in Aromatic Molecules and Cation-π Complexes Using Molecular Electrostatic Potential**" is an independent work carried out by me at the Chemical Sciences and Technology Division, National Institute for Interdisciplinary Science and Technology (NIIST-CSIR), Trivandrum, under the supervision of Dr. C. H. Suresh and it has not been submitted elsewhere for any other degree, diploma or title.

Fareed Bhasha Sayyed Meerasaheb

Council of Scientific & Industrial Research
National Institute for Interdisciplinary Science & Technology
(Formerly Regional Research Laboratory)
Thiruvananthapuram-695 019, Kerala, India

Dr. C. H. Suresh
Chemical Sciences and Technology Division

Tel: +91- 471-2515381
E-mail: sureshch@gmail.com

December 13, 2012

CERTIFICATE

This is to certify that the work embodied in the thesis entitled "**Quantification and Prediction of Substituent Effects in Aromatic Molecules and Cation-π Complexes Using Molecular Electrostatic Potential**" has been carried out by Mr. Fareed Bhasha Sayyed Meerasaheb under my supervision and guidance at the Chemical Sciences and Technology Division, National Institute for Interdisciplinary Science and Technology (NIIST-CSIR), Trivandrum and this work has not been submitted elsewhere for a degree.

Dr. C. H. Suresh
(Thesis Supervisor)

ACKNOWLEDGEMENT

I find immense pleasure in expressing my sincere regards and profound gratitude to my research supervisor Dr. C. H. Suresh, Scientist, Chemical Sciences and Technology Division, National Institute for Interdisciplinary Science and Technology (NIIST)-CSIR, Trivandrum. I owe the greatest depth of gratitude for his invaluable guidance, strong motivation, timely advice, encouragement and support.

I express my profound thanks to the Director Dr. Suresh Das, former Directors Dr. B. C. Pai and Prof. T. K. Chandrasekhar for giving me an opportunity to carry out my doctoral work in this institution.

I take immense pleasure to offer my special thanks to Dr. Roschen Sasikumar, Dr. Elizabeth Jacob and Dr. S. Savithri for their encouragement and support. I also extend my sincere thanks to Dr. K. P. Vijayalakshmi for her valuable encouragement.

I wish to thank my friends at Computational Modeling and Simulation Section Jomon, Sajith P. K, Neetha M, Sandhya K. S, Ajitha M. J, Remya H, Lincy, Rakhi, Remya P. R, Rejitha, Manoj M, Manju M. S, Jijoy J, Alex A, Dr. Panneer Selvam, Sudeep P. M, Gopika, Hareesh R. S, Fathima, and Adersh V. K.

The friendship and support of Prashant S, Hari, Adersh, Suresh N, Vinayakan, Ramesh Reddy, Ravi Kiran, Jayaram, Anas, Shafeekh, Anees, Rahim, Prakash, Dr. Khurshid Ahmad, Nagendra, Jaggaiah, Ashok, and Chandrasekhar will be cherished. I wholeheartedly extend my thanks to all my friends at NIIST.

Council of Scientific and Industrial Research (CSIR) and Department of Science and Technology (DST) are acknowledged for their support through a network project NWP-53, and Project No. SR/S1/OC-41/2006, respectively. High Performance Computational Facility at CSIR centre for Mathematical Modelling and Computer Simulation (C-MMACS), National Chemical Laboratory (NCL), and Centre for Modelling Simulation and Design (CMSD) is greatly acknowledged.

I am deeply grateful to my family members for their constant love and care and especially my wife for her constant support during my Ph. D work.

Finally, CSIR India is highly acknowledged for the financial support.

Fareed Bhasha Sayyed Meerasaheb

CONTENTS

List of Tables

List of Figures

List of Schemes

List of Abbreviations

BSSE	: Basis Set Superposition Error
CI	: Configuration Interaction
CCSD	: Coupled Cluster Single and Double
DFT	: Density Functional Theory
ECP	: Effective Core Potential
GGA	: Generalized Gradient Approximation
HF	: Hartree-Fock
HK	: Hohenberg-Kohn
LDA	: Local-Density Approximation
MP	: Moller-Plesset Perturbation Theory
CC	: Coupled Cluster
MESP	: Molecular Electrostatic Potential
MO	: Molecular Orbital
STO	: Slater-Type Orbitals
GTO	: Gaussian-Type Orbitals
TS	: Through-space Effect
TB	: Through-bond Effect
ED	: Electron donating
EW	: Electron withdrawing
DSP	: Dual Substituent Parametric
SIR	: Steric Inhibition of Resonance
LFER	: Linear Free Energy Relation
NMR	: Nuclear Magnetic Resonance
XC	: Exchange Correlation
QSAR	: Quantitative Structure Activity Relationship
QSPR	: Quantitative Structure Property Relationship
QM	: Quantum Mechanics
MM	: Molecular Mechanics
MD	: Molecular Dynamics

Preface

Understanding the correlation between structure of the molecules and their chemical reactivity is one of the most important topics of chemistry. Hammett introduced an empirical equation to quantify the substituent effects. The wide applications of this equation and the transferability of substituent effect from one system to another system lead to a new era of QSAR/QSPR.

Computational chemistry is one of the most rapidly expanding and exciting area of scientific endeavors. Computational chemistry has evolved as one of the most important approach to study a wide range of chemical problems, including enzymatic reactions, thermochemistry, material science, catalysis, structure-reactivity correlations and reaction mechanisms.

In this thesis, quantum chemically derived descriptor, molecular electrostatic potential (MESP) is used to quantify various aspects of substituent effects such as proximity effect, resonance effect and through-space effect in a variety of aromatic molecules. These developed methods are applied on a variety of substituted cation-π complexes to unravel the origin of substituent effects and also a MESP method was established to predict the cation-π interaction energies. The thesis entitled "**Quantification and Prediction of Substituent Effects in Aromatic Molecules and Cation-π Complexes Using Molecular Electrostatic Potential**" is divided into four chapters.

The first part of the Chapter 1 summarizes a brief history and the importance of substituent effects. The second part of the Chapter 1 gives a brief account of various computational methods and their theoretical basis.

Chapter 2 of the thesis deals with the development of quantitative methods for proximity effect, resonance effect, through-space and through-bond substituent effects using MESP. *Ortho*, *meta* and *para* substituent effects in benzoic acid derivatives have been quantified using MESP and is established as a quantitative descriptor for substituent effects. The total proximity effect

has been quantified separately using a molecular fragment approach in conjunction with a rotation experiment on the benzoic acid. These two methods allowed the assessment of *ortho*, *meta* and *para* interrelationships. Further, an electrostatic scale for the substituent resonance effect is also proposed using substituted benzenes. The proposed electrostatic resonance constants have been validated using several isodesmic reactions. Using MESP, a quantitative method for the through-bond (TB) and through-space (TS) effects was established.

In the third chapter, the quantification of substituent effects in $C_6H_5X\cdots Na^+$ systems and characterization of substituent effects in the cation-π complexes of $C_6H_5X\cdots M^+$ (Li^+, Na^+, K^+ and NH_4^+) using NMR shielding constants is described. The dependence of the electronic nature of substituent effects on the NMR shielding parameters is discussed and deshielding at the carbon and hydrogens of the phenyl ring is proposed as a signature of cation-π interaction. Further, to unravel the origin of substituent effects in cation-π interactions several theoretical models have been designed. These models suggests a unified view that the total substituent effect is the sum of the inductive, resonance and through-space effects.

A detailed quantitative methodology for the prediction of substituent effects in the cation-π interactions using MESP was demonstrated in the fourth chapter. An emperical equation was developed to predict the cation-π interaction energy of a substituted cation-π complex using MESP minimum obtained over the π-region of the moleule. The reliability of this equation has been tested over a variety of π-systems, cations and substituents. Further, the MESP approach is extended to multiple substituted complexes and observed that the substituent effects in cation-π interactions are largely additive.

Chapter 1

Introduction

Part A – Substituent Effects
&
Part B – Computational Chemistry

Part A – Substituent Effects

1.1 Substituent Effects

1.1.1 Linear free Energy relationships

Understanding the correlation between structure and reactivity of molecules is one of the most important concepts in chemistry [Jaffe 1953]. Several attempts have been made to establish correlations between the reactivities of two different reactions and also to predict the reactivities of unknown reaction series [Wells 1963]. Among these correlations, linear free energy relations (LFER) are found to be useful and these relationships are linear of the form,

$$\log K_A = m\log K_B + c \qquad \text{(Eq. 1.1)}$$

where K_A and K_B are the equilibrium constants of reactions A and B, respectively, m is the slope and c is a constant. The logarithm of equilibrium constant (K) is directly related to the standard free energy change of the reaction as shown in Eq. 1.2.

$$\log K = \frac{-\Delta G^{o}}{2.303RT} \qquad \text{(Eq. 1.2)}$$

Substituting Eq. 1.2 in Eq. 1.1 for the reactions A and B,

$$\frac{-\Delta G_A{}^{o}}{2.303RT} = m\frac{-\Delta G_B{}^{o}}{2.303RT} + c \qquad \text{(Eq. 1.3)}$$

Therefore, Eq. 1.1 can be treated as a LFER and can be written as

$$\Delta G_A{}^{o} = m'\Delta G_B{}^{o} + c' \qquad \text{(Eq. 1.4)}$$

Where m' is the slope and c' is a constant.

Under given conditions, if the magnitude of changes in reaction properties of A is affected in a similar way for the reaction B either by varying the electronic nature of substituents or reactants then we can say that there exists an linear free energy relationship between A and B [Wells 1963].

1.1.2 Hammett Equation

Hammett equation is one of the earliest and the most popular LFER. Let us consider a molecule X-G-Y, where X is substituent, Y is reaction centre and G is the transmitting moiety to which X and Y are attached. Hammett observed that by varying X, the rate of reaction, *k* is changing by a constant factor which is characteristic to a substituent. Hammett estimated rate constants for a large number of *meta* and *para* substituted benzoic acids (Scheme 1.1), and proposed an empirical equation to quantify

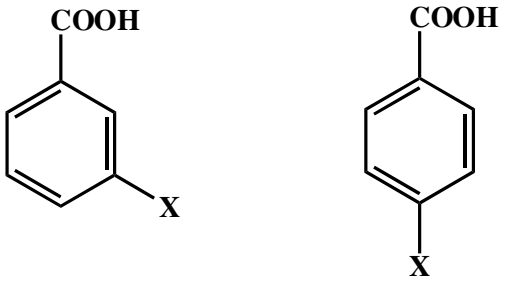

***meta* substituted benzoic acid** ***para* substituted benzoic acid**

Scheme 1.1 *Meta* and *para* substituted benzoic acids. X represents a substituent.

the effect of structure on the chemical reactivity [Hammett 1937]. This LFER is referred as Hammett equation which can be expressed as Eq. 1.5.

$$\log\left(\frac{k}{k_0}\right) = \sigma\rho \qquad \text{(Eq. 1.5)}$$

where k and k_0 are the rate constants for substituted and unsubstituted compounds. σ is the substituent constant which depends on the position, the transmitting moiety with respect

to the reaction centre and ρ is the reaction constant depends on the reaction, medium and temperature. For *meta* and *para* substitutions, the corresponding substituent constants are represented as σ_m and $\sigma_{p,}$ respectively. From Eq. 1.5, the only data available is the product of $\sigma\rho$, therefore to assign some arbitrary values for σ and ρ; Hammett assigned ρ value to be unity for ionization of benzoic acids in water at 25° C. By substituting ρ = 1, the difference between the ionization constants of substituted and unsubstituted benzoic acid is estimated which will give the value of σ. The values of σ_m and σ_p that are originally reported by Hammett are presented in Table 1.1. It can be noticed that some of the substituents showing positive σ value while some are showing negative value. Based on the sign of the σ, the electronic nature of substituents are

Table 1.1 Hammett's σ_m and σ_p substituent constants derived from the ionization of substituted benzoic acids.

Substituent	σ_m	σ_p
$N(CH_3)_2$	0.211	-0.205
NH_2	-0.161	-0.660
OCH_2CH_3	0.150	-0.250
OCH_3	0.115	-0.268
CH_3	0.069	-0.170
H	0.000	0.000
F	0.337	0.620
Cl	0.373	0.227
Br	0.391	0.232
I	0.352	0.276
CN	0.678	1.000
NO_2	0.710	1.270

characterized as electron-donating for negative sign and electron-withdrawing for positive sign. These substituent constants have been successfully correlated for a large variety of reaction series [Krygowski and Stepien 2005]. However, the applicability of Hammett equation for some of the reactions have shown systematic deviations and in such cases the use of substituent constants is limited [Jaffé 1953, Exner and Bohm 2006]. Hammett interpreted that the substituent constants can be used as a measure of electron density produced by a substituent at the reaction centre [Price 1940]. Based on the assumption that electron density produced by the substituents is directly proportional to the substituent constants, Jaffe calculated σ values using quantum chemical methods [Jaffé 1952]. Hansch *et al*. did an extensive survey of Hammett constants for a large variety of substituents and derived σ_m and σ_p values based in regression analysis [Hansch *et al*. 1991]. The Hammett constants derived from Hansch *et al*. is one of the most widely used for structure-activity or structure-property correlations.

1.1.3 Failure of Hammett Constants

In certain reactions, Hammett constants are not correlated with reaction rates. For example, Hammett constants are failed for reactions in which direct conjugation between electron-donating reaction centre and electron-withdrawing substituent and vice-versa [Jaffé 1953]. The deviation of σ-constants is mainly attributed to resonance effect or mesomeric effect occurred between substituent X and reaction centre Y. In Scheme 1.2, an example for the existence of the resonance structures between electron-donating reaction centre (Y) and electron-withdrawing substituent (X) are shown.

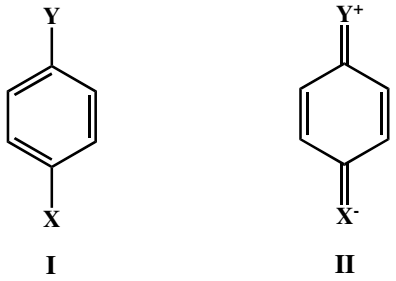

Scheme 1.2 Resonance structures of *para* substituted compounds. X is a electron-withdrawing substituent and Y is electron-donating reaction centre.

Substituents which are electron-donating through resonance effect are classified under +M (M corresponds to mesomeric) group while substituents which are electron-withdrawing through resonance effect are classified under -M group. Hammett proposed the σ_p values from the ionization of *para* substituted benzoic acids which is thought to be contaminated with the substituent resonance effect [Hammett 1937]. Therefore, Van Bekkum *et al*. studied the ionization constants of *para* substituted phenyl acetic acids and phenyl propionic acids wherein the direct conjugation between the substituent and the reaction centre is absent [Van Bekkum *et al.* 1959]. From these two reaction series, the derived substituent constants are designated as σ^n and these constants are concluded to be free from mesomeric interactions [Wells 1963]. Taft introduced a dual substituent parametric (DSP) equation wherein the total substituent effect can be expressed as a sum of inductive and resonance effects [Taft 1953]. Taft's DSP equation is shown below.

$$\sigma_p = \sigma_I + \sigma_R \qquad \text{(Eq. 1.6)}$$

where σ_I and σ_R are inductive and resonance parameters.

With the introduction of Eq. 1.6, naturally a question arises in this context is "To what extent does a substituent contributes to the inductive and resonance effects"? To

understand the inductive and resonance effect of substituent, several molecular models have been designed and these will be discussed in the sections 1.1.4 and 1.1.5. Further, the Hammett constants are also failed in the case of *ortho* substitution [Exner and Böhm 2006]. In *ortho* substitution, the substituent is in close proximity with the reaction centre which can exert steric effect and intramolecular hydrogen bonding. These aspects will be discussed in detail in section 1.1.6.

1.1.4 Substituent Inductive Effect

To quantify the inductive substituent effect, three models *viz*. 4-substituted bicyclo [2.2.2]octane-l-carboxylic acids (**1**), [Roberts and Moreland 1953] and 1,4-*trans*-cyclohexanes (**2**) and quinuclidine (**3**) derivatives have been investigated.

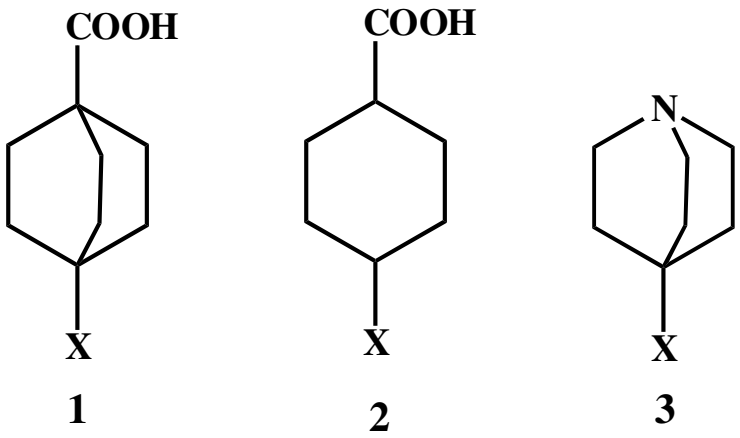

Scheme 1.3 Model systems considered for quantifying the inductive substituent effect.

In the case of **1**, the effect of X on the ionization of COOH is assumed to be free from steric, and through resonance interactions [Hansch *et al.* 1991]. Therefore, total substituent effect observed in **1** can be treated as inductive effect. By applying the Hammett equation (Eq. 1.5), the σ values are evaluated from **1** and the corresponding substituent constants are designated as σ_I. These σ_I constants will be referred as inductive

substituent constants. The ionization constants of **1** are correlated with that of *meta* and *para* substituted benzoic acids to understand the transmission of inductive effect through the π-electrons of phenyl ring [Roberts and Moreland 1953]. It was observed that the linear correlation between rate constants of *para* substituted benzoic acids and rate constants of **1** are significantly deviated while *meta* substituents are in good agreement to that of **1** suggesting that inductive effect does not transmit through conjugated π-electrons. In a later study, Baker, Parish and Stock studied systems **4** and **5** (Scheme 1.4) to understand transmission of substituent effect through unsaturated carbon-carbon bonds [Baker *et al*. 1967]. In Figure 1.1, $\log(K/K_H)$ values of **1** are plotted with $\log(K/K_H)$ values of **4** and **5**. The correlation clearly suggests that transmission of substituent effects in both **1** and **4** are of similar magnitude with a slope of 1.07. On the other hand, slope of the correlation between **1** and **5** is significantly less than unity, suggesting that the substituent effect in dibenzo-octane acids is just 0.79 times to that of **1**.

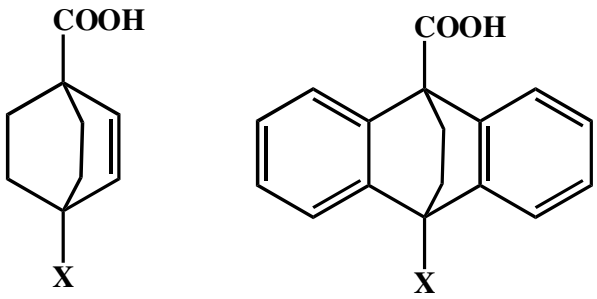

4 **5**

Scheme 1.4 Model systems considered to understand the transmission of substituent effect through unsaturated double bond.

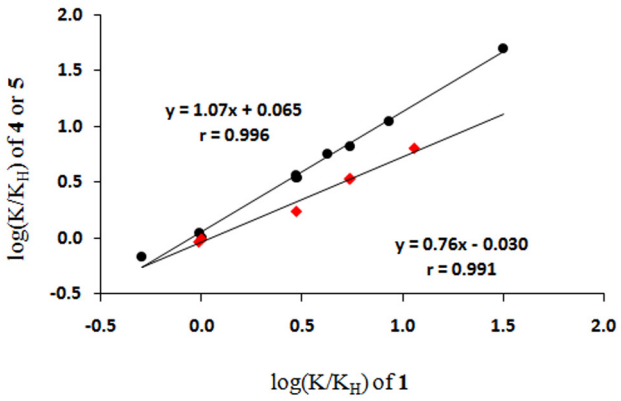

Figure 1.1 Corelaton betwen log (K/K_H) of **1** with log (K/K_H) of **4** (●) and **5** (◆).

Wiberg studied the acidities of 3- and 4-substituted bicyclooctane-1-carboxylic acids (**1** and **6**) and 3-substituted bicyclo-[1.1.1]pentane-1-carboxylic acids (**7**) to understand the mode of transmission of inductive effect with respect to distance. It was observed that substituent effect in **7** is more sensitive than **6** (Scheme 1.5) showing that inductive is significant at smaller distance [Wiberg 2002[a]]. Further, he proposed that substituent effects in these bicyclo carboxylic acids are mainly due to through-space

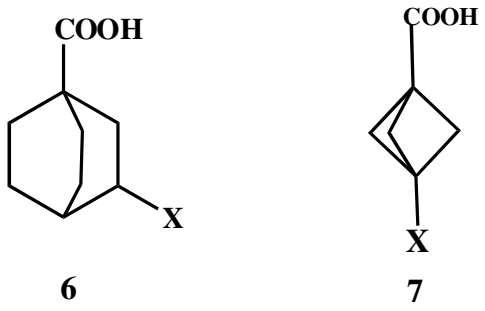

Scheme 1.5 Substituent effects studied by Wiberg to understand mode of transmission of inductive effect [Wiberg 2002[a]].

effect, arises from the polarization of bonding electrons. However, total substituent effect in bicyclooctane systems is considered as the sum of through-bond inductive and through-space effects. Using quantum theory of atoms in molecules (QTAIM) [Bader 1991] Nolan and Linck analyzed 75 substituted ethanes and higher alkanes and supported the

transmission of through-space effects over through-bond effects [Nolan and Linck 2000]. Ponec and Van Damme revisited the gas phase acidities on the compounds **1**, **2**, **3**, **4**, and **6** to evaluate the mode of transmission of substituent effect [Ponec and Van Damme 2007]. They suggested that variation of substituent effects is due to electrostatic field effect which is another formulation for through-space effect. Recently, Mawhinney and co-workers have investigated substituent effects in bicyclo[1.1.1]pentane-1-carboxylic acid systems using isodesmic reaction energies (Scheme 1.6) and QTAIM parameters [Smith *et al.* 2011]. They demonstrated that total inductive effect comprises of through-bond and through-space contributions. The isodesmic reaction energy is poorly correlated with substituent electronegativity (χ) and a good correlation with the field effect parameters σ_F indicating through-space effect is significant than through-bond effect.

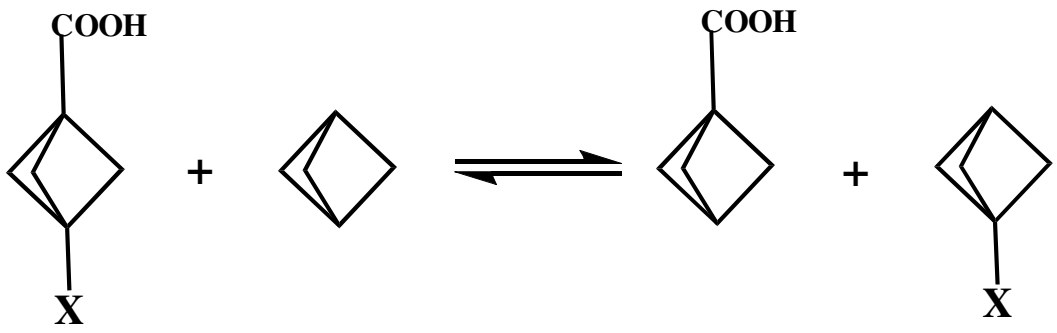

Scheme 1.6 Isodesmic reactions for quantifying the inductive effects in 3-substituted bicyclo[1.1.1]pentane-1- carboxylic acid.

Campanelli *et al*. investigated Bicyclo[1.1.1]pentane and [n] Staffane derivatives to understand the transmission of electronic substituent effects through these systems (Scheme 1.7) [Campanelli *et al.* 2010]. They observed that structural variations that occurred on benzene ring of **8**, is mainly due to through-space substituent effects in these systems. With increasing 'n' value, the effect of substituent falls off linearly by a factor of n^{-3}.

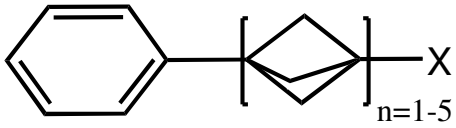

8

Scheme 1.7 Substituent effects transmitted through the Bicyclo[1.1.1]pentane monitored on the phenyl ring.

Using models **1**, and **4**, inductive constants can be evaluated and several descriptors have been evolved for an alternative measurement of inductive effect. One of the most popular ways of quantifying the inductive effect is the use of isodesmic reactions with appropriate systems. For instance, the most widely used systems are 4-substituted bicyclo[2.2.2]octane systems (Scheme 1.8). Exner and co-workers in a series of papers have shown the use of isodesmic reaction approach as an accurate measure of inductive effect [Bohm and Exner 2007, Exner and Bohm 2004, Exner and Bohm 2006].

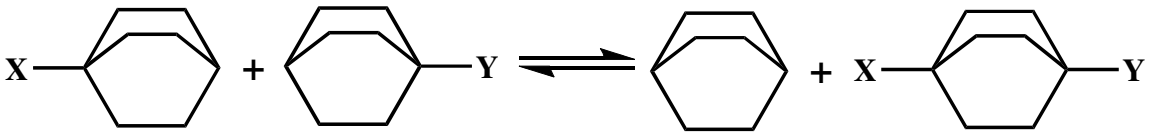

Scheme 1.8 Isodesmic reaction for the quantification of inductive effect. X is a substituent and Y is the reaction centre.

The above isodesmic reaction has the disadvantage that to get an inductive contribution of a single substituent one has to perform the energy calculation four molecules. Moreover, these isodesmic reaction energies depend on the calculating method and also demand more accurate calculations. In order to overcome the discrepancy, Suresh *et al*. have introduced a molecular electrostatic potential (MESP) topographical method for the quantification of substituent inductive effects [Suresh *et al*. 2008]. They measured MESP minimum (V_{min}) over the 20 substituted systems of **1**, **3** and also anionic

bicyclo[2.2.2]octane carboxylic acids. In Figure 1.2, and Figure 1.3, the MESP isosurfaces of **1** and **3** are shown respectively for a representative set of substituents (NH_2, CH_3, H and CN). It can be seen that the V_{min} value varies with respect to the change in electronic nature of the substituent. The correlation between V_{min} of **1** and **3** with inductive constants, σ_I shown in Figure 1.4, strongly suggest V_{min} can be used as a good measure of inductive substituent effect.

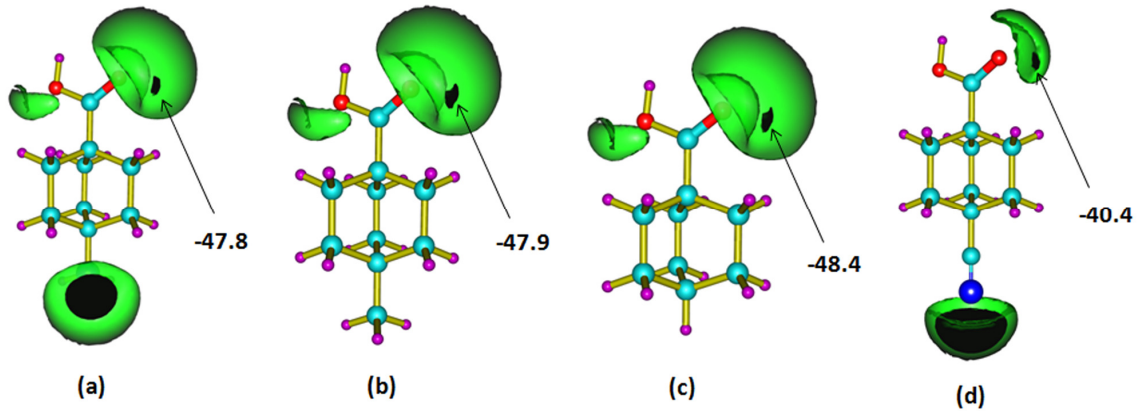

Figure 1.2 MESP isosurfaces of substituted bicyclo[2.2.2]octane carboxylic acids (**1**). (a) X = NH_2 (b) X = CH_3 (c) X = H, (d) X = CN. All the isosurfaces are drawn at -31.4 kcal/mol. The exact location of V_{min} (in kcal/mol) is depicted with an arrow.

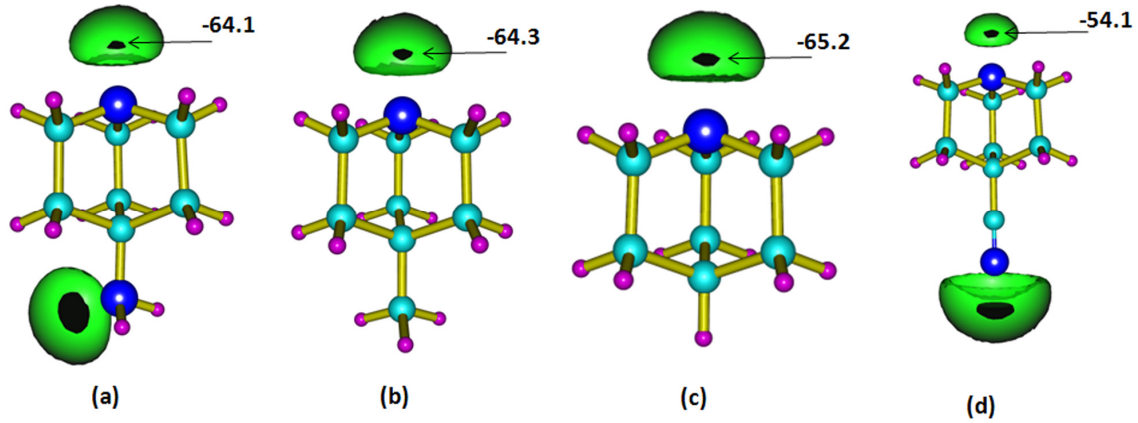

Figure 1.3 MESP isosurfaces of substituted quinuclidines (**3**). (a) X = NH_2 (b) X = CH_3 (c) X = H, (d) X = CN. All isosurfaces are drawn at -18.8 kcal/mol. The exact location of V_{min} (in kcal/mol) is depicted with an arrow.

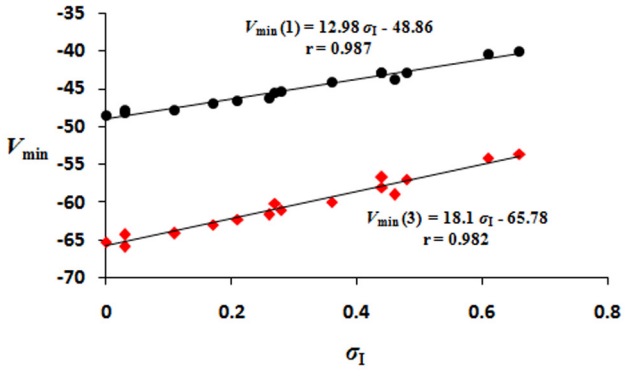

Figure 1.4 Correlation between V_{min} of **1** and **3** with the corresponding inductive constants, σ_I.

1.1.5 Substituent Resonance Effect

In section 1.1.3, it was showed that the Hammett equation fails with a -M substituent in *para* position interacting with +M reaction centre or +M substituent interacting with -M reaction centre in *para* position. The classical examples for this deviation are the acid-base equilibrium of 4-nitro anilinium and 4-amino benzoic acid. In order to circumvent this deviation, Jaffe [Jaffe 1953] suggested two procedures for the evaluation of substituent (X) constants which are free from resonance viz. (i) the reaction centre should not be in conjugation with the benzene ring, (ii) the side chain should not facilitate conjugation between X and reaction centre. Based on these suggestions, Van Bekkum *et al*. introduced σ_n constants from ionization of *para* phenyl substituted acetic acids and this method also failed for some -M substituents [Van Bekkum *et al.* 1959]. Therefore, Hoefnagel and Wepster studied the thermodynamic dissociation constants of a large number of phenyl acetic acids and introduced new constants namely σ_R^+ [Hoefnagel and Wepster 1973].

Resonance effect is a qualitative concept but very important to understand many chemical problems [Exner and Bohm 2005]. Several efforts have been made to quantify

the substituent resonance effects. Taft *et al*. quantified the substituent resonance effects using ^{19}F-NMR on the **9** and **10** systems [Taft *et al.* 1959]. The difference between ^{19}F-NMR chemical shifts of *para* and *meta* substituted systems is quantified as substituent resonance effects and the substituent resonance constants are represented with σ_R^o. However, basic assumption lies under the Taft's scale is in considering the total substituent effect as sum of inductive and resonance effect. Katritzky and co-workers also proposed a resonance scale based on the integrated infrared intensities of CC stretching bands of monosubstituted benzenes [Katritzky and Topsom 1977]. This method is complicated as identifying the most appropriate stretching intensities that exclusively differentiates the resonance interactions is difficult .

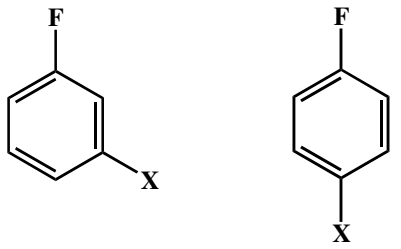

9 **10**

Scheme 1.9 *meta* and *para* substituted flourobenzenes studied by Taft et al. using ^{19}F-NMR for evaluating the substituent resonance constant.

Recently, Exner and Bohm have revisited the DSP equation, Eq. 1.6 and found that this equation is not valid as a general case for all types of substituents [Exner and Böhm 2007]. They designed two isodesmic reactions shown in Scheme 1.10 and observed that resonance scale is unsatisfactory as the reaction energies are not properly expressing X and Y when X and Y belongs to +M group and also when X and Y belongs to -M group vice-versa. They suggested two different scales should be used for donor and

acceptor substituents. Thus, to evaluate substituent resonance effect, an easy, reliable and efficient method through an observable molecular property is yet to be established.

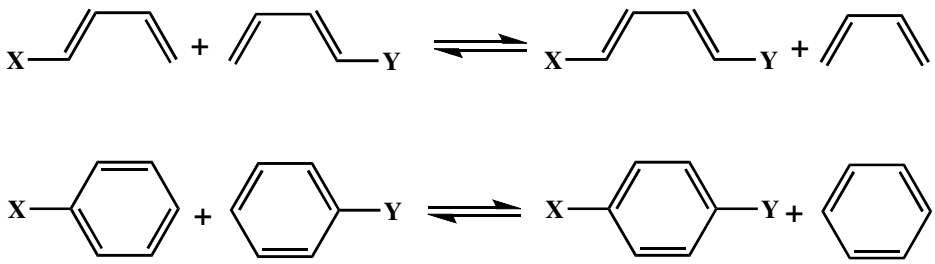

Scheme 1.10 Isodesmic reactions designed by Exner and Bohm for quantifying the substituent resonance effect.

Since the substituent resonance effect depends on the extent of interaction between substituent and reaction centre [Niwa 1989], a resonance scale must also interpret accurately the electron-donating as well as electron-withdrawing ability of the substituent. Thus, in this thesis, we attempted to develop a descriptor for the quantification of resonance effects.

1.1.6 *Ortho* substituent Effect

Ortho substituent effect has been remained as a special case in interpreting the reactivities using Hammett equation due to the interplay of proximity effects that occur between the reaction centre and the substituent [Exner and Böhm 2006]. The proximity effect corresponds to combined effects of steric inhibition of resonance, steric effect, intramolecular hydrogen bonding etc [Exner and Böhm 2006]. Due to the failure of Hammett equation for *ortho* substituents, these systems are less studied than the corresponding *meta* and *para* substituted systems. In view of introducing *ortho* substituent constants, Charton studied a diversified set of 32 reaction series and proposed

that *ortho* constants are different for different reactions [Charton 1969]. Charton assumed that the *ortho* substituent constant (σ_o) can be expressed as the sum of inductive, resonance combinations and any correlation between these 32 sets will be considered as free from steric effect.

$$\sigma_o = a\sigma_I + b\sigma_R + c \qquad \text{(Eq. 1.7)}$$

From the data of all these 32 sets of reactions and the correlation between σ_o values and the corresponding molecular properties Charton reported that "*only in an exceptional case is the ortho-electrical effect likely to have the same composition as the para-electrical effect*" [Charton 1969].

Bohm, Fielder and Exner analyzed the *ortho* effect by studying eleven substituted 2-substituted benzoic acids and the corresponding benzoates [Bohm *et al.* 2004] with the aid of isodesmic reactions (Scheme 1.11), they attempted to separate the polar and steric effects by approximating that the total *ortho* and *para* substituent effects are equal. The correlation between acidities of *ortho* and *para* substituted benzoic acids suggested that *ortho* effect is 0.81 times to that of *para* and the rest of the substituent effect is considered as the steric effect. However, in their correlation, bulky substituents t-butyl and CH_2Cl are eliminated. To understand the effect of bulky groups several efforts have been made to unravel the origin of *ortho* effect by investigating various aspects such as steric inhibition of resonance (SIR) and role of steric effect. SIR is the phenomenon in which the reaction centre is twisted out of the ring plane by a torsion angle ϕ to prevent the resonance delocalization. Exner and co-workers have studied SIR concept in the case of methyl substituted acetophenones and they observed that a significant increase in the ϕ for the substituents that shows strong steric hindrance [Kulhanek *et al.* 2004]. They also

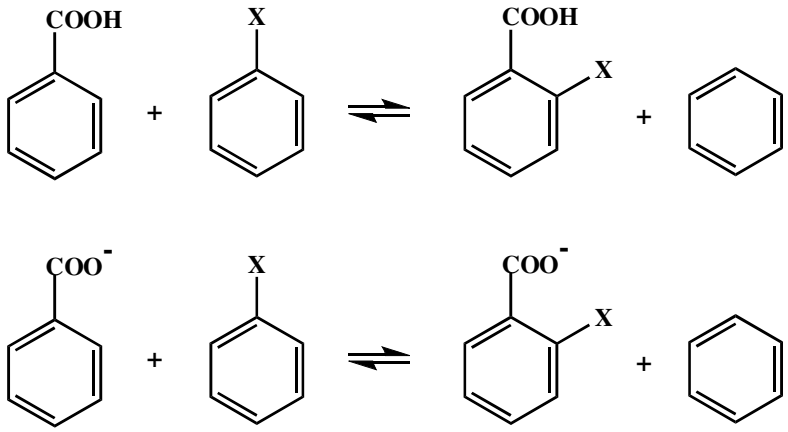

Scheme 1.11 Isodesmic reactions designed for quantifying the *ortho* substituent effect.

concluded that ϕ is not a good measure of SIR, and isodesmic reaction (Scheme 1.12) strategy is a good measure of steric hindrance. However, in this case also the polar effect of methyl group is approximated as similar for *ortho* and *para* substitutions.

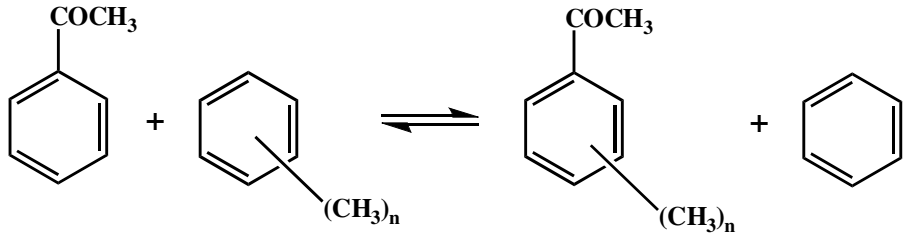

Scheme 1.12 Isodesmic reaction to measure the steric inhibition of resonance for ortho substituted acetophenones.

Segurado *et al*. measured the rate constants for the oxidative chlorodehydration of *ortho*, *meta* and *para* substituted 2- phenoxy propanoic acid using 1-chloro-3-methyl-2,6-diphenylpiperidin-4-one [Segurado *et al.* 2007]. From the correlation of activation enthalpies for the chlorination of 2-*ortho* versus *para* phenoxy propanoic acids, the *para*/*meta* substituent effects are found to be in the ratio of 0.926 and 1.038 for *ortho*/*para*. However, the electrostatic modeling on the benzoate ion is found to be very low, 0.397 compared to that of the ratio, 0.81 obtained by Exner and co-workers, calculated from the acidity of benzoic acids [Bohm *et al.* 2004]. Despite of advances in

understanding the *ortho* substituent effect, there is a need for evaluating *ortho* substituent constant which is free from proximity effect.

1.1.7 Cation-π Interaction

Cation-π interaction can be defined as the interaction between a cation and electron rich π-system [Ma and Dougherty 1997]. This interaction is conceptually treated as the electrostatic interaction between any positively charged cation and the electron-rich π-cloud [Keiluweit and kleber 2009]. The pioneering work from Dougherty and co-workers evolved a new type of non-covalent binding force, the cation-π interaction [Ma and Dougherty 1997]. This interaction has been created a great interest among the chemists as energetically the cation-π interaction is stronger or comparable to that of the hydrogen bonding interaction. The nature of this interaction has been studied in detail and reported that electrostatic effect controls the interaction between the cation and the electron rich π-system [Soteras *et al.* 2008,Tsuzuki *et al.* 2001]. A typical cation-π interaction between benzene and Na^+ is represented in the Scheme 1.13.

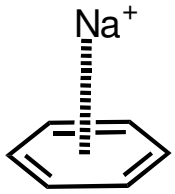

Scheme 1.13. Cation-π interaction between a positively charged sodium cation and electron rich benzene.

Several theoretical works have been devoted to understand the origin of cation-π interactions by decomposing the total interaction energy into electrostatic, induction, charge-transfer, Pauli repulsion and dispersion components [Engerer and Hanusa 2011, Kim *et al.* 2003, Kim *et al.* 2007, Liu *et al.* 2001, Liu *et al.* 2004, Marshall *et al.*

2009,Tsuzuki *et al.* 2001,Yi *et al.* 2009]. Depending on the type of cation that interacts with the π-system, electrostatic, induction and dispersion effects play significant roles in stabilizing the interaction [Liu *et al.* 2001]. For instance, Soteras *et al*. showed that induction effect is more dominant in the $C_6H_6\cdots Li^+$ complex while electrostatic contribution is more important in the case of $C_6H_6\cdots Na^+$ and $C_6H_6\cdots K^+$ [Soteras *et al.* 2008]. Dispersion effect is also important in the case of cation-π complexes of the type, $C_6H_6\cdots N(CH_3)_4^+$. Further, experimental studies have been made to quantify the cation-π interaction using threshold collision induced dissociation technique. These studies discussed mainly the interaction of alkali metal ions with aromatic systems such as substituted benzenes, naphthalenes and indole [Amicangelo and Armentrout 2000, Amunugama and Rodgers 2002[a], Amunugama and Rodgers 2002[b], Amunugama and Rodgers 2002[c], Amunugnama and Rodgers 2003, Ruan *et al.* 2007]. Recently, Wu and Mcmahon studied the cation-π complexes of Na^+ and NH_4^+ with the Phenylalanine, tyrosine and tryptophan using high pressure mass spectroscopy and they proposed a protocol for estimating the cation-π binding energies [Wu and McMahon 2008].

Theoretically, several studies have been made to quantify substituent effects in cation-π interactions using electrostatic potential,[Mecozzi *et al.* 1996] electron density topological parameters [Cubero *et al.* 1999]. Dougherty proposed that the electrostatic potential calculated above the substituted arenes at the equilibrium distance of the cation or directly at the cation of the cation-π complex can be used to quantify cation-π interaction energies [Mecozzi *et al.* 1996]. Wheeler and Houk confirmed the Dougherty model by studying 25 substituted $C_6H_5X\cdots Na^+$ complexes and they obtained good correlation between the calculated interaction energies and the electrostatic potential [Raju *et al.* 2011]. Cubero, Orozco and Luque performed QTAIM analysis on a series of cation-π complexes of substituted arenes and heterocyclics and found a linear correlation

between the cage critical point and the binding energies [Cubero *et al.* 1999]. Recently, Deya and co-workers also reported a similar type of correlation between the cation-π complexes of substituted ethynyl benzenes [Lucas *et al.* 2010]. Jiang and co-workers also found a linear correlation between the binding enthalpies of cation-π complexes of substituted benzenes and Li^+, Na^+, K^+, Be^{2+}, Mg^{2+} and Ca^{2+} and ($\sigma_{total} = \sigma_{meta} + \sigma_{para}$) [Zhu *et al.* 2003]. However, the above methods require computations that involves the cation-π complex while in this thesis work a simple and efficient method for the calculation of cation-π interaction energies just from the π-system is outlined.

Part B – Computational Chemistry

1.2 Computational Chemistry

Computational chemistry is a branch of theoretical chemistry that is mainly used to understand chemical problems with the aid of computational resources. Computational chemistry is used to investigate the molecular geometries, conformational energies, reaction mechanisms, reaction kinetics, spectroscopic properties such as IR, NMR, Raman, UV and also to study enzymatic reactions etc. In order to understand all these molecular properties, several theoretical parameters should be calculated. These calculations can be done by using computational methods which are broadly divided into five types *viz*. (a) molecular mechanics (b) semi-empirical methods (c) ab initio quantum chemical methods (d) density functional theory methods and (e) molecular dynamics methods. A brief theoretical background of all these methods will be discussed in detail in the following sections.

1.2.1 Molecular Mechanics

Molecular mechanics (MM) or force field methods are based on the use of classical mechanics to predict structure and energies of molecules. In MM methodology, atoms in a molecule are treated as hard spheres and chemical bonds are treated as springs. MM method calculates the energy based on geometry or conformations of a molecule. The theory behind molecular mechanics is based on the assumption that the total energy (E) in a molecule is due to the energy arise from stretching (E_{str}), bending of bonds

(E_{bend}), torsional energy (E_{tor}) due to the twisting of bonds, energy due to the van der Waals non-bonded interactions (E_{vdw}) and electrostatic interactions (E_{elec}).

$$E = E_{str} + E_{bend} + E_{tor} + E_{vdw} + E_{elec} \quad \text{(Eq. 1.8)}$$

Bond stretching: E_{str} is the energy due to the stretching and compression of bonds. In the theory of molecular mechanics, the chemical bonds are treated as a model of springs. According to Hook's law, energy required to stretch or compress the bond between two atoms A and B which are separated by an equilibrium bond length of r_{eq} is as follows.

$$E_{str} = \sum \frac{1}{2} k_{str} (r_{AB} - r_{eq})^2 \quad \text{(Eq. 1.9)}$$

where k_{str} is the stretching force constant for the bond A-B and r_{AB} is the stretched or compressed bond length.

Bending: E_{bend} is the energy required to bend a bond from an equilibrium angle θ_{eq}. The deformation of bond from θ_{eq} will lead to a change in the potential energy which can be expresses as

$$E_{bend} = \sum \frac{1}{2} k_{\theta} (\theta_{ABC} - \theta_{eq})^2 \quad \text{(Eq. 1.10)}$$

where k_{θ} is the bending force constant and θ_{ABC} is the angle that is deformed between the atoms A, B and C from the θ_{eq}.

Torsion: E_{tor} *is* the energy required to rotate about two bonds. The torsional energy can be expressed as

$$E_{tor} = \sum \frac{1}{2} k_{\tau 1} (1 + cos\,\phi) + \sum \frac{1}{2} k_{\tau 2} (1 + cos\,2\phi) + \sum \frac{1}{2} k_{\tau 3} (1 + cos\,3\phi) \quad \text{(Eq. 1.11)}$$

where ϕ is the dihedral angle about the bond, $k_{\tau 1}$, $k_{\tau 2}$, and $k_{\tau 3}$ are the torsional constants for one-fold, two-fold and three-fold rotations, respectively. This torsional energy is very important for molecules having single bonds due to the possibility of eclipsed, gauche and staggered conformations whereas double and triple are rigid, free rotation is restricted.

van der Waals non-bonded interactions: van der Waals energy (E_{vdw}) is due to the interaction of the energy clouds between two non-bonded atoms. When two atoms are at short distance, strong repulsion will arise while at long range attraction will be present. The non-bonded interactions can be calculated by Lennard-Jones potential.

$$E_{vdw} = \sum \left[\left(\frac{\sigma}{r} \right)^{12} - \left(\frac{\sigma}{r} \right)^{6} \right] \qquad \text{(Eq. 1.12)}$$

Where r is the distance between the two nuclei of the atoms and 'σ' depends on the identity of the two atoms at a distance r.

***Electrostatic Interactions*:** Electrostatic energy is due to the Coulomb force between two atoms A and B with charges q_A and q_B, respectively. The electrostatic interaction can be estimated using Coulombic potential.

$$E_{elec} = \sum \frac{q_A q_B}{\varepsilon r_{AB}} \qquad \text{(Eq.1.13)}$$

Where ε the effective dielectric constant and for vacuum ε value is 1.

When all these energy terms are substituted in the Eq. 1.8, a model which is called the functional form of the force field is obtained. The process of finding the actual numbers k_{str}, k_{θ}, $k_{\tau 1}$, $k_{\tau 2}$, and $k_{\tau 3}$ of Eq. 1.9 to 1.11 is called force field parameterization. The advantage of MM method is that it requires less computational time to calculate the theoretical properties of molecules compared to other methods and it is highly useful to

study large molecules such as proteins. Major disadvantage of using MM method is that the force field parameters derived for one set of molecules is not likely to perform well for other set of molecules.

1.2.2 Quantum Chemical Methods

Quantum chemical methods describe the molecules in terms of the interactions of electrons and nuclei. All quantum chemical methods are based on the Schrödinger equation,

$$\mathbf{H}\Psi = E\Psi \qquad \text{(Eq.1.14)}$$

where **H** is the Hamiltonian operator comprising of the nuclear and electronic kinetic energy operators and the potential energy operators corresponding to the nuclear-nuclear, nuclear-electron and electron-electron interactions. Ψ is a many electron wavefunction. E is the energy eigenvalue of the system. The Hamiltonian operator for N electron and M nucleus system can be written as

$$\mathbf{H} = -\sum_{i=1}^{N}\frac{1}{2}\nabla_i^2 - \sum_{A=1}^{M}\frac{1}{2M_A}\nabla_A^2 - \sum_{i=1}^{N}\sum_{A=1}^{M}\frac{Z_A}{r_{iA}} + \sum_{i=1}^{N}\sum_{j>i}^{N}\frac{1}{r_{ij}} + \sum_{A=1}^{N}\sum_{B>1}^{M}\frac{Z_A Z_B}{R_{AB}} \qquad \text{(Eq. 1.15)}$$

where, r_{iA} is the distance between the i^{th} electron and A^{th} nucleus, r_{ij} is the distance between i^{th} and j^{th} electrons and the distance between the A^{th} nucleus and B^{th} nucleus is R_{AB}. M_A is the ratio of the mass of the nucleus to the mass of an electron and Z_A is the nuclear charge of nucleus A. ∇_i and ∇_A are the Laplacian operators which involves the second order differentiation with respect to the coordinates of the i^{th} electron and A^{th} nucleus, respectively. The many electron Schrödinger equation for a simple two electron system such as Helium atom and hydrogen molecule is difficult to solve due to practical

limitations. In order to provide practical application some approximations have been introduced.

1.2.2.1 Born-Oppenheimer Approximation

Born-Oppenheimer approximation states that in a molecule, the nuclear motion is negligible compared to the electronic motion [Born and Oppenheimer 1927]. It means that electrons are moving in a field of fixed nuclei, kinetic energy of the nucleus can be negligible while nuclear-nuclear repulsion will be a constant. Therefore, Eq. 1.15 leads to an electronic Schrödinger equation which can be written as follows

$$\mathbf{H}_{\text{elec}} = -\sum_{i=1}^{N}\frac{1}{2}\nabla_i^2 - \sum_{i=1}^{N}\sum_{A=1}^{M}\frac{Z_A}{r_{iA}} + \sum_{i=1}^{N}\sum_{j>i}^{N}\frac{1}{r_{ij}} \qquad \text{(Eq. 1.16)}$$

The first term is the electronic kinetic energy operator summed over N electrons. The second term represents attraction between i^{th} electron and nuclei A and Z_A is the nuclear charge. The last term in the Eq.1.16 corresponds to Coulombic repulsion between i^{th} and j^{th} electrons. The eigenvalue equation for the electronic Hamiltonian can be written as

$$\mathbf{H}_{\text{elec}}\Phi_{\text{elec}}\left(\{\mathbf{r}_i\};\{\mathbf{R}_A\}\right) = E_{\text{elec}}\Phi_{\text{elec}}\left(\{\mathbf{r}_i\};\{\mathbf{R}_A\}\right) \qquad \text{(Eq. 1.17)}$$

The electronic Hamiltonian depends explicitly on the electronic coordinates and parametrically on the nuclear coordinates. Therefore, the total energy of a system with fixed nuclei can be obtained by adding E_{elec} to the nuclear term.

$$E_{\text{total}} = E_{\text{elec}} + \sum_{A=1}^{N}\sum_{B>1}^{M}\frac{Z_A Z_B}{R_{AB}} \qquad \text{(Eq. 1.18)}$$

Once the wavefunction Ψ is obtained by solving the Schrödinger equation, any experimental observable can be computed as the expectation value of appropriate

operator, $\langle \Psi | \boldsymbol{O} | \Psi \rangle$.

1.2.2.2 Hartree-Fock Approximation

The electronic Hamiltonian defined in Eq. 1.16, $\mathbf{H}_{elec}$ depends on the spatial coordinates of the electron. The necessary conditions for a wave function of the Schrodinger equation is that the wavefunction should be finite, single valued, continuous, quadratically integrable and obeying the appropriate boundary conditions. Further, a many electron wave function must be antisymmetric with respect to the spin of any two electrons. The individual electrons are confined to functions referred as molecular orbitals, and they are determined by assuming that the electron is in the average of other electrons. However, Hartree's approximation relies on the assumption that one electron is independent of the other [Hartree 1928]. Since the molecular Hamiltonian is the sum of many one-electron Hamiltonians, the total molecular wavefunction can be written as the product of spin orbital wave function χ_i and χ_j which is termed as Hartree product determinant [Fock 1930, Slater 1930].

$$\Psi^{HP}(\mathbf{x}_1, \mathbf{x}_2, ..., \mathbf{x}_N) = \chi_i(\mathbf{x}_1)\chi_j(\mathbf{x}_2).....\chi_k(\mathbf{x}_N) \qquad \text{(Eq. 1.19)}$$

Ψ^{HP} is an uncorrelated or independent electronic wavefunction. Further, Ψ^{HP} does not distinguishes the identical electrons, it does not follow the antisymmetry principle, total wavefunction is written in the form of a single determinant named as Slater determinant.

$$\Psi(\mathbf{x_1}, \mathbf{x_2}, ..., \mathbf{x_N}) = \frac{1}{\sqrt{N!}} \begin{vmatrix} \chi_i(\mathbf{x_1}) & \chi_j(\mathbf{x_1}) & ... & \chi_N(\mathbf{x_1}) \\ \chi_i(\mathbf{x_2}) & \chi_j(\mathbf{x_2}) & ... & \chi_N(\mathbf{x_2}) \\ . & . & ... & . \\ \chi_i(\mathbf{x_N}) & \chi_j(\mathbf{x_N}) & ... & \chi_N(\mathbf{x_N}) \end{vmatrix} \qquad \text{(Eq. 1. 20)}$$

The normalized Slater determinant can also be represented in the short from as

$$\Psi(\mathbf{x}_1, \mathbf{x}_2 ....., \mathbf{x}_N) = \left| \chi_i \chi_j .....\chi_N \right\rangle \qquad \text{(Eq. 1. 21)}$$

According to the variational theorem, the best wavefunction is the one which produce lowest energy to the system by determining the correct choice of the spin orbitals. The set of molecular orbitals leading to the lowest energy can obtained using Hartree-Fock (HF) equation as shown below.

$$f(i)\chi(x_i) = \varepsilon\chi(x_i) \qquad \text{(Eq. 1. 22)}$$

where f(i) is the effective one electron operator called as the Fock operator. The procedure for solving the Hartee-Fock equation is called self-consistent-field (SCF) procedure. Fock proposed an extension to the Hartree's SCF procedure of obtaining Slater determinant wavefunctions. Similar to the Hartree product orbitals, the HF molecular orbitals can be individually determined as eigenfunctions of a set of one-electron operators, the interaction of each electron with the static field of all of the other electrons includes exchange effects on the Coulomb repulsion. Later, Roothaan and Hall formulated matrix algebraic equations that permitted HF calculations to be carried out using a basis set representation for the molecular orbitals [Hall 1951, Roothaan 1951]. The Fock operator f(i) can be written as

$$f(i) = -\frac{1}{2}\nabla_i^2 - \sum_{A=1}^{M} \frac{Z_A}{r_{iA}} + V^{HF}(i) \qquad \text{(Eq. 1. 23)}$$

where $V^{HF}(i)$ is the HF potential which is the average potential experienced by the i^{th} electron in the presence of other electrons. Thus, the HF approximation replaces the complicated many electron problem by a one electron problem in which electron-electron repulsion is treated in an average way.

Hartree-Fock theory and linear combination of atomic orbitals (LCAO) approximations applied together to Schrodinger equation lead to Roothan-Hall equations

$$FC = \varepsilon SC \qquad \text{(Eq. 1. 24)}$$

where F is the Fock matrix, S is the overlap matrix and ε is the orbital energies. The methods resulting from the Roothan-Hall equations are treated as Hartree-Fock models and the resultant energy is called HF energy. The Hartree-Fock theory is slightly varied depends on the molecular spin, for example, if the molecule is having singlet spin, the same orbital spatial function can be used for the α and β spin pairs. This procedure is called restricted Hartee-Fock method (RHF).

However, in the case of molecules with unpaired electrons, two HF methods *viz.* (i) unrestricted Hartee-Fock method (UHF) (ii) restricted open shell Hartee-Fock method (ROHF) have been developed [McWeeny and Dierksen 1968, Pople and Nesbet 1954]. In UHF method, two separate sets of orbitals for α and β electrons will be used. The unpaired electrons will have the same spatial orbitals while the paired electrons will not have the same spatial orbitals. Due to this fact, the calculation will results an error called spin contamination. A wavefunction for a particular spin state results another with mixed spin states due to spin contamination, often the total computed energy will be lowered due to high degrees of vibrational freedom. In the case of ROHF method, the paired electrons will have the same spatial orbital functions, spin contamination is absent. ROHF calculations are computationally expensive than the UHF or RHF method.

1.2.2.3 Basis sets

HF calculations essentially use the basis set expansion to express the unknown set of molecular orbitals to a set of known functions. According to LCAO molecular orbital

theory, a molecular orbital can be expressed as a linear combination of many atomic orbitals. Initially Slater types of orbitals (STOs) are used as good approximations but the calculations of two electron integrals are time consuming [Allen and Karo 1960]. Later Boys suggested the use of Gaussian type of orbitals (GTOs) [Boys 1950]. The STO (Eq. 1. 25) and GTO (Eq. 1. 26) for *1s* orbital is shown below.

$$\phi_{1s}^{SF}\left(\xi, \mathbf{r}-\mathbf{R}_{\mathbf{A}}\right)=\left(\xi^{3}/\pi\right)^{1/2} e^{-\xi|\mathbf{r}-\mathbf{R}_{\mathbf{A}}|} \qquad \text{(Eq. 1.25)}$$

where ξ is the Slater orbital exponent.

$$\phi_{1s}^{GF}\left(\alpha, \mathbf{r}-\mathbf{R}_{\mathbf{A}}\right)=\left(2\alpha/\pi\right)^{3/4} e^{-\alpha|\mathbf{r}-\mathbf{R}_{\mathbf{A}}|^{2}} \qquad \text{(Eq.1.26)}$$

where α is the Gaussian orbital exponent. The, p and d orbitals for STO and GTO type are of the general form of Eq. 1.25 and Eq. 1.26, with polynomial equations with exponents $e^{-\xi r}$, $e^{-\alpha r^{2}}$, respectively. It may be noted that compared to STO, the GTO is only a poor approximation to the nearly ideal description of atomic wavefunction. For electronic wavefunction calculations, Slater type of orbitals can yield more accurate features of molecular orbitals. However, the main advantage of GTO is that at large values are *r*, Gaussian function decays much faster than the Slater function. A Cartesian Gaussian function used in electronic structure calculations has the form,

$$g\left(\alpha,l,m,n;x,y,z\right)=N_{l\,m\,n}\left(x-x_{A}\right)^{l}\left(y-y_{A}\right)^{m}\left(z-z_{A}\right)^{n} e^{-\alpha\,|\mathbf{r}-\mathbf{R}_{\mathbf{A}}|^{2}} \qquad \text{(Eq.1.27)}$$

where, α is the orbital exponent and l, m, n are the powers of Cartesian components x, y and z respectively. The center of a Gaussian function is denoted by $\mathbf{R_A}$= (x_A, y_A, z_A). The computational advantage of GTOs over STOs is due to the product of two Gaussian orbitals is again a GTO. The STO-NG basis function is a contracted Gaussian consisting of N primitive Gaussians which has a contraction coefficient [Hehre *et al.* 1969]. The

notation STO-3G means Slater type of orbital is approximated by three Gaussians. The STO-3G basis set is the smallest basis function used in commercial molecular modeling softwares. The STO-3G basis set has the disadvantage that it describes the atoms as spherical environments than the atoms with non-spherical environments and also it restricts the flexibility to describe the electron distribution around the nuclei. To overcome these shortcomings, split valence basis sets and polarization basis sets are formulated.

Split-valence basis set represents the core atomic orbitals by one set of functions and the valence atomic orbitals by two set of functions. Hydrogen is provided by two s-type functions and the main-group elements are provided by two sets of valence s and p-type functions. The simplest split-valence basis sets are 3-21G and 6-31G [Ditchfield *et al.* 1971]. The 6-31G basis sets denote that the core atomic orbital is denoted by six Gaussians and valence orbitals split by three and one Gaussians. For higher basis sets like 6-311G the valence shell can be written in three, one and one Gaussians [McLean and Chandler 1980]. The d-type functions on the main group elements and p-type functions on the hydrogen allow the displacement of the electron distributions away from the nuclear positions. This basis set is called as the polarization basis set and they are represented as 6-31G* and 6-311G*. The symbol * represent d-type polarization functions are written on the non-hydrogen atoms. Similarly 6-31G** and 6-311G** are identical to 6-31G* and 6-311G* except the fact that in the former p-type polarizations are added to hydrogen.

Calculations involving anions are often include diffuse functions which are represented by + indicating the p-type functions on heavy atoms while ++ indicating p,s-type functions to non-hydrogen and hydrogen atoms respectively. Calculations involving transition metals are simplified by considering only the valence electrons as they involved

in bonding, the basis functions corresponding to core electrons can be replaced by an Effective core potential (ECP) [Hay and Wadt 1985]. These basis functions are generated from relativistic atomic calculations, hence this includes some relativistic effects on the system studied.

1.2.2.4 Basis Set Superposition Error

It may be noted that in solving HF equations in conjunction with LCAO approximation, complete set of orbitals are not considered for practical reasons of calculation. This non-completeness of the basis set generates a truncated error of that basis set. When two molecules A and B are interacting to form a complex AB and the interaction energy can be calculated by the following the formula,

$$E_{int} = E_{AB} - (E_A + E_B) \qquad \text{(Eq.1.28)}$$

where E_{AB} is the energy of the complex, E_A and E_B are the energies of the monomer A and B, respectively. The total energy of AB is a representative of the energy calculated at a basis set defined for AB rather than the monomer's basis sets [Chałasiński and Szczgsniak 1994]. The difference between E_A calculated at the basis set defined for the complex and E_A from the monomer's basis set is large and this phenomenon is known as basis set extension effect (BSE). The BSE effect on the monomer energies is termed as basis set superposition error (BSSE). To solve the inconsistency due to the BSE effect, Boys and Bernadi formulated a procedure named as counterpoise procedure [Boys and Bernardi 1970]. This procedure suggests that E_{int} calculated using Eq. 1.28, all the E_{AB}, E_A and E_B should be calculated with the basis set defined for the complex AB. For larger basis sets, the interaction energy is improved and the BSSE will be negligible. But in practical use of larger basis sets are computationally expensive and hence Gutowski and Chalasinski [Gutowski and Chałasiński 1993] recommended the use of counterpoise correction for

evaluating the E_{int}.

1.2.3 Post Hartree-Fock Methods

One of the disadvantage of the HF theory is the electron-electron correlation effect. HF theory assumes the electron repulsion with the average field of electrons but not the electron-electron interaction. It means that the probability of finding the electron around the nucleus is with respect to the nucleus but not with the other electrons. The correlation effect is important for several reasons; mainly it improves the molecular geometries, computed total energies, to study the noncovalent interactions where dispersion effect play a dominant role. To overcome this discrepancy, post HF methods are developed to improve electron correlation which is a more accurate way. The most popular methods which treat electron correlation explicitly are configuration interaction methods (CI), Moller-Plessett (MPn) perturbation methods, coupled cluster methods (CC) , multiconfiguration self-consistent methods (MCSCF). Calculations of all these methods begin with HF and then correlation effect will be included.

1.2.3.1 Configuration Interaction

The correlation energy is defined as the difference between the exact energy (ε_0) and the HF energy.

$$E_{corr} = \varepsilon_0 - E_{HF} \qquad \text{(Eq. 1. 29)}$$

According to the variation theorem, the HF energy is always above ε_0 and hence the E_{corr} is always negative. In configuration interaction (CI) method, excited states are included in to describe the total electronic state of a molecule. In principle, CI method provides an exact solution to the many electron problem. HF wavefunction is used as the reference determinant and the energy is minimized variationally with respect to the determinant expansion coefficients. The possible Slater determinants of HF orbitals to the total exact wavefunction is given by

$$\Phi_0 = \sum_{\substack{all\ Slater\ det \\ of\ HF\ orbitals}} c_k \phi_k \qquad \text{(Eq. 1. 30)}$$

The complete CI wavefunction is a linear combination of Slater determinants with all the permutations of electron occupancies expanded as shown below.

$$\left|\Phi_0\right\rangle = c_0\left|\Psi_0\right\rangle + \sum_{ir} c_i^r \left|\Psi_i^r\right\rangle + \sum_{\substack{i<j \\ r<s}} c_{ij}^{rs} \left|\Psi_{ij}^{rs}\right\rangle + \sum_{\substack{i<j<k \\ r<s<t}} c_{ijk}^{rst} \left|\Psi_{ijk}^{rst}\right\rangle + \sum_{\substack{i<j<k<l \\ r<s<t<u}} c_{ijkl}^{rstu} \left|\Psi_{ijkl}^{rstu}\right\rangle + \ldots \qquad \text{(Eq. 1.31)}$$

The first term in Eq. (1.31) represents the ground state Slater determinant corresponding to the HF wavefunction. The 2nd term represents the Slater determinant with an electron excited from the i^{th} orbital to the r^{th} unoccupied (virtual) orbital. Similarly, rest of the terms constitute triply, quadruply, etc excited determinants with appropriate expansion coefficients. CI method calculations are accurate but computationally very expensive. These calculations are classified by the number excitations used to make each determinant as shown in Eq. 1.31. If only one electron has been moved from each determinant, it is called a configuration interaction single-excitation (CIS) calculation [Foresman *et al*. 1992]. CIS calculations give an approximation to the excited states of the molecule, but do not change the ground-state energy. Single-and double excitation (CISD) calculations yield a ground-state energy that has been corrected for correlation. Triple-excitation (CISDT) and quadruple-excitation (CISDTQ) calculations are done only

when very-high-accuracy results are desired. The configuration interaction calculation with all possible excitations is called a full CI. The full CI calculation using an infinitely large basis set will give an exact quantum mechanical result. Full CI calculation is computationally very expensive and its cost can be related to a binomial coefficient.

$$\binom{K}{N} = \frac{(K)!}{(K-N)!N!} \qquad \text{(Eq. 1.32)}$$

where K is the total number of HF orbitals and N is the number of electrons.

1.2.3.2 Coupled Cluster Methods

Coupled cluster (CC) calculations are very similar to the CI calculations, the difference is that excitations are treated perturbatively rather than the exactly. Coupled cluster is a numerical method used for describing the many body systems and this is considered to be one of the most important practical advancement over the CI method [Čizek 1966]. CC method is a size-extensive method and often CC method is more accurate than the equivalent size CI calculation. The CC wavefunction can be written as exponential functions,

$$\psi_{CC} = e^{T}\ \psi_{HF} \qquad \text{(Eq. 1.33)}$$

ψ_{HF} is a Slater determinant constructed from HF molecular orbitals and T is known as excitation operator which produces linear combination of excited Slater determinants. The cluster operator can be written as

$$T = T_1 + T_2 + T_3 + \ldots + T_n \qquad \text{(Eq. 1.34)}$$

where T_1 is the operator of all single excitations and T_2, T_3 are the operator for all double and triple excitations etc. Therefore, the CC wavefunction can be rewritten as

$$\psi_{CC} = \left(1 + T + \frac{1}{2}T^2 + \frac{1}{6}T^3 + \ldots\right) \psi_{HF} \qquad \text{(Eq. 1.35)}$$

substituting the Eq. 1.34 in Eq.1.35

$$\psi_{CC} = \left(1 + \left(T_1 + T_2 + T_3 + \ldots + T_n\right) + \frac{1}{2}\left(T_1 + T_2 + T_3 + \ldots + T_n\right)^2 + \ldots\right) \psi_{HF} \qquad \text{(Eq. 1.36)}$$

In practice, the expansion of T into individual components is terminated at 2nd excitation. Based on the number of excitations allowed in the calculation of T, the abbreviations for CC methods are of the form, CCN. (N = S for single excitation, N = D for double excitations and N = T for triple excitations etc). The notation CCSD corresponds that the cost of single excitations (T_1) are included with doubles and this type of methods are gives more accurate results. Further, most popular CCSD(T) is that the singles and doubles are fully considered while the triples are calculated with perturbation theory.

1.2.3.3 Moller-Plesset Perturbation Theory

In the sections 1.2.3.1 and 1.2.3.2 we have discussed about adding electron correlation methods to the HF results. Both the CI and CC methods are computationally expensive due to the large number of excited state Slater determinants and hence Möller and Plesset introduced a method for estimating the electron correlation energy using perturbation theory which is generally referred as MPn theory, n stands for order of perturbation. MPn method includes the HF method by adding electron correlation effects using Rayleigh-Schrodinger perturbation theory (RSPT) [Krishnan and Pople 1978; Bartlett and Silver 1975]. According to the RSPT, Hamiltonian can be partitioned as

$$H = H_0 + P \qquad \text{(Eq. 1.37)}$$

where H_0 is the Hartree-Fock Hamiltonian and P is the perturbation given by

$$H_0 = \sum_i f(i) = \sum_i [h(i) + V^{HF}(i)] \qquad \text{(Eq. 1.38)}$$

$$P = \sum_{i<J} \frac{1}{r_{ij}} - \sum_i V^{HF}(i) \qquad \text{(Eq. 1.39)}$$

where $V^{HF}(i)$ is the Coulomb and exchange interaction of electron i other electrons. The expectation value for the V^{HF} for an orbital r is given by

$$[r \mid V^{HF} \mid r] = \sum_s [rr \mid ss] - [rs \mid sr] \qquad \text{(Eq. 1.40)}$$

For the Hamiltonian, H_0, the eigen value is $E_0^{(0)}$, then the first order correction to the energy can be written as

$$E_0^{(1)} = \int \psi_0^{(0)} P \psi_0^{(0)} d\tau \qquad \text{(Eq. 1.41)}$$

Substituting Eq. 1.39 in Eq. 1.41

$$E_0^{(1)} = \int \psi_0^{(0)} \sum_{i<J} \frac{1}{r_{ij}} \psi_0^{(0)} d\tau - \int \psi_0^{(0)} \sum_i V^{HF}(i) \psi_0^{(0)} d\tau \qquad \text{(Eq. 1.42)}$$

$$E_0^{(1)} = -\frac{1}{2} \sum_r \sum_s [rr \mid ss] - [rs \mid sr] \qquad \text{(Eq. 1.43)}$$

Eq. 1.43 clearly represents that the HF energy is the sum of the zeroth and 1st order perturbation energy. Further, the correlation energy can be obtained by the 2nd or higher order perturbation energy. Therefore, for MP2 method, the energy of the system is

$$E_0^{(MP2)} = E_0^{(0)} + E_0^{(1)} + E_0^{(2)} \qquad \text{(Eq. 1.44)}$$

1.2.4 Semi-empirical methods

Semi-empirical models are also based on the Schrodinger equation and follow directly from HF models. Due to the large computational demand in calculation for the ab initio quantum chemical methods, several approximations have been made to ease the computational expense and introduced semi-empirical methods. These methods are based on the treatment of only the valence electrons while the core electrons are neglected in the calculation of the certain integrals that are associated with the HF calculation. Semi-empirical methods are parameterized to produce results such as geometry, energy, electronic spectra, dipolemoments, heats of reactions and NMR chemical shifts.

The most commonly used semi-empirical methods are CNDO, MINDO, MNDO, INDO, ZINDO, AM1 [Dewar and Thiel 1977], PM3 [Stewart 1989] and PM6 [Stewart 2007] etc. The approximation in these methods is that atomic orbitals on different atomic centers will not overlap and is referred as neglect of differential overlap (NDO). The CNDO method is the complete neglect of differential overlap and is proved to be useful for the hydrocarbons. MNDO method is the modified neglect of differential overlap, this method has shown qualitatively incorrect results in the excitation energies and activation barriers and the use of AM1 and PM3 methods has surpassed due to the relative accuracy. PM3 method is the parameterization method 3 which uses almost the same equations to that of AM1. PM6 method is the parameterized method 6 which is known to be superior than the AM1 and PM3 methods.

1.2.5 Density Functional Theory (DFT)

Density functional theory models are fundamentally based on the electron density $\rho(\mathbf{r})$. The electron density is a physically observable quantity. Hohenberg, Kohn and

Sham proposed that the sum of the exchange and correlation energies of a uniform electron gas can be calculated by knowing the electron density [Hohenberg and Kohn 1964]. The main aim of the DFT theory is to introduce some functional that connects to the electron density and the energy of the system. According to Kohn-Sham formalism, the electronic energy can be expressed as a sum of the kinetic energy (E_{KE}), electron-nuclear interaction energy or simply the external potential (E_V), electron-electron interaction energy (E_{ee}) and the exchange-correlation energy (E_{XC}).

$$E(\rho) = E_{KE} + E_V + E_{ee} + E_{XC} \qquad \text{(Eq. 1.45)}$$

In 1964, a fundamental basis for the density functional theory has been established by Hohenberg and Kohn [Hohenberg and Kohn 1964]. They proposed two theorems viz (i) the external potential can be determined by electron density, $\rho(\mathbf{r})$ or the energy is a functional of electron density (ii) Given an external potential, the correct ground state density minimizes the energy functional, $E(\rho)$. These two theorems have lead a fundamental statement for the DFT.

$$\delta\left[E(\rho) - \mu\left(\int \rho(\mathbf{r})\,d\mathbf{r} - N\right)\right] = 0 \qquad \text{(Eq. 1.46)}$$

where N is the number of electrons, $E(\rho)$ is the energy functional and μ is the chemical potential. In the above equation, the kinetic energy term, E_{KE} and the electron-electron interaction term E_{ee} are unknown values. By making some good approximations to these two quantities, the energy minimization can be achieved. Further, the interaction with the external potential is given by

$$E_V = \int E_V\, \rho(\mathbf{r})\,d\mathbf{r} \qquad \text{(Eq. 1.47)}$$

Kohn and Sham introduced an imaginary system of N non-interacting electrons which can

be represented by single determinant wavefunction in N orbitals , ψ_i. the kinetic energy and electron density can be determined from these orbitals

$$E_{KE} = -\frac{1}{2}\sum_{i}^{N}\left\langle \Psi_i \mid \nabla^2 \mid \Psi_i \right\rangle \qquad \text{(Eq. 1.48)}$$

Since the kinetic energy is due to the motion of the molecule, except E_{KE}, all other E_V, E_{ee} and E_{XC} are dependent on the $\rho(\mathbf{r})$. The electron density, $\rho(\mathbf{r})$ is related to the one electron component of orthonormal orbitals, $\rho(\mathbf{r})$ can be expressed as

$$\rho(\mathbf{r}) = \sum_{i=1}^{N}\left|\psi_i^{\,2}\right| \qquad \text{(Eq. 1.49)}$$

The electron-electron interaction is

$$E_{ee} = \frac{1}{2}\int \frac{\rho(\mathbf{r}_1)\rho(\mathbf{r}_2)}{\left|\mathbf{r}_1 - \mathbf{r}_2\right|} d\mathbf{r}_1 d\mathbf{r}_2 \qquad \text{(Eq. 1.50)}$$

It may be noted that in the Eq. 1.45 the E_{XC} is the sum of the error that came from the assumption of non-interacting electron-electron interaction. By applying the variation theorem and introducing the orbitals in the DFT equation, the energy of the system which minimizes follows the equation

$$\left\{-\frac{1}{2}\nabla^2 + E_V + \frac{\rho(\mathbf{r}')}{|\mathbf{r}-\mathbf{r}'|} d\mathbf{r}' + E_{XC}(\mathbf{r})\right\}\psi_i(\mathbf{r}) = \varepsilon_i \psi_i(\mathbf{r}) \qquad \text{(Eq. 1.51)}$$

In the above equation, $E_{XC}(\mathbf{r})$ is the local multiplicative potential which is the functional derivative of the exchange correlation energy with respect to density and it can be expressed as

$$E_{XC}(\mathbf{r}) = \frac{\delta E_{XC}[\rho]}{\delta \rho} \qquad \text{(Eq. 1.52)}$$

The Kohn-Sham equations are similar to that of the Hartree-Fock equations wherein the non-local exchange potential replaced by the local exchange-correlation potential, E_{XC}. The computational cost of solving Kohn-Sham equations is of the order N^3. However, in practice the use of DFT theory is mainly depends on the approximation used in E_{XC}. For a thorough understanding in the formulation of E_{XC}, the E_{XC} is separated into pure exchange part E_X and pure correlation part E_C.

$$E_{XC} = E_X + E_C = \int \rho(r)\varepsilon_x[\rho(r)]dr + \int \rho(r)\varepsilon_c[\rho(r)]dr \qquad \text{(Eq. 1.53)}$$

For practical applications of DFT, several methods have been designed by modifying the exchange-correlation potential viz. (i) Local density approximation (LDA) (ii) Generalized gradient approximation (GGA) (iii) meta-GGA (iv) Hybrid functionals.

(i) Local density approximation (LDA)

LDA is based on the approximation that density can be treated as uniform electron gas. According to Dirac, the exchange from is given by equation (following).

$$E_X^{LDA} = -\frac{3}{4}\left(\frac{3}{\pi}\right)^{1/3} \int \rho^{4/3} dr \qquad \text{(Eq. 1.54)}$$

The correlation functional was determined using Monte Carlo simulations for different densities. To make use of these results for DFT calculations, Vosko, Wilk and Nusair (VWN) has proposed an analytic interpolation formula [Vosko *et al.* 1980].

(ii) Generalized Gradient Approximation (GGA)

Though the model for computing exchange functional through LDA approximation, for improvements the non-uniform electron gas was considered. It lead to an important step to consider that exchange correlation functional depends on both electron density and the

gradient of electron density, $\nabla\rho$. These methods are known as Gradient Corrected or Generalized Gradient Approximation (GGA) methods. Perdew and Wang (PW86) [Perdew 1986, Perdew *et al.* 1992] proposed a modified expression for the exchange functional in which the gradient expansion for slowly varying uniform electron gas is given by

$$x = \frac{\nabla\rho}{\rho^{4/3}} \qquad \text{(Eq. 1.55)}$$

$$\varepsilon_x^{\mathrm{PW86}} = \varepsilon_x^{\mathrm{LDA}} \left(1 + ax^2 + bx^4 + cx^6\right)^{1/15} \qquad \text{(Eq. 1.56)}$$

Becke proposed another correction to the $\varepsilon_x^{\mathrm{LDA}}$ which is given by the following formula [Becke 1988]

$$\varepsilon_x^{\mathrm{B888}} = \varepsilon_x^{\mathrm{LDA}} + \Delta\varepsilon_x^{\mathrm{B888}} \qquad \text{(Eq. 1. 57)}$$

$$\Delta\varepsilon_x^{\mathrm{B888}} = -\beta\rho^{1/3} \frac{x^2}{1 + 6\beta x \sinh^{-1} x} \qquad \text{(Eq. 1. 58)}$$

the x value is fitted to the known atomic data according to the Eq. 1.55 and the corresponding parameter β is obtained.

Perdew and Wang also proposed another exchange functional similar to that of the Becke's functional which is given below

$$\varepsilon_x^{\mathrm{PW91}} = \varepsilon_x^{\mathrm{LDA}} \left(\frac{1 + xa_1 \sinh^{-1} xa_2 + x^2(a_3 + a_4 e^{-bx^2})}{1 + xa_1 \sinh^{-1} xa_2 + a_5 x^2} \right) \qquad \text{(Eq. 1. 59)}$$

where a and b are constants.

(iii) meta-GGA functional

With the development of LDA and GGA designing in the DFT functionals has been improved to a great extent. As a further development for the exchange correlation functional is the consideration to include the higher derivatives of the density. The term

meta-GGA is proposed by Perdew and Schmidit. The meta-GGA functional not only depends on the electron density, its gradient but it also depends on the non interacting kinetic energy density.

$$T = \frac{1}{2}\sum_{i}(\nabla\Psi_{i})^{2} \qquad \text{(Eq. 1. 60)}$$

$$\mathrm{E_X^{MGGA}} = \int f(\rho(\mathrm{r}),\nabla\rho(\mathrm{r}),T(\mathrm{r}))d^{3}\mathrm{r} \qquad \text{(Eq. 1. 61)}$$

(iv) Hybrid functional

In hybrid functionals, the Hartree-Fock exchange is added based on the Hamiltonian and the exchange-correlation energy, a connection between the correlation potential of fictitious reference system and the actual systems with the exact exchange correlation energy. This connection is termed as adiabatic connection formula (ACM). The ACM shows that exchange-correlational energy, E_{XC} can be taken as a weighted sum of the DFT and HF exchange energies. Originally it was proposed by Becke which gives rise to a new functional knows as BHLYP [Becke 1998].

$$\mathrm{E_X^{BHH}} = \frac{1}{2}\mathrm{E_X^{HF}} + \frac{1}{2}\mathrm{W_1^{LDA}} \qquad \text{(Eq. 1. 62)}$$

Later, by incorporating some experimental data in to the above equation, the exchange energy is modified as a combination of LDA, exact exchange and gradient correction term.

$$\mathrm{E_{XC}^{B3}} = a\mathrm{E_X^{HF}} + (1-a)\mathrm{E_X^{LDA}} + b\mathrm{E_X^{B88}} + c\mathrm{E_C^{GGA}} + (1-c)\mathrm{E_C^{LDA}} \qquad \text{(Eq. 1. 63)}$$

where *a*, *b* and *c* are the fitting parameters from the experimental data. Further by incorporating the LYP functional and VWN functional to the equation (above), a new functional namely B3LYP was developed and this is most widely used DFT functional for understanding a variety of chemical problems [Becke 1993].

$$\mathrm{E_{XC}^{B3LYP}} = 0.2\mathrm{E_X^{HF}} + 0.8\mathrm{E_X^{LDA}} + 0.72\mathrm{E_X^{B88}} + 0.81\mathrm{E_C^{LYP}} + 0.19\mathrm{E_C^{VWN}} \qquad \text{(Eq. 1. 64)}$$

1.2.6 Molecular Dynamics and Monte Carlo Simulations

The molecular dynamics (MD) and Monte Carlo (MC) simulation methods uses the classical equations of motion that allows the chemists to understand the dynamical behavior of gases, liquids, solids, surfaces and clusters. MD simulations for liquids are often started in a predefined lattice grid, the momentum and velocity of atoms are computed from the initial geometry. The forces on each atom are calculated from the energy expression which is usually calculated by the molecular mechanics method. A cycle of this procedure will be repeated until the system reaches the equilibrium and the corresponding atomic coordinates are used for further computations of thermodynamic quantities, diffusion constants etc. Monte Carlo methods are based on some sort of random sampling simulated with a random number generating algorithm. In the MC simulation, the molecular geometry is designed according to the statistical distribution. Further, the energy of the system is computed from the initial atomic positions and randomly a trial move for the system will be chosen and again the energy of the system will be calculated for the new configuration. MC simulations are computationally less expensive than the MD simulation for a given system.

1.2.7 Molecular Electrostatic Potential (MESP)

According to Coulomb's law, the electrostatic force of attraction or repulsion between two stationary point charges q_1 and q_2 separated by a distance r is given by

$$F = \frac{q_1 q_2 \hat{r}}{4\pi\varepsilon_0 r^2} \qquad \text{(Eq. 1. 65)}$$

Where ε_0 is a constant known as the permittivity of the free space, $\hat{r}$ is the unit vector joining the point charges q_1 and q_2. The positive sign of F it indicates that both q_1 and q_2

repel each other while a negative sign indicate the attraction between them.

The work done in bringing the unit test positive from infinity to a point of reference R is given by

$$W = \int_{\infty}^{R} \boldsymbol{F} \cos\theta d\boldsymbol{r} \qquad \text{(Eq. 1. 66)}$$

Where θ is the angle between $\boldsymbol{F}$ and $d\boldsymbol{r}$

Substituting the Eq. 1.65 in Eq. 1.66,

$$W = \int_{\infty}^{R} \frac{q_1 q_2}{4\pi\varepsilon_0 r^2} \cos\theta d\boldsymbol{r} \qquad \text{(Eq. 1. 67)}$$

When θ is 180°, cosθ = -1 and when θ is 0°, cosθ = 1, in these cases, the work done or the interaction energy is attractive and repulsive, respectively. On integrating the equation,

$$W = \frac{q_1 q_2}{4\pi\varepsilon_0 r} \qquad \text{(Eq. 1. 68)}$$

Dividing the equation by q_2 gives the electrostatic potential, $V(r)$ generated by the q_1 at a distance r is

$$V(r) = \frac{1}{4\pi\varepsilon_0}\frac{q_1}{r} \qquad \text{(Eq. 1. 69)}$$

The above equation represents the electrostatic potential created by a point charge q_1, but a molecule contains several electrons and nucleus. Therefore, the total electrostatic potential is given by the following formula. For nucleus, according to Born-Oppenheimer approximation, the nuclei can be considered as stationary point charges and the corresponding electrostatic potential for such a group of point charges can be written as

$$V(\mathbf{r}) = \frac{1}{4\pi\varepsilon_0}\sum_i \frac{q_i}{r} \qquad \text{(Eq. 1. 70)}$$

The electrons are not stationary point charges and hence it always contains a continuous charge distribution represented as ρ(**r'**). The charge contained in an infinitesimal volume element $d^3\mathbf{r'}$ around a point r' is $\rho(\mathbf{r'})d^3\mathbf{r'}$.

$$V(\mathbf{r}) = \frac{1}{4\pi\varepsilon_0}\int \frac{\rho(\mathbf{r}')d^3\mathbf{r}'}{|\mathbf{r}-\mathbf{r}'|} \qquad \text{(Eq. 1. 71)}$$

Combining the above two equations, we will get an equation of the following form

$$V(\mathbf{r}) = \frac{1}{4\pi\varepsilon_0}\left[\sum_A \frac{Z_A}{|\mathbf{R_A}-\mathbf{r}|} + \int \frac{\rho(\mathbf{r}')}{|\mathbf{r}-\mathbf{r}'|} d^3\mathbf{r}'\right] \qquad \text{(Eq. 1. 72)}$$

and conveniently it can be written as

$$V(\mathbf{r}) = \sum_A^N \frac{Z_A}{|\mathbf{R_A}-\mathbf{r}|} - \int \frac{\rho(\mathbf{r}')d^3\mathbf{r}'}{|\mathbf{r}-\mathbf{r}'|} \qquad \text{(Eq. 1. 73)}$$

The Eq. 1.73 represents the electrostatic potential at a point **r**, Z_A is the nuclear charge at a distance $\mathbf{R_A}$ and $\mathbf{R_A}$-**r** is the distance from **r**. The first term in the equation corresponds to the bare nuclear potential and second term corresponds to the electronic contributions. It is customary to represent V(**r**) in the units of energy. The MESP, V(**r**), is scalar and real physical property of a molecule, which can attain positive, zero or negative values and this value can be experimentally obtained using x-ray diffraction techniques [Stewart 1979]. In most of the computational programmes, the MESP is often calculated over a cubical grid and the corresponding file can be visualized. In the valence region of a molecule, MESP is positive in the region close to nuclei and negative in the electron-rich region such as lone-pairs and unsaturated π-systems.

The MESP at a particular nucleus A can be calculated using the formula,

$$V(R_B) = \sum_{A \neq B}^{N} \frac{Z_A}{|R_B - R_A|} - \int \frac{\rho(r')d^3r'}{|R_B - r'|} \quad \text{(Eq. 1. 74)}$$

In Eq. 1.74, Z_A represents the nuclear charge, $\rho(r)$ is the electron density of the molecule, r' is the dummy integration variable. The equation contains summation over all the atomic nuclei which are treated as positive point charges as well as integration over the continuous distribution of the electronic charge. The topographical features of MESP can be characterized in terms of nondegenerate critical points *viz.* minima, saddle and maxima [Balanarayan and Gadre 2003; Pinjari and Gejji 2008]. A critical point is typically represented in the form (R, S), where R is rank and S is the signature of the Hessian matrix. Electron rich regions like lone-pair of electrons and π-bonds shows (3, +3) critical points which is the local minima on the MESP isosurface. On the other hand, (3, -1) saddle will represent a covalent bond. Similar to the electron density based critical points, rings will show a ring critical point in the case of MESP topography and is represented as (3, +1) critical point.

In Figure 1.5, the MESP surfaces for ethylene, benzene, N-heterocyclic carbene, water and pyridine are shown. Ethylene is an unsaturated double bonded system while benzene is an aromatic system. N-heterocyclic carbene is a reactive intermediate which has a lone pair of electrons on the carbon and water has a two non-bonded lone pairs on the oxygen. Further, pyridine is also an aromatic compound in which nitrogen has a lone pairs electrons. Benzene has electrostatic potential isosurface above and below the ring plane while in pyridine the isosurface is at the nitrogen atom indicating the depletion of electron density on the aromatic part. Water is having two lone pair of electrons showing the electron rich character reflected in the isosurface. The MESP value at which the

isosurface vanishes is called as the MESP minimum and represented as V_{min}.

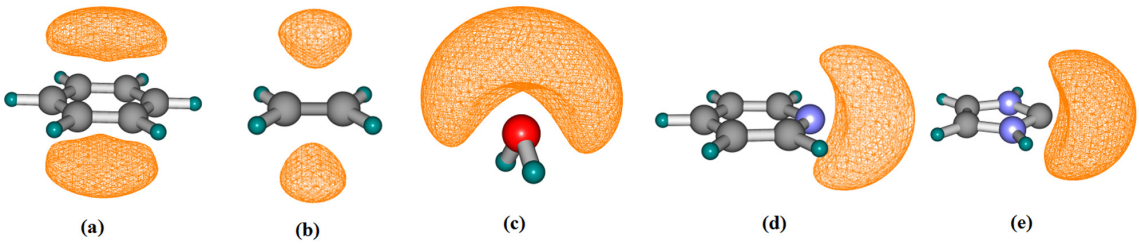

Figure 1.5 MESP isosurfaces of (a) Benzene (b) Ethylene (c) Water (d) Pyridine (e) N-heterocyclic carbene drawn at -0.02, -0.02, -0.04, -0.035 and -0.04 au, respectively.

MESP has been widely used as a qualitative descriptor for identifying the reactive sites in a variety of contexts. For instance, Gadre and co-workers have explored the use of MESP topography to study the reactive behavior of 1,3 dipolar cycloaddition reactions between acetylene and fulmunic acid, diazomethane [Balanarayan *et al.* 2003]. Haeberlein and Brinck calculated the deepest MESP point designated as V_{min} of *para* substituted phenoxide ions at the BLYP and HF methods and found a linear correlation between V_{min} and σ_p^- [Haeberlein and Brinck 1996]. Gadre and Suresh studied the monosubstituted benzenes and emphasized the use of MESP based critical points to predicting the substituent effects [Gadre and Suresh 1997]. They classified electron-donating and electron-withdrawing substituents in straightforward way that any substituent which produces more negative MESP value than the benzene is electron-donating and the one which produces higher MESP value than the benzene is electron-withdrawing. Later this MESP approach was extended to V_{min} approach to the multiple substituted benzenes and showed that the quantity ΔV_{min} (difference between the V_{min} of substituted benzene and the unsubstituted benzene) can be used as a direct measure of substituent effect [Suresh and Gadre 1998]. For disubstituted benzenes, three quantities namely substituent pair constants, D_o, D_m and D_p are proposed for *ortho*, *meta* and *para*

substitutions. The D_o, D_m and D_p is defined as the difference between the actual V_{min} of a disubstituted benzene and the corresponding predicted V_{min} obtained by adding the ΔV_{min} of different substituents for *ortho*, *meta* and *para* combinations. The parameters D_o, D_m and D_p are useful for predicting the combination of substituents in a multiple substituted systems especially for (*ortho*,*ortho*), (*ortho*,*meta*) and (*ortho*,*para*) combinations as there is no *ortho* constant.

Galabov *et al*. evaluated the MESP at the nuclei of fifteen monosubstituted benzenes using B3LYP and BPW91 methods [Galabov *et al.* 2006]. They observed linear correlations between the MESP at the nuclei of *meta* and *para* carbons and σ_m^0 and σ_p^0 suggesting that MESP at the nuclei can be used as a good descriptor for quantification of substituent effects. Suresh and Gadre compared the use of MESP at the nuclei of *para* carbon with V_{min} for the monosubstituted benzenes at different levels of theory and recommended the use of V_{min} as it can represent the exact locations of electron-rich centers in three-dimensions [Suresh and Gadre 2007]. The calculations carried out at the B3LYP, B3PW91, and MP2 levels suggested that the absolute values of V_{min} may vary with respect to the methods but the overall trend of substituent effects is unaffected.

1.2.8 NMR Chemical Shifts

Nuclear magnetic resonance spectroscopy (NMR) is one of most powerful technique used by the chemists for the interpretation of structures of molecules. The NMR measurements are very sensitive to the small changes of molecules. The NMR chemical shift of a nucleus can be defined as the difference between the resonance frequency of a particular nucleus relative to the reference nucleus. NMR chemical shifts can be computed using DFT and ab initio methods using many molecular modelling softwares like Gaussian, Gammess, Turbomole, and NWchem etc. These softwares

calculate the isotropic nuclear magnetic shielding tensors, from which the chemical shifts are calculated by subtracting the nuclear shielding tensors of reference compound such as TMS (trimethylsilane) [Vaara 2007]. To calculate the NMR shielding tensors, the euqillibrium geometry must be optimized at higher accuracy level. Helgakar *et al*. suggested using at least triple zeta quality basis sets for optimizing the structures [Helgaker *et al.* 1999].

For computing the NMR properties, several methods viz. (i) Guage invariant atomic orbitals (GIAO) [Ditchfield 1974] (ii) individual guage for localized orbitals (IGLO) [Schindler and Kutzelnigg 1982] (iii) localized orbital local origin (LORG) (iv) individual gauges for atoms in molecules (IGAIM) [Keith and Bader 1992]. Among these methods, the most widely used method is GIAO which is based on the perturbation theory. IGAIM is based on the Bader's theory of atoms in molecules which requires large computer time and hence this method is rarely used. Further, computing NMR tensors for organic molecules is relatively easy compared over the transitions metal complexes. Since, the NMR property is a nuclear effect, for calculating NMR shielding constants effective core potentials should not be used.

1.3 Conclusions

In the first part of the introduction, a detailed description about origin of the Hammett equation was derived using the linear free energy relationships. The electron donating and withdrawing power is characterized by Hammett substituent constants and these are designated as σ_m and σ_p for *meta* and *para* substitution. These σ_m and σ_p constants have been failed in several reaction series wherein an electron donating substituent interacts with an electron withdrawing reaction centre and vice-versa. As a consequence, σ_I and σ_R constants have been evolved to quantify the substituent effect in terms of inductive and resonance effects. A detailed literature survey about the quantitative methods for the inductive, resonance and proximity substituent effects was discussed. Further, a brief introduction about the cation-π interactions factors that are responsible for this strong interaction was demonstrated. The fine tuning of cation-π interactions can be done by tuning the electronic nature of substituents and the quantitative methods for the substituent cation-π interaction energies are also discussed. In the second part of introduction, an overview of theoretical background of computational methods is discussed. A brief account on the molecular mechanics methods, semi-empirical methods, Hartree-Fock theory, post Hartree-Fock methods, density functional theory and molecular dynamics methods are outlined. Moreover, molecular properties such as NMR calculations and molecular electrostatic potential are also discussed.

Chapter 2

Development of Quantitative Methods for Proximity, Resonance, and Through-space Substituent Effects

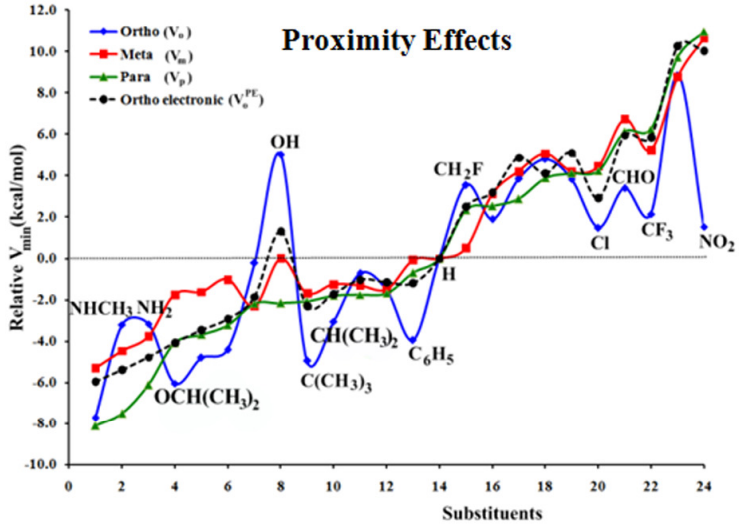

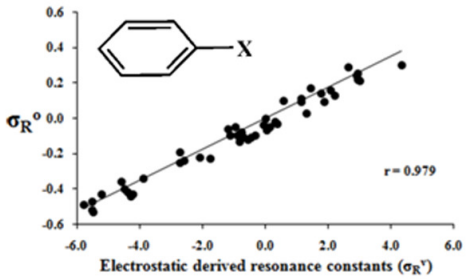

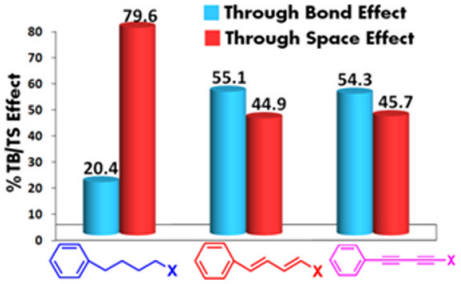

2.1 Abstract

In part A of this chapter, several ortho, meta, and para substituted benzoic acids have been studied to quantify the substituent effects by analyzing subtle variations in the molecular electrostatic potential minimum (V_{min}) at the response site of the carboxylic acid moiety using density functional theory. V_{min} of meta and para substituted benzoic acids is directly proportional to the σ_m and σ_p values suggesting that V_{min} can be used as a good measure of substituent effect. The total ortho substituent effect is separated into contributions from electronic and proximity effects. A molecular fragment approach in conjunction with a rotation experiment on the COOH moiety of benzoic acid is used to quantify the proximity effect. The quantified proximity effect for the alkyl groups is in accord with the steric parameters proposed by Taft (E_s), Proft and Schlosser. The proximity effect-corrected V_{min} of ortho systems showed excellent linear correlations to both the V_{min} of meta and para substituted systems which enabled the computation of meta:para, ortho:para and meta:ortho electronic effect ratios and their respective values are 1:1.108, 1:1.042 and 1:1.047. Further, additive nature of substituent effect is also tested using the V_{min} on multiple substituted benzoic acids. It is found that total substituent effect is approximately 86.3% of the sum of the individual contributions.

In part B of this chapter, the MESP approach is applied to monosubstituted benzenes to quantify the substituent resonance effect. The MESP based resonance constant, σ_R^v is proposed as a quantitative measure of substituent resonance effect. A linear correlation between σ_R^v and resonance constants (σ_R^o) derived from infrared intensities is obtained. This correlation indicates that MESP can be used as an alternative descriptor for quantification of substituent resonance effect. The reliability of σ_R^v is rigorously verified using three isodesmic reactions and found that the energy component of substituent resonance effect is proportional

to σ_R^v. Thus, MESP approach enabled the definition to an electrostatic scale of substituent resonance effect. In part C of this chapter, through-bond (TB) and through-space (TS) substituent effects in substituted alkyl, alkenyl and alkynyl arenes are quantified separately using MESP. The deepest MESP point over the aromatic ring (V_{min}) is considered as a probe for monitoring these effects for a variety of substituents. In the case of substituted alkyl chains, the TS effect (79.6%) dominates the TB effect whereas in the unsaturated alkenyl and alkynyl analogues, the TB effect (~55%) overrides the TS effect.

Part A: Quantification of Proximity Effects

2.2 Introduction

Understanding the correlation between structure of molecules and their chemical reactivity is one of the fundamental objectives in modern chemistry [Jaffé 1953]. When 'X' derivative of a molecule 'M-H' is made, the 'X' will have a direct and significant effect on the chemical properties of 'M' and this effect in comparison with 'H' is considered as substituent effect [Exner and Krygowski 1996, Krygowski and Stepien 2005]. To quantify the substituent effects, Hammett introduced substituent constants which are primarily derived from the ionization of substituted benzoic acids [Hammett 1937]. These substituent constants [Shorter 1994, 1997] successfully explained the reactivities of a variety of aromatic molecules, when the substituent is at *meta* or *para* position with respect to the reaction centre [Exner and Böhm 2002, Gross *et al.* 2001, Klein and Lukeš 2006, McDaniel and Brown 1958, Wiberg 2002[a], 2003]. On the other hand, the Hammett substituent constants for *ortho* substitution have been rarely used to understand the chemical reactivity as they failed in many cases due to interplay of proximity effects at the reaction centre [Taft 1960]. In a recent review, Exner and Bohm have pointed out that applying the Hammett equation to *ortho* systems is difficult due to the existence of intramolecular hydrogen bonds, steric inhibition of resonance, steric hindrance and short-range polar effects [Exner and Böhm 2006]. These effects are collectively termed as '*ortho* effect' or 'proximity effect'. In the case of *ortho* substitution, steric inhibition of resonance describes that any structural modification leading to distortion in the coplanarity between reaction centre and phenyl group which reduces the electron delocalization between them. Exner and co-workers have investigated steric inhibition of resonance in the case of *ortho* alkyl substituted benzoic acids, methyl

substituted acetophenones and concluded that the substituents which exhibit strong steric hindrance at the reaction centre will show significant torsion angle (Figure 2.1) and substituents which exhibits weak steric hindrance remains planar with the phenyl ring [Bohm and Exner 2000, 2001, Kulhanek *et al.* 2004]. For instance, in the *o*-*t*-butyl benzoic acid, the bulky *ortho* substitution inhibits the coplanarity between COOH and phenyl ring and this in turn enhances its acidity to a value 0.74 higher than benzoic acid (the pK_a (H) = 4.20, pK_a (*o*-*t*-butyl) = 3.46, pK_a (*m*-*t*-butyl) = 4.28, and pK_a (*p*-*t*-butyl) = 4.40) [Exner and Böhm 2006].

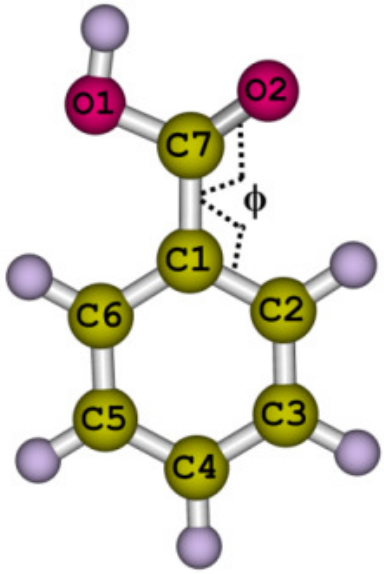

Figure 2.1 Definition of torsion angle $\phi(O_2C_7C_1C_2)$.

Several experimental studies have been employed to understand the nature of *ortho* electronic substitution effect [Charton 1969[b], 1971, Charton and Charton 1971, Fiedler *et al.* 2006]. All these experimental results have limitations to quantify the exact electronic nature of *ortho* substituent effects such as, eliminating the bulky *ortho* substituent effect in correlating with *para* substituent effect and approximating the *ortho*, *para* electronic effects to be the same [Bohm *et al.* 2004, Charton 1969[b]]. However, a method which can accurately quantify the electronic as well as proximity effects of *ortho* substituents is yet to be established. Attempts have been made by many research groups to establish a theoretical

basis for quantifying the substituent effects using computed quantum chemical descriptors such as, total core-electron binding energy shifts [Takahata and Chong 2005], atomic charges [Fourré *et al.* 2007, Klein and Lukes 2007], electrophilicity index [Elango *et al.* 2005], QSAR studies [Gieleciak and Polanski 2007, Girones *et al.* 2003, Sullivan *et al.* 2000] and energy of protonation [Hollingsworth *et al.* 2002]. Molecular electrostatic potential (MESP) is a well established electronic descriptor to study noncovalent interactions, electrophilic substitution reactions and for a variety of chemical phenomenon [Bonnaccorsi *et al.* 1975, Galabov *et al.* 2008, Kushwaha and Mishra 2006, Murray and Politzer 2009, Tiwari *et al.* 2008]. From a number of studies based on topological properties of MESP, it has been recognized that MESP is one of the most promising molecular properties that can accurately interpret the electron-donating as well as electron-withdrawing ability of the substituents [Gadre and Suresh 1997, Galabov *et al.* 2006, Suresh *et al.* 2008, Suresh and Gadre 1998, 2007]. Thus, MESP based method may be useful to quantify the proximity effects which facilitates the interrelationships among *ortho*, *meta* and *para* substituent effects.

2.3 Computational Details

Computational calculations involved on the substituted benzoic acids have been performed with density functional theory (DFT) by incorporating Becke's three parameter exchange functional with Lee, Yang and Parr`s (B3LYP) [Becke 1993, Lee *et al.* 1988] method as implemented in the Gaussian03 suite of programme [Frisch *et al.*]. The split valance basis set with polarization functions 6-31G(d,p) is employed in all the calculations. Suresh and Gadre have shown that B3LYP/6-31G(d,p) level wave function is adequate for studying the MESP features of organic systems [Suresh and Gadre 2007]. The MESP, $V(\mathbf{r})$ at a point $\mathbf{r}$ due to a molecular system with nuclear charges located at $\mathbf{R_A}$ and electron density

$\rho(\mathbf{r})$ is expressed in Eq.2.1 where N is the total number of nuclei in the molecule [Gadre and Shirsat 2000, Politzer and Murray 2002].

$$V(\mathbf{r}) = \sum_{A=1}^{N} \frac{Z_A}{|\mathbf{r} - \mathbf{R}_A|} - \int \frac{\rho(\mathbf{r}')\mathrm{d}^3\mathbf{r}'}{|\mathbf{r} - \mathbf{r}'|} \qquad \text{(Eq. 2.1)}$$

MESP is an experimentally derived property using X-ray diffraction techniques [Naray-Szabo and Ferenczy 1995] and it interprets the reactivities of organic molecules. To quantify the proximity effects and also to understand the *ortho* electronic effect with respect 23 substituted derivatives of *ortho*, *meta* and *para* benzoic acids are considered. Substituents which will exhibit inductive, steric, resonance and hyper conjugative effects are included. Various possible conformers of all substituents for *meta* and *para* positions are studied and most stable conformers are considered. In the case of *ortho* systems, proximity effect operates and therefore the substituent can either orient towards carbonyl group of the COOH or hydroxyl group of the COOH. Therefore, to describe relative values of proximity effects using same type of reference structures, the orientation of the substituent towards the carbonyl of the COOH moiety is selected for all *ortho* systems.

2.4 Results and Discussion

2.4.1 MESP and Hammett Substituent Constants

Aromatic ring, hydroxyl oxygen and carbonyl oxygen are the electron rich sites of benzoic acid and at these sites one can locate negative valued MESP minimum (V_{min}) (Figure 2.2). In benzoic acid, the V_{min} on the aromatic ring (-9.89 kcal/mol) is located near the *meta* carbon. At the OH of the COOH, the V_{min} is -24.07 kcal/mol whereas CO of COOH shows a V_{min} value of -44.59 kcal/mol. The carbonyl oxygen is clearly more electron rich than the OH due to the sp^2 hybridization of the former. All the systems except $COCH_3$, $CONH_2$, CN, and

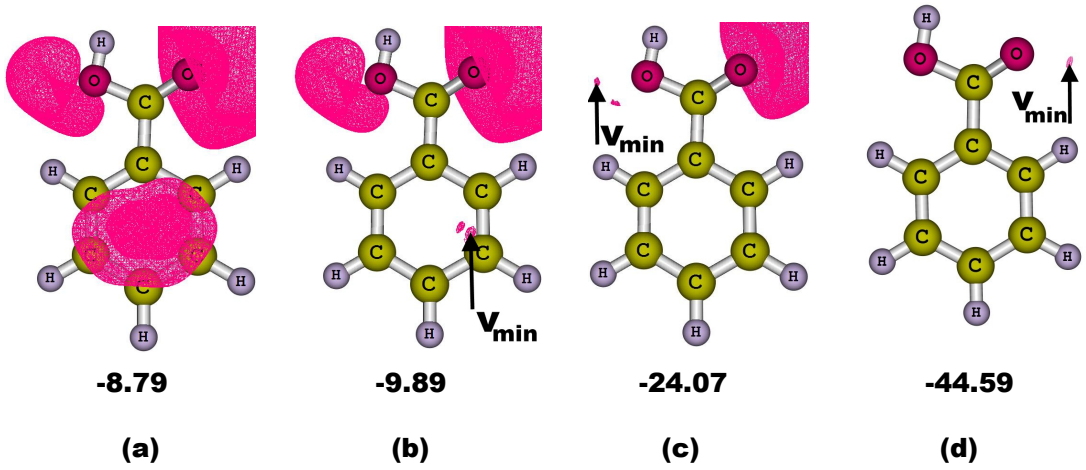

Figure 2.2 In (a), (b), (c) and (d) different values (-8.79, -9.89, -24.07, and -44.59 kcal/mol, respectively) of MESP isosurface of benzoic acid is shown. In (b), (c), and (d), the location of V_{min} is depicted.

NO_2 substituents showed V_{min} on the aromatic ring. Lack of negative V_{min} on the aromatic ring is due to strong electron-withdrawing substituent effect. In all *ortho* systems, CO of the COOH experiences more proximity interactions from the substituent compared to OH of the COOH. Therefore, among the three V_{min} sites, the V_{min} at the OH is considered for assessing the substituent effects.

The relative V_{min} obtained at OH of the COOH with respect to the V_{min} of unsubstituted benzoic acid (-24.07 kcal/mol) is designated as V_o for *ortho*, V_m for *meta* and V_p for *para* substituted benzoic acids and these values are presented in Table 2.1. Based on the relative V_{min} values, electron-donating and withdrawing ability of substituent can be predicted. For instance, in *para* substituted benzoic acids, the electron donating ability of the substituent is of the following order, $N(CH_3)_2 > NHCH_3 > NH_2 > OCH(CH_3)_2 > OCH_2CH_3 > OCH_3 > NHOH \sim OH > C(CH_3)_3 > CH(CH_3)_2 > CH_3 > CH_2CH_3 > C_6H_5 > H > CH_2F > F > CONH_2 > COCH_3 > Br > Cl > CHO > CF_3 > CN > NO_2$. The halogens (F, Cl, Br) are the

Table 2.1 Relative V_{min} values of *ortho* (V_o), *meta* (V_m) and *para* (V_p) substituted benzoic acids and Hammett substituent constants.

S.No	Substituent[a]	V_o	V_m	V_p	σ_m	σ_p
1	$N(CH_3)_2$	-7.72	-5.30	-8.13	-0.21	-0.83
2	$NHCH_3$	-3.19	-4.46	-7.50	-0.21	-0.70
3	NH_2	-3.16	-3.76	-6.12	-0.16	-0.66
4	$OCH(CH_3)_2$	-6.04	-1.74	-4.08	0.08	-0.45
5	OCH_2CH_3	-4.79	-1.62	-3.67	0.08	-0.24
6	OCH_3	-4.40	-1.02	-3.21	0.06	-0.27
7	NHOH	-0.22	-2.31	-2.18	-0.04	-0.34
8	OH	5.03	0.02	-2.17	0.05	-0.37
9	$C(CH_3)_3$	-4.94	-1.68	-2.07	-0.10	-0.20
10	$CH(CH_3)_2$	-3.04	-1.24	-1.79	-0.04	-0.15
11	CH_3	-0.72	-1.30	-1.76	-0.07	-0.17
12	CH_2CH_3	-1.52	-1.49	-1.68	-0.07	-0.15
13	C_6H_5	-3.95	-0.06	-0.70	0.06	-0.01
14	H	0.00	0.00	0.00	0.00	0.00
15	CH_2F	3.56	0.52	2.35	0.12	0.11
16	F	1.89	3.11	2.54	0.34	0.06
17	$CONH_2$	3.85	4.21	2.87	0.28	0.31
18	$COCH_3$	4.81	5.06	3.89	0.38	0.47
19	Br	3.85	4.21	4.12	0.39	0.23
20	Cl	1.49	4.47	4.25	0.37	0.23
21	CHO	3.41	6.75	6.12	0.40	0.42
22	CF_3	2.15	5.23	6.24	0.43	0.54
23	CN	8.88	8.79	9.71	0.62	0.66
24	NO_2	1.53	10.67	10.98	0.71	0.78

[a] All the substituents are arranged in accord with the V_p values.

only *ortho*, *para* directing substituents placed below the 'H'. V_m and V_p showed good linear relationships to Hammett constants σ_m and σ_p, respectively (Figure 2.3) suggesting that the true nature of substituent effect is associated with these electronic descriptors (V_m and V_p) and they may be used as alternate measure of substituent effect. However, V_o showed poor linear correlation (correlation coefficient (r) is 0.583) to σ_o constant (Figure 2.4). It may be noted that in the case of *ortho* systems, the σ_o values differ considerably for various set of reactions [Charton 1969[a]], unlike the σ_m and σ_p, it cannot be universally applied to various types of reaction series. The poor correlation between V_o and σ_o can be mainly attributed to the proximity effects.

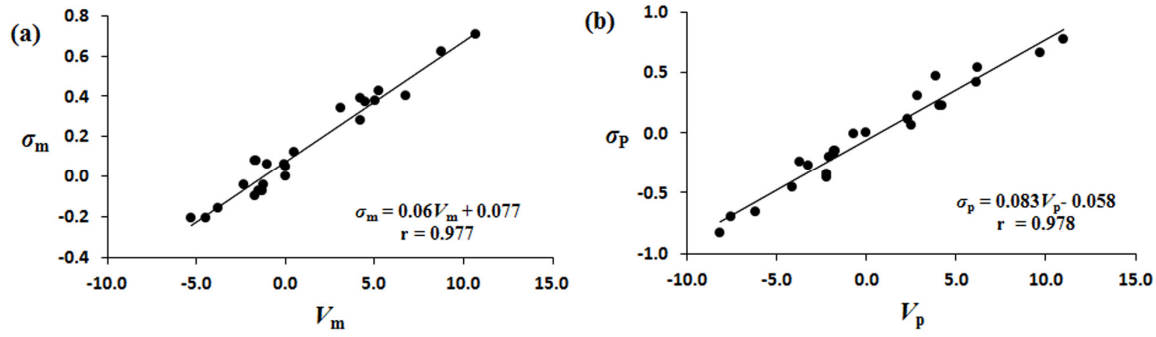

Figure 2.3 Relative V_{min} at the OH of COOH in *meta* and *para* substituted benzoic acids plotted with Hammett constants. (a) V_m vs σ_m (b) V_p vs σ_p.

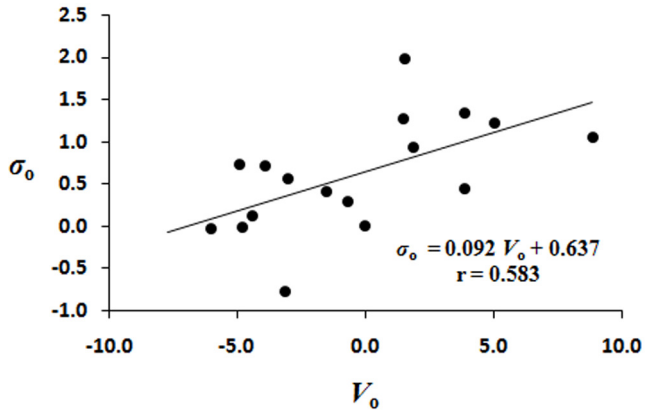

Figure 2.4 Relative V_{min} at the OH of COOH in *ortho* substituted benzoic acids plotted with σ_o constants.

2.4.2 MESP Approach to Quantify Proximity Effects

Two types of proximity effects exist in *ortho* substituted systems, *viz*. (i) through-space COOH···X interactions and (ii) steric effect of X. In order to quantify the first effect, a molecular fragment approach is developed. In this approach, at first a fragment showing the proximity effect should be identified and separated from the remaining portion of the molecule (Figure 2.5a and 2.5b). In the next step, the unused valence of carbon atoms (C_1 and C_2 in Figure 2.5b) of the fragment is filled by adding hydrogen atoms at optimum distance through a constrained optimization (only the new C-H distances are optimized) to generate a new structure and this will resemble the *cis*-(COOH, X) form of ethylene (Figure 2.5c). The corresponding *trans* form is then generated by rotating the C_1-C_2 bond by 180° (Figure 2.5d).

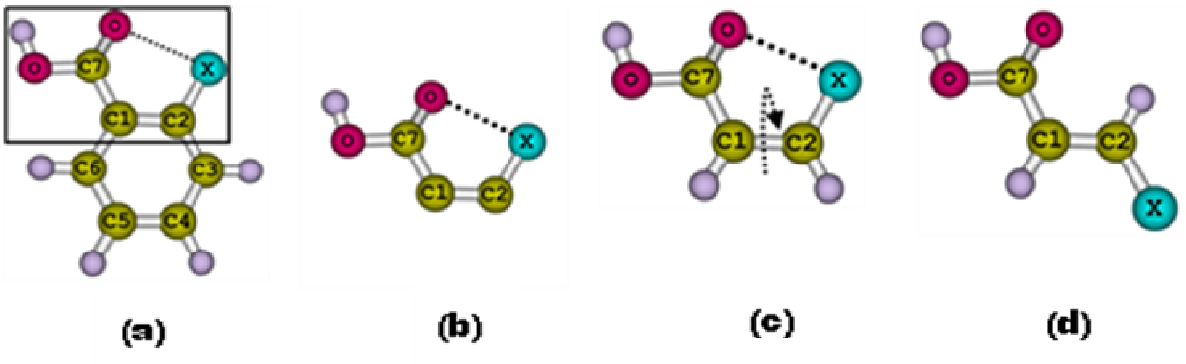

Figure 2.5 Model systems constructed for quantification of proximity effects. Dotted line represents the proximity interaction between X and COOH.

The relative V_{min} with respect to 'X = H' for both *cis* and *trans* forms is designated as V_c for *cis* and V_t for *trans*. In *cis*-form, proximity effect is preserved nearly to the same extent as that of the parent molecule while C_1-C_2 rotation leading to the *trans* form will remove this

effect. Therefore, we can expect the difference between V_c and V_t to be a measure of proximity effect.

When bulky substituents like $CH(CH_3)_2$, $C(CH_3)_3$, and C_6H_5 are present at *ortho* position, an increase in ϕ value (for definition of ϕ, see Figure 2.1) is obtained due to steric hindrance. In the molecular fragment procedure, since *cis* and *trans* form of the fragments retain the same ϕ value of parent molecule, the steric-induced proximity effect which leads to the twisting of COOH is not accounted in the ($V_c - V_t$) values. In order to assess the effect of ϕ on the V_{min}, a free model experiment with unsubstituted benzoic acid was carried out. In this procedure, benzoic acid is modeled for ϕ values in the range of 0–90° at an interval of 4.5°. This experiment was done by fixing the C_1-C_7 distance and the ∠C_2-C_1-C_7 angle to those of the planar benzoic acid (Figure 2.1). The V_{min} for the OH moiety of the COOH is determined at each interval of ϕ. The V_{min} value for ϕ = 0 is set as zero and the relative V_{min} of other ϕ values are designated as V_ϕ. The ϕ values are plotted with V_ϕ to fit to a 2nd order polynomial which indicates that V_ϕ is highly sensitive to the twisting of the COOH group (r = 0.999, Figure 2.6). As the ϕ value increases, negative value of V_ϕ is increased (Table 2.2), suggesting that a bulky group capable of producing considerable twist at the COOH group can significantly affect the overall electron distribution in the system through strong steric-induced proximity effect.

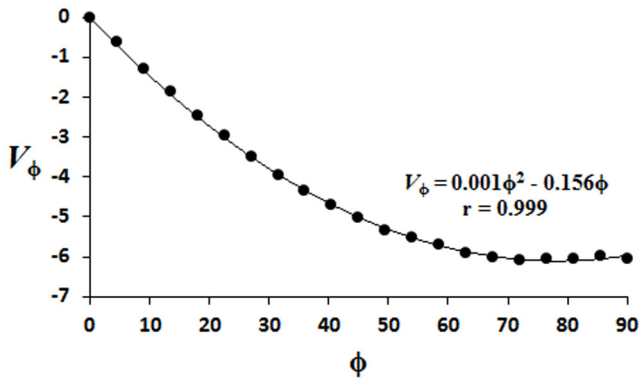

Figure 2.6 Dependence of V_ϕ with ϕ in the unsubstituted benzoic acid.

Table 2.2 ϕ (in degrees) and V_ϕ (in kcal/mol) values obtained by modeling the free benzoic acid.

ϕ	V_ϕ[a]
0.0	0.00
4.5	-0.59
9.0	-1.27
13.5	-1.86
18.0	-2.46
22.5	-2.97
27.0	-3.50
31.5	-3.95
36.0	-4.35
40.5	-4.69
45.0	-5.02
49.5	-5.33
54.0	-5.52
58.5	-5.69
63.0	-5.90
67.5	-6.03
72.0	-6.08
76.5	-6.07
81.0	-6.07
85.5	-5.98
90.0	-6.04

[a] V_{min} value is -24.08 kcal/mol for ϕ = 0

Thus, total proximity effect, V_{PE} in *ortho* substituted system can be represented as a sum of ($V_c - V_t$) and V_ϕ (Eq. 2.2).

$$V_{PE} = (V_c - V_t) + V_\phi \qquad \text{(Eq. 2.2)}$$

Both V_m and V_p represent purely the electronic effects (transmitted through the σ and π bonds) of substituents as they are nearly unaffected by proximity effects while V_o represents the total of electronic and proximity effects. Therefore, the through-bond electronic effect of an *ortho* substituent (designated as V_o^{PE}) can be obtained by correcting the V_o value with the corresponding V_{PE} values as defined in Eq. 2.3.

$$V_o^{PE} = V_o - V_{PE} \qquad \text{(Eq. 2.3)}$$

In Table 2.3, the values of V_c, V_t, V_ϕ, V_{PE}, and V_o^{PE} are presented along with the ϕ values. In the case of alkyl groups, the proximity effect V_{PE} is mainly due to steric hindrance and accordingly the order is as follows $C_6H_5 > C(CH_3)_3 > CH(CH_3)_2 > CH_2CH_3 > CH_3$. This order is in accord with the steric constants proposed by Taft (E_s) and the B-value proposed by Schlosser [Ruzziconi *et al*. 2009]. Further, the V_{PE} is also validated by a linear correlation (correlation coefficient is 0.910) with the electron density based steric constants ($E_S[\rho(r)]$) [Torrent-Sucarrat *et al*. 2009] (Figure 2.7).

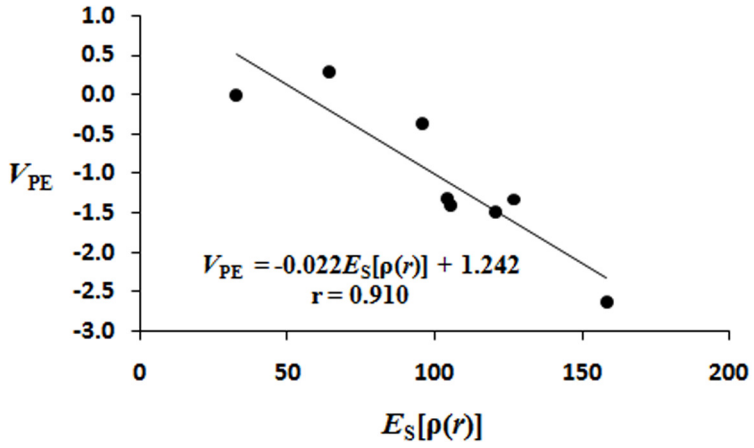

Figure 2.7 Correlation between $E_S[\rho(r)]$ and V_{PE}.

In Figure 2.8, values of V_o, V_o^{PE}, V_m, and V_p for all the substituents are compared to show the ability of molecular fragment approach and free model experiment. V_m and V_p values show similar substituent effect pattern as they are not affected by proximity effect whereas V_o is highly deviated from the corresponding V_m and V_p values. The proximity effect corrected V_o^{PE} parameter shows nearly the same substituent effect trend to those of V_m and V_p. Thus, it is clear that V_o^{PE} represents the through-bond electronic effect similar to V_m and V_p. Further, the *ortho* electronic nature of V_o^{PE} is validated by finding a linear correlation between V_o^{PE} and Exner's polar effect parameters (polar effects transmitted through bonds derived by approximating *ortho* and *para* effects are same) where a correlation coefficient

Table 2.3 V_{min} based parameters for the quantification of proximity effect. All values in kcal/mol.

Substituent	ϕ	$V_\phi{}^b$	V_c	V_t	V_c - V_t	V_{PE}	$V_o{}^{PE}$
$N(CH_3)_2$	16.28	-2.27	-12.39	-12.89	0.50	-1.78	-5.95
$NHCH_3$	0.01	0.00	-10.98	-13.15	2.17	2.17	-5.36
NH_2	0.93	-0.14	-10.04	-11.80	1.76	1.62	-4.77
$OCH(CH_3)_2$	4.22	-0.64	-11.04	-9.71	-1.33	-1.97	-4.07
OCH_2CH_3	-0.04	0.01	-10.13	-8.79	-1.35	-1.34	-3.45
OCH_3	0.16	-0.03	-9.72	-8.26	-1.46	-1.49	-2.91
NHOH	2.09	-0.32	-5.06	-7.01	1.95	1.63	-1.85
OH	0.01	0.00	1.00	-2.70	3.71	3.71	1.33
$C(CH_3)_3$	38.82	-4.55	-2.15	-4.06	1.91	-2.64	-2.30
$CH(CH_3)_2$	17.15	-2.38	-2.98	-4.03	1.05	-1.33	-1.71
CH_3	-0.03	0.00	-3.40	-3.70	0.29	0.30	-1.02
CH_2CH_3	8.12	-1.20	-2.92	-3.75	0.83	-0.37	-1.15
C_6H_5	21.78	-2.92	-2.85	-3.01	0.16	-2.76	-1.19
H	0.00	0.00	0.00	0.00	0.00	0.00	0.00
CH_2F	0.00	0.00	2.29	1.24	1.05	1.05	2.50
F	-0.03	0.00	-0.11	1.20	-1.31	-1.31	3.20
$CONH_2$	31.79	-3.95	8.21	5.29	2.92	-1.03	4.88
$COCH_3$	4.99	-0.75	5.20	3.75	1.44	0.69	4.12
Br	-0.03	0.00	1.71	2.97	-1.26	-1.26	5.10
Cl	0.00	0.00	1.81	3.25	-1.44	-1.44	2.93
CHO	0.14	-0.02	2.97	5.50	-2.53	-2.55	5.96
CF_3	18.84	-2.58	5.90	7.02	-1.12	-3.70	5.85
CN	-0.01	0.00	9.29	10.69	-1.40	-1.40	10.28
NO_2	42.65	-4.83	8.96	12.63	-3.67	-8.51	10.04

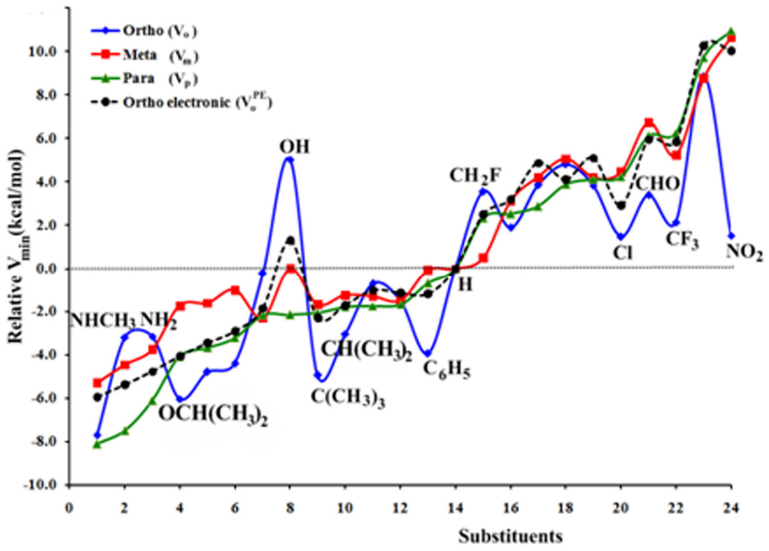

Figure 2.8 A comparative diagram representing the relative V_{min} of *ortho* (V_o), *meta* (V_m), and *para* (V_p) substituted benzoic acids, the proximity effect-corrected parameter (V_o^{PE}). Dotted horizontal line differentiates the electron activating and electron deactivating nature of substituents. For the numbering of substituents, see Table 2.1.

of 0.957 is obtained (Figure 2.9). In summary, the combination of both molecular fragment approach and free model experiment can exclusively quantify the proximity effects and V_o^{PE} can be considered as a proximity effect free *ortho* substituent constant.

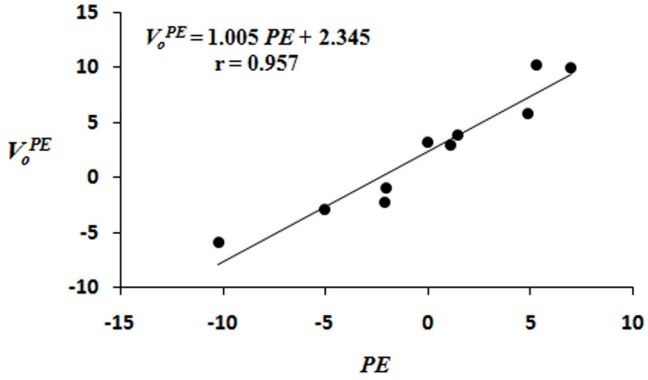

Figure 2.9 Correlation between V_o^{PE} and the Exner's PE values.

2.4.3 *Ortho*, *Meta* and *Para* Relationships

To address *ortho-para* relationships, Charton mentioned that "*only in an exceptional case is the ortho-electrical effect likely to have the same composition as the para-electrical effect"* [Charton 1969[a]]. On the other hand, some authors approximated that the *ortho* and *para* electronic effects are similar in magnitude. More than a decade ago, Pytela [Pytela 1996] described the ratio of *para*/*meta* substituent effects on the basis of a classification of substituents into three groups *viz.* donors, acceptors, and neutral ones. Recently, Exner and co-workers [Exner and Böhm 2002] studied these relationships by classifying the substituents into two categories *viz.*(i) those having lonepair of electrons at α-position and (ii) those having no lonepair at α-position and estimated that the *para*/*meta* ratio [Exner and Böhm 2002] is 1.20 for the second category. Using an isodesmic reaction approach Bohm *et al*. also derived the *ortho*/*para* ratio to a value of 0.81 for substituted benzoic acids [Bohm *et al*. 2004]. Very recently, Segurado *et al*. used an electrostatic modeling approach to benzoate anions and reported a value of 0.985 for *para*/*meta* ratio and a substantially small value of 0.397 for *ortho*/*para* ratio [Segurado *et al.* 2007]. All these treatments on substituent effects were based on the classification of substituents into different categories and a single line correlation leading to *para*/*meta*, *para*/*ortho*, and *ortho*/*meta* ratio was elusive. The single line correlation approach is more useful for comparing the general trend of substituent effects than the sophisticated approaches involving classification of substituents into different categories. Plots shown in Figure 2.8 strongly suggest that the proximity effect-corrected V_o^{PE} and the proximity effect-free V_m and V_p follow nearly a parallel trend and therefore these parameters may be used in a single line correlation approach to compare the substituent effects. We find that $V_p = 1.108\ V_m$ (r is 0.958), $V_p = 1.042\ V_o^{PE}$ (r is 0.972), and $V_o^{PE} = 1.047\ V_m$ (r is 0.969), respectively where the y-intercept is set as zero. Therefore, the ratios

para:*meta*, *para*:*ortho* and *ortho*:*meta* electronic substituent effect are 1.108:1, 1.042:1 and 1.047:1, respectively and electronic substituent effect follow the order *para* > *ortho* > *meta*.

2.4.4 Additive Nature of Substituent Effects

Additive nature of substituent effects arises when the total substituent effect observed in a multiple substituted compound is equal to sum of the effect produced by the individual substituents. For example, in the case of saturated hydrocarbons, the total inductive effect observed by the multiple substituents is the sum of inductive effect of individual substituents [Suresh *et al*. 2008]. In several reaction series, the activation energy of a multiple substituted compound is expressed in terms of individual contribution of substituents [Jones and Robinson 1950, Shorter and Stubbs 1949]. In the present work, the additive nature of substituent effects is analyzed by using the V_{min} approach through a representative set of substituents *viz*. NH_2, OH, CH_3, Cl, and CN. The selected systems and the notation of the structures are shown in Scheme 2.1.

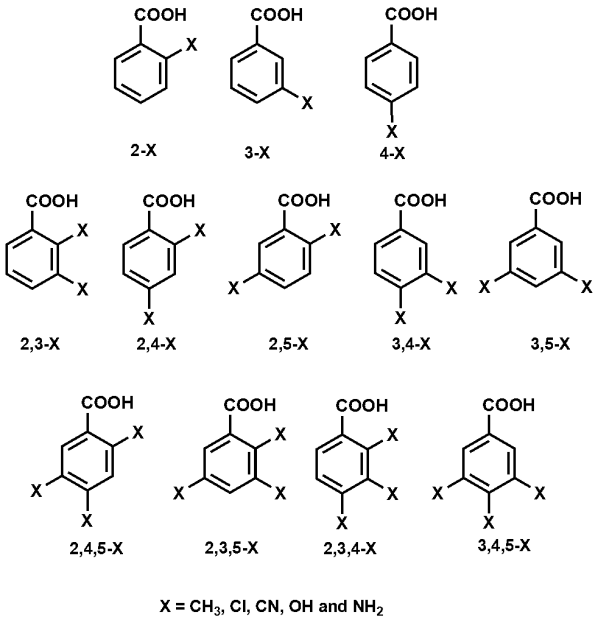

Scheme 2.1 Substituted systems considered for testing the additive nature of substituent effects.

In the multiple substituted systems, the calculated relative V_{min} with respect to 'X = H' is designated as V_{cal} and the predicted relative V_{min} is designated as V_{pred}. The V_{cal} and V_{pred} observed on the OH moiety of the COOH for all the structures are presented in Table 2.4.

Table 2.4 V_{cal} and V_{pred} values (in kcal/mol) are presented for mono and multiple substituted benzoic acids.

System	V_{cal}	V_{pred}[a]	System	V_{cal}	V_{pred}	System	V_{cal}	V_{pred}
2-Cl	3.75	-	2,3,4-Cl	10.08	12.47	2,4,5-OH	1.05	2.88
3-Cl	4.47	-	2,3,5-Cl	11.06	12.69	3,4,5-OH	-3.58	-2.13
4-Cl	4.25	-	2,4,5-Cl	10.46	12.47	2,3-NH_2	-4.22	-6.92
2- CH_3	-0.72	-	3,4,5-Cl	10.56	13.19	2,4- NH_2	-8.11	-9.28
3- CH_3	-1.30	-	2,3-CH_3	-0.54	-2.02	2,5- NH_2	-4.57	-6.92
4- CH_3	-1.76	-	2,4- CH_3	-0.74	-2.48	3,4- NH_2	-7.25	-9.88
2-OH	5.03	-	2,5- CH_3	0.06	-2.02	3,5- NH_2	-5.41	-7.52
3-OH	0.02	-	3,4- CH_3	-0.96	-3.06	2,3,4-NH_2	-9.24	-13.04
4-OH	-2.17	-	3,5- CH_3	-2.28	-2.60	2,3,5-NH_2	-5.14	-10.68
2- NH_2	-3.16	-	2,3,4- CH_3	-4.79	-3.78	2,4,5-NH_2	-8.21	-13.04
3- NH_2	-3.76	-	2,3,5- CH_3	-3.41	-3.32	3,4,5-NH_2	-7.40	-13.64
4- NH_2	-6.12	-	2,4,5- CH_3	-1.59	-3.78	2,3-CN	17.10	17.67
2-CN	8.88	-	3,4,5- CH_3	-1.84	-4.36	2,4-CN	17.55	18.59
3-CN	8.79	-	2,3-OH	5.49	5.05	2,5-CN	16.72	17.67
4-CN	9.71	-	2,4-OH	2.94	2.86	3,4-CN	17.68	18.50
2,3-Cl	7.34	8.22	2,5-OH	3.40	5.05	3,5-CN	17.53	17.58
2,4-Cl	7.72	8.00	3,4-OH	-2.45	-2.15	2,3,4-CN	24.23	27.38
2,5-Cl	7.81	8.22	3,5-OH	2.81	0.04	2,3,5-CN	24.05	26.46
3,4-Cl	7.64	8.72	2,3,4-OH	3.45	2.88	2,4,5-CN	23.92	27.38
3,5-Cl	8.74	8.94	2,3,5-OH	3.78	5.07	3,4,5-CN	23.98	27.29

[a] V_{cal} and V_{pred} of monosubstituted systems are same and not included in correlation shown in Figure 2.10.

V_{pred} values are calculated by adding the of total individual substituent effects that are presented in the multiple substituted compound. For example, the V_{pred} of 2,3,5-methyl benzoic acid can be calculated as V_{pred} (2,3,5-CH_3) = V_{cal} (2-CH_3) + V_{cal} (3-CH_3) + V_{cal} (5-CH_3) = -0.72 -1.30 -1.30 = -3.32 kcal/mol and the actual V_{cal} is -3.41 kcal/mol. The V_{pred} and the V_{cal} showed an excellent linear correlation (Figure 2.10) indicating that the substituent

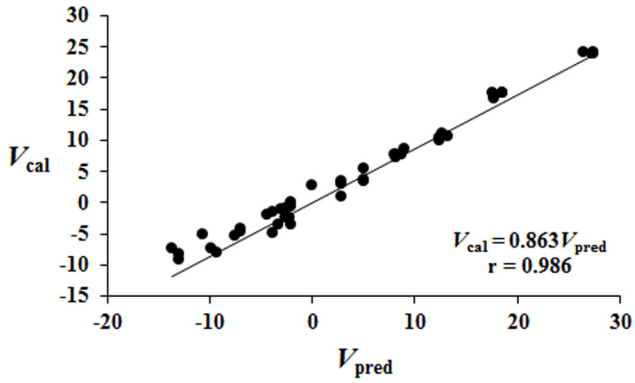

Figure 2.10 Correlation between V_{cal} and V_{pred}.

effects largely follow an additive rule. However, this additive rule is not perfect as the V_{cal} is 0.863 times to the V_{pred} and the majority of the systems showed that the difference between V_{pred} and V_{cal} is less than 2 kcal/mol. In general, for electron-withdrawing groups, the actual electron deactivation is less than the expected value. Similarly, for electron donating groups, the actual electron activation is less than the expected value. It may be noted that a perfect additive rule cannot be expected because in multiple substitution when two groups occupy adjacent positions (e.g. 2,3,4-X and 3,4,5-X) significant proximity effects may operate and this was pointed out earlier by Jaffe [Jaffé 1953].

Part B: Quantification of Substituent Resonance Effect

2.5 Introduction

Resonance effect is one of the most widely used qualitative concept in chemistry [Exner and Bohm 2000]. Though it is not considered as an observable property, its use is wide spread to interpret molecular stability, reactivities of conjugated molecules [Silva 2009], rationalizing hydrogen bonding [Krygowski and Zachara-Horeglad 2009, Liu *et al.* 2008] and in understanding the coordination of ligands to metals [Ott *et al.* 2009]. Substituents exhibit profound influence on the molecular properties of attached molecular units and the resonance contribution of a substituent is quantified as resonance constant (σ_R) [Krygowski *et al.* 2004, Krygowski and Stepien 2005]. Taft *et al*. introduced the dual substituent parametric (DSP) equation ($\sigma_p = \sigma_I + \sigma_R$) to derive the σ_R [Krygowski and Stepien 2005, Taft 1953]. However, Exner *et al*. found that the validity of DSP equation is limited as the acceptor substituents are properly not expressed by σ_R and suggested two different resonance scales for both acceptors and donors [Exner and Böhm 2007]. Several scales have been proposed as an alternative to resonance constants; based on infrared intensities (IR) [Angelelli *et al.* 1969, Brownlee *et al.* 1974, Katritzky and Topsom 1977], NMR chemical shifts [Taft and Lewis 1959, Taft *et al.* 1963], and isodesmic reaction energies [Exner and Bohm 2000, 2002, 2005]. The energies of substituent resonance effects turned out to be an unsatisfactory scale [Exner and Bohm 2000, Krygowski and Stepien 2005], IR scale requires a detailed spectral analysis [Palat Jr *et al.* 2001]. Thus, to evaluate substituent resonance effect, an easy, reliable and efficient method through an observable molecular property is yet to be established. Since the substituent resonance effect depends on the extent of interaction between substituent and reaction centre [Niwa 1989], a resonance scale must also interpret accurately the electron-donating as well as electron-withdrawing ability of the substituent. Previous work has shown that MESP is an

excellent descriptor to interpret the substituent effects [Gadre and Suresh 1997, Galabov *et al*. 2006, Gross *et al*. 2001, Mathew *et al.* 2007, Suresh and Gadre 1998, 2007]. Since MESP is an experimentally observable property [Naray-Szabo and Ferenczy 1995] and intimately related to the electron distribution, the use of MESP to quantify the resonance effect is highly desirable.

2.6 Computational Details

Fifty mono substituted benzenes are selected to quantify the substituent resonance effect. All these systems are optimized at the B3LYP/6-31G(d,p) level of theory. The MESP is calculated at B3LYP/6-31G(d,p) level [Becke 1993]. The MESP at a particular nucleus A can be calculated using the formula,

$$V(R_B) = \sum_{A \neq B}^{N} \frac{Z_A}{|R_B - R_A|} - \int \frac{\rho(r')d^3r'}{|R_B - r'|} \qquad \text{(Eq. 2.4)}$$

In the above equation, Z_A represents the nuclear charge, $\rho(r)$ is the electron density of the molecule, r' is the dummy integration variable. The equation contains summation over all the atomic nuclei which are treated as positive point charges as well as integration over the continuous distribution of the electronic charge.

2.7 Results and Discussion

In Figure 2.11, the MESP isosurfaces of benzene, flourobenzene, aniline and benzonitrile are shown to illustrate the effect of substituent over the π-region of various carbon atoms of the phenyl ring. In benzene, the D_{6h} symmetry guarantees equal distribution of MESP in all the carbon atoms. In fluorobenzene and aniline, the most negative-valued MESP or the MESP minimum (V_{min}) is observed near the *para* carbon whereas in benzonitrile V_{min} is observed near the *meta* carbons. V_{min} also indicate electron rich character

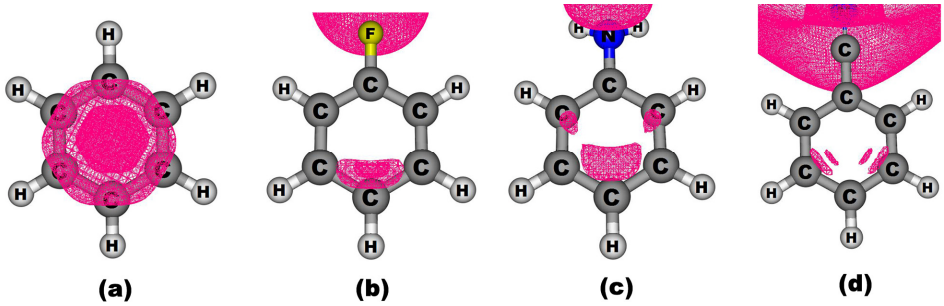

Figure 2.11 MESP isosurfaces of mono substituted benzenes (C_6H_5X). (a) X = H (b) X = F (c) X = NH_2 (d) X = CN. The isosurface values in kcal/mol are -16.32, -12.24, -23.03 and -2.95, respectively for H, F, NH_2 and CN substituents.

over the respective carbon atoms. In general, when an electron-donating substituent is attached to phenyl ring, the region close to *ortho* and *para* carbons is more electron rich [Roberts and Moreland 1953] than the vicinity near *meta* whereas in the case of electron withdrawing substituents *meta* carbons are the most electron rich (Scheme 2.2). Similarly,

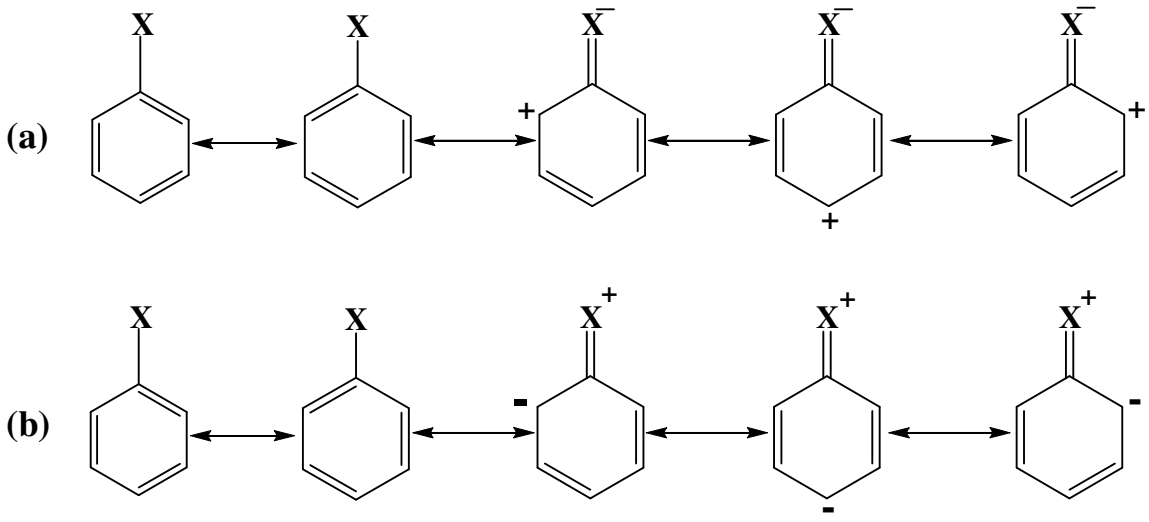

Scheme 2.2 Canonical structures with charge separation are shown for substituted benzene. (a) X is an electron-withdrawing substituent showing the delocalization of positive charge over the aromatic nucleus (b) X is an electron donating substituent showing the delocalization of negative charge over the aromatic nucleus.

the features observed over π-region of C_6H_5X are also reflected at the nuclei of carbon atoms of phenyl ring. The MESP at *meta* carbon atom (V_m^N) is more negative than the MESP at *para* carbon atom (V_p^N) for electron withdrawing substituent and V_p^N is more negative than V_m^N for electron donating substituent. For instance, NH_2 shows V_m^N value of -9253.95 kcal/mol and V_p^N value of -9259.47 kcal/mol whereas CN shows V_m^N value of -9232.74 kcal/mol and V_p^N value of -9231.61 kcal/mol. It may be noted that the substituent effect on the *meta* carbon is primarily due to inductive effect ($\rho_I\sigma_I = 0.86\rho\sigma_m$) [Holtz and Stock 1964] while the substituent effect on comprises of both resonance and inductive effects [Brownlee *et al.* 1965]. Thus, difference between V_p^N and V_m^N can be primarily due to resonance contribution of 'X'. Roberts and Moreland reported that inductive substituent effect is nearly same on all the *para* carbon carbons of aromatic ring [Roberts and Moreland 1953]. Following this argument, we define the MESP based resonance constant (σ_R^v) as $V_p^N - V_m^N$. The V_p^N and V_m^N values are evaluated for a set of fifty monosubstituted benzenes and the corresponding values are presented in Table 2.5. Interestingly, substituents classified as '*ortho-para* directing' in electrophilic substitution reactions showed negative sign for σ_R^v and the rest (*meta* directing) showed positive sign. The linear correlation between σ_R^v and σ_R^o (resonance constants derived from IR [Katritzky and Topsom 1977] shown in Figure 2.12 suggests that MESP is a vital tool for the estimation of the resonance effect of substituents and serves as alternate measure of the resonance constants.

Table 2.5 Molecular electrostatic potential (MESP) at the *meta* (V_m^N) and *para* (V_p^N) carbons of monosubstituted benzenes and MESP derived resonance constants (σ_R^v). V_m^N and V_p^N value are in au and σ_R^v in kcal/mol.

Substituent	V_m^N	V_p^N	$\sigma_R^{o\,a}$	σ_R^v	Substituent	V_m^N	V_p^N	$\sigma_R^{o\,a}$	σ_R^v
H	-14.7409	-14.7409	0.00	0.00	Br	-14.7251	-14.7279	-0.23	-1.76
CH_3	-14.7440	-14.7454	-0.10	-0.88	CHO	-14.7237	-14.7191	0.24	2.89
C_2H_5	-14.7448	-14.7466	-0.10	-1.13	$COCH_3$	-14.7301	-14.7254	0.22	2.95
$CH(CH_3)_2$	-14.7442	-14.7451	-0.12	-0.56	$CONH_2$	-14.7319	-14.7284	0.13	2.20
$C(CH_3)_3$	-14.7447	-14.7460	-0.13	-0.82	$CSNH_2$	-14.7279	-14.7244	-	2.20
$CH=CH_2$	-14.7392	-14.7390	-0.05	0.13	COOH	-14.7283	-14.7241	0.29	2.64
C_6H_5	-14.7395	-14.7400	-0.10	-0.31	$COOCH_3$	-14.7307	-14.7274	0.16	2.07
CH_2OH	-14.7440	-14.7459	-0.06	-1.19	CN	-14.7133	-14.7115	0.09	1.13
CH_2SH	-14.7366	-14.7368	-	-0.13	NO_2	-14.7094	-14.7071	0.17	1.44
CH_2Cl	-14.7306	-14.7300	-0.03	0.38	CF_3	-14.7226	-14.7217	0.10	0.56
NH_2	-14.7471	-14.7559	-0.47	-5.52	COCl	-14.7139	-14.7091	0.21	3.01
$NHCH_3$	-14.7496	-14.7584	-0.52	-5.52	Li	-14.7804	-14.7776	0.14	1.76
$N(CH_3)_2$	-14.7515	-14.7602	-0.53	-5.46	$SICl_3$	-14.7175	-14.7145	0.09	1.88
N=NH	-14.7171	-14.7177	-	-0.38	$Si(CH_3)_3$	-14.7437	-14.7416	0.03	1.32
$NHCOCH_3$	-14.7368	-14.7438	-0.42	-4.39	PH_2	-14.7354	-14.7369	-0.05	-0.94
OH	-14.7395	-14.7466	-0.40	-4.46	$P(CH_3)_2$	-14.7401	-14.7413	-0.08	-0.75
OCH_3	-14.7420	-14.7487	-0.43	-4.20	$NHNH_2$	-14.7506	-14.7598	-0.49	-5.77
OCH_2CH_3	-14.7430	-14.7498	-0.44	-4.27	SO_2Cl	-14.7131	-14.7113	0.11	1.13
$OCH(CH_3)_2$	-14.7435	-14.7518	-0.43	-5.21	$SOCH_3$	-14.7259	-14.7258	-0.07	0.06
OC_6H_5	-14.7391	-14.7464	-0.36	-4.58	BCl_2	-14.7237	-14.7168	0.30	4.33
$OCOCH_3$	-14.7333	-14.7374	-0.24	-2.57	NO	-14.7152	-14.7105	0.25	2.95
SH	-14.7328	-14.7371	-0.19	-2.70	CH_2CHO	-14.7317	-14.7324	-0.11	-0.44
SCH_3	-14.7376	-14.7419	-0.25	-2.70	$CH_2CH_2CH_3$	-14.7440	-14.7451	-0.11	-0.69
F	-14.7284	-14.7346	-0.34	-3.89	CH_2Br	-14.7307	-14.7302	-0.02	0.31
Cl	-14.7248	-14.7281	-0.22	-2.07	CH_2OCH_3	-14.7449	-14.7450	-0.04	-0.06

[a] Values are taken from Ref. [Katritzky and Topsom 1977].

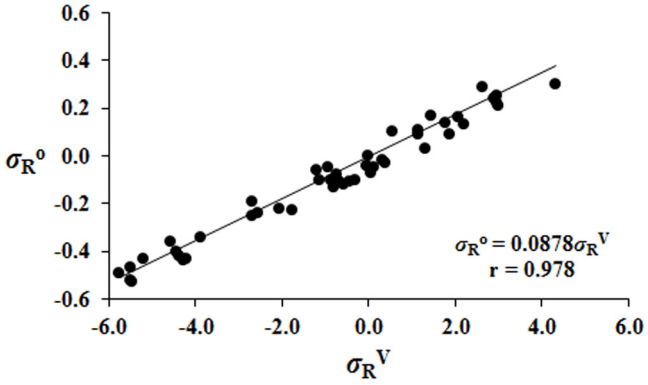

Figure 2.12 Correlation between the σ_R^o and MESP derived σ_R^v values.

The efficacy of σ_R^v is rigorously tested in substituted phenols by considering 26 substituents using three sets of isodesmic reactions (Scheme 2.3).

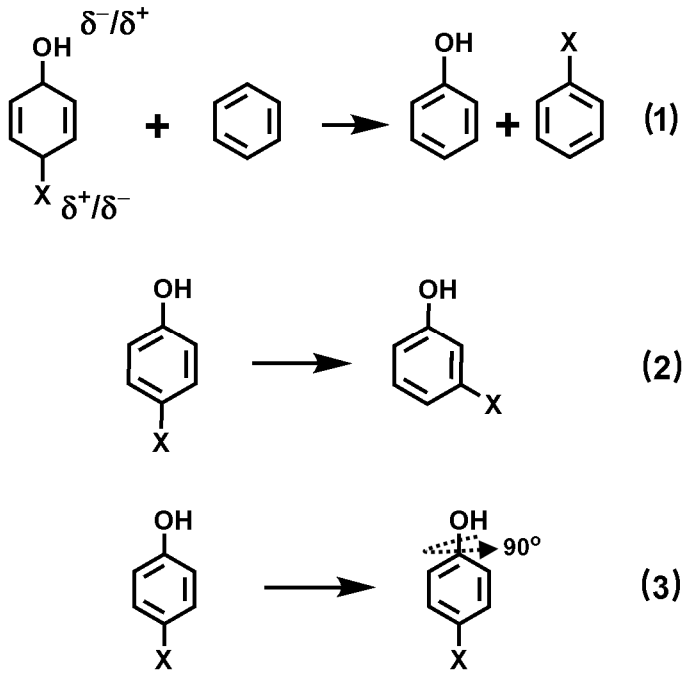

Scheme 2.3 Isodesmic reactions studied to validate the electrostatic scale of resonance effect. X = substituent.

The isodesmic reaction energies of the reactions, (1), (2), and (3) are designated as ΔE_1, ΔE_2 and ΔE_3, respectively. The reaction (1) quantifies energy component of the resonance contribution of 'X' with the OH. The correlation between ΔE_1 and σ_R^v (r = 0.988) illustrates the use of σ_R^v as a measure of substituent effect where the 'through conjugation effect' occurs between the reaction centre and the substituent (Figure 2.13a). Regarding isodesmic reaction (2), the *meta* substituent can interact with 'OH' mainly through inductive effect whereas the *para* substituent interacts with 'OH' through both inductive and resonance effects [Holtz and Stock 1964]. Therefore, ΔE_2 will serve as a good measure of resonance

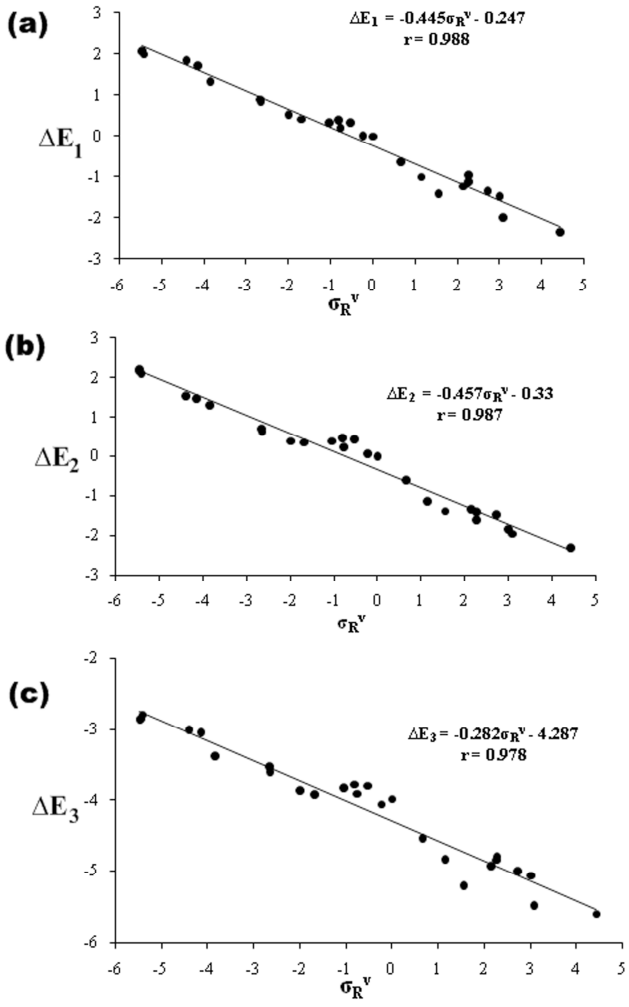

Figure 2.13 Dependence of isodesmic reaction energies and the MESP derived resonance constants (σ_R^v).

effect of 'X'. The linear correlation between ΔE_2 and σ_R^v (r = 0.987) strongly supports this argument and validates the use of MESP approach to estimate resonance effects (Figure 2.13b). The isodesmic reaction (3) corresponds to the rotation of OH group wherein the OH group is rotated by 90° with respect to the phenyl ring, the X...OH resonance interaction will be effectively removed and no significant change will occur to the inductive effect [Silva 2009]. The correlation of ΔE_3 with σ_R^v is linear with r = 0.978 (Figure 2.13c). Thus, three linear correlations of isodesmic reaction energies with σ_R^v, suggest that σ_R^v is a reliable measure of substituent resonance effect. The proposed electrostatic scale of substituent resonance effect is easy to compute and is expected to be useful in QSAR and QSPR studies of organic molecules.

Part C: Quantification of Through-bond and Through-space Effects

2.8 Introduction

The concept of substituent effects is widely used in chemistry for understanding the physicochemical and biological properties of a variety of substituted molecules [Fersner *et al.* 2009, Jaffé 1953, Krygowski and Stepien 2005]. In 1937, Hammett introduced an empirical equation, *viz*. log $(k/k_o) = \rho\sigma$ (where k and k_o are rate constants for the reactions of the substituted and unsubstituted compound, ρ is the reaction constant, and σ, the substituent constant) for throwing light on structure property correlations [Hammett 1937]. These σ-constants are known to be prone to failure in the case of molecules in which a strongly electron-withdrawing substituent is interacting with an electron-donating reaction centre and *vice-versa* [Hansch *et al.* 1991]. In 1953, Taft proposed a dual parametric equation, $\sigma_p = \sigma_I + \sigma_{R,}$ (where σ_I and $\sigma_{R,}$ represent the inductive and resonance effects of the substituents, respectively) by considering that the total substituent effect is a combination of inductive and resonance effects [Taft 1953]. A question naturally arising in this context is: *To what extent does a substituent contribute to inductive and resonance effects?* Several molecular models have been designed for the quantification of these effects, individually in terms of σ_I and $\sigma_{R,}$ respectively [Hansch *et al*. 1991, Katritzky and Topsom 1977, Roberts and Moreland 1953, Suresh *et al*. 2008]. The inductive effect is quantified successfully from the dissociation constants of bicyclooctane carboxylic acids and protonated quinuclidine derivatives, wherein the total substituent effect is considered as the sum of the through-space (TS) and through-bond (TB) effects [Hansch *et al*. 1991, Roberts and Moreland 1953]. In the case of saturated systems, the TS effect is termed as field effect which is purely electrostatic in nature and the

term inductive effect is employed for describing the TB effect [Galkin 1999]. Further, many groups have designed models to unravel the origin of TB and TS effects, reaching a general consensus that the TS effects dominates the TB ones [Adcock and Trout 1999, Bowden and Grubbs 1996, Charton 1999, Exner 1999, Nolan and Linck 2000]. Recently, Wheeler and Houk [Wheeler and Houk 2008, Wheeler and Houk 2009[a], Wheeler and Houk 2009[b]] also demonstrated the dominance of TS substituent effects. However, the separation and quantification of TB and TS effects has remained elusive. The TB and TS contributions varies significantly [Wheeler and Houk 2009[b]] depending upon the electronic nature of the substituent and hence their quantification is essential for a complete understanding of substituent effects. Thus, it is clear that a method is needed for the estimation of relative contributions of TB and TS effects.

In part A of this chapter, the use of MESP approach to quantify the proximity effects in *ortho* substituted benzoic acids, the additivity effect in multiple substituted benzoic acids is discussed. In part B and part C of this chapter, a MESP based method for the quantification of substituent resonance effect and through-bond and through-space effects, respectively was developed.

2.9 Methodology and Computational Details

An appraisal for the TB and TS substituent effects using MESP has been carried out on several model systems shown in Scheme 2.4. The molecules, **1a**-**3b** are chosen so as to cover adequate test cases for appraisal of the inductive (**1a**), inductive-resonance (**2a**, **3a**) and, through-space (**1b**, **2b** and **3b**) substituent effects. **1b**, **2b** and **3b** are derived from **1a**, **2a** and **3a**, respectively by removing the CC linkages between phenyl ring and substituent (X) which exclusively provide the models for TS effects. All these structures are optimized at B3LYP/6-31G(d,p) level [Becke 1993] and the MESP computations for all the systems in

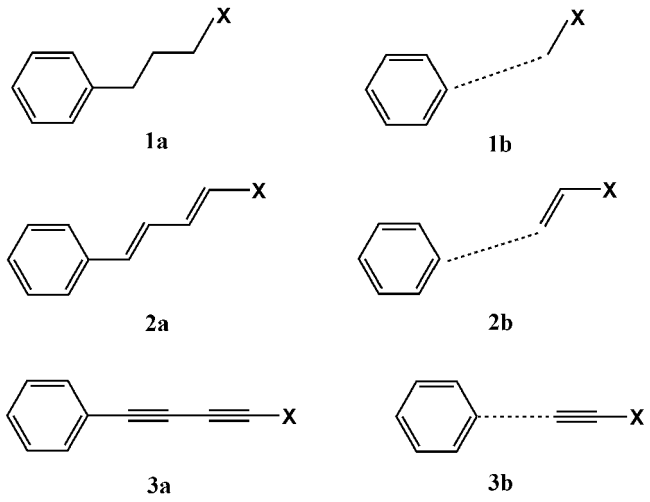

Scheme 2.4 Systems considered for the assessment of through bond (TB) and through space (TS) substituent effects. The TS interaction is shown with dotted lines.

their optimized geometries are also done at the same level of theory. Previous works [Gadre *et al.* 1995, Suresh *et al*. 2008, Suresh and Gadre 2007, Wheeler and Houk 2009[b]] demonstrate that the essential topographical features of MESP are rather insensitive to the basis set and B3LYP/6-31G(d,p) level of theory is adequate for a very good representation of substituent effects. Using the optimized geometries, the MESP is computed at the B3LYP/6-31G(d,p) level of theory using the Eq. 2.1. All the computations are carried out using Gaussian03 programme [Frisch *et al*.].

In **1b**, **2b**, and **3b** the newly added hydrogen atoms are optimized by fixing all other coordinates, the distance between 'H' atom of phenyl ring and the 'H' of the corresponding fragment (shown by dotted lines in Scheme 2.4) is in the range 3.254 - 3.301 Å, 1.902 - 1.907 Å, and 1.849 - 1.879 Å, respectively. In all the substituted systems, phenyl ring is used as a probe for observing MESP minimum (V_{min}). The relative V_{min} of the substituted molecule (substituent = X) with respect to the corresponding unsubstituted one, is denoted as ΔV_{min} which exclusively represents the total of TB and TS effects of substituent, X. Thus, for a particular substituent, a negative sign of ΔV_{min} is an indicator of the overall electron donating

nature, while a positive sign indicates the electron withdrawing nature . Further, the notation $\Delta\Delta V_{min}$ is employed for denoting the difference between the ΔV_{min} of the TB model (**1a**, **2a**, and **3a**) and the ΔV_{min} of the corresponding TS model (**1b**, **2b**, and **3b**). Since the ΔV_{min} of the TS model exclusively represents the TS effect, the $\Delta\Delta V_{min}$ could be considered as a faithful measure of the TB effect. Ten substituents, *viz.* $N(CH_3)_2$, NH_2, OCH_3, CH_3, H, F, Cl, CF_3, CN and NO_2 which exhibit hyperconjugation, electron donating and electron withdrawing effects, are considered for the present study.

2.10 Results and Discussion

Table 2.6 shows V_{min} values of systems **1a** and **1b**. In **1a**, the substituent of phenyl ring is $–CH_2CH_2CH_2CH_2$-X. It is a general thought that electronic effect of 'X' transmitted to the aromatic ring through the CC σ-bonds is inductive in nature [Katritzky and Topsom 1971]. When X = H, the V_{min} value is -19.26 kcal/mol. When the 'H' is replaced by CH_3, V_{min}

Table 2.6. V_{min} (in kcal/mol) obtained over the phenyl ring of systems **1a** and **1b**.

X	V_{min}(**1a**)	V_{min}(**1b**)	ΔV_{min}(**1a**)	ΔV_{min}(**1b**)	$\Delta\Delta V_{min}$(**1**)
$N(CH_3)_2$	-18.99	-17.33	0.27	0.21	0.06
NH_2	-19.21	-17.59	0.05	-0.05	0.10
OCH_3	-17.53	-16.60	1.74	0.94	0.79
CH_3	-19.35	-17.60	-0.09	-0.06	-0.03
H	-19.26	-17.54	0.00	0.00	0.00
F	-16.78	-15.41	2.48	2.13	0.35
Cl	-15.89	-14.94	3.37	2.60	0.77
CF_3	-15.86	-15.28	3.40	2.26	1.14
CN	-14.53	-13.67	4.73	3.87	0.86
NO_2	-14.40	-13.65	4.86	3.89	0.97

becomes deeper by 0.09 kcal/mol and this could be due to higher electron donating effect of the methyl group as compared to that of 'H'. Similarly, when X = NH_2, the V_{min} is 0.05 kcal/mol higher than that of X = H system, suggesting a slight electron withdrawing nature of -NH_2 group. Increasingly, more electron withdrawing effect is noticeable for -OCH_3, -F, Cl, CF_3 and -NO_2 as reflected by the respective MESP minimum values are -17.53, -16.78, -15.89, -15.86 and -14.40, kcal/mol.

For **1b** systems, 'X' does not have any through σ-bond interaction with phenyl ring, which means that the inductive effect is absent in these systems. Interestingly, V_{min} values of all the **1b** systems show nearly a parallel trend to that of their **1a** counterparts. Further, the V_{min} values of **1b** are seen less negative than the corresponding values of **1a** systems. To gain further insights into the electronic effects, we define the following three quantities.

$$\Delta V_{min}(\mathbf{1a}) = V_{min}(X) - V_{min}(H) \text{ for } \mathbf{1a} \text{ systems.}$$

$$\Delta V_{min}(\mathbf{1b}) = V_{min}(X) - V_{min}(H) \text{ for } \mathbf{1b} \text{ systems.}$$

$$\Delta\Delta V_{min}(\mathbf{1}) = \Delta V_{min}(\mathbf{1a}) - \Delta V_{min}(\mathbf{1b})$$

A similar trend exhibited by $\Delta V_{min}(\mathbf{1a})$ and $\Delta V_{min}(\mathbf{1b})$ means that substituent effect is very much present on the aromatic ring of **1b** system even though the substituent is not connected to the ring via a σ-bond. Thus, to justify this observation, substantial through-space effect must be invoked for **1a** and **1b** systems. If we consider the $\Delta V_{min}(\mathbf{1b})$ value as indicator of TS effects, the $\Delta\Delta V_{min}(\mathbf{1})$ brings out the TB effects and the values of these two quantities (Table 2.6) clearly suggest that the TB effects are quite small compared to the corresponding TS effects for these systems.

Prior work reported that it is difficult to distinguish the through bond inductive effect from the field effect as there is no way to correctly define these two phenomena by

experimental means [Exner 1999]. The IUPAC compendium of chemical terminology states that '*Ordinarily the inductive effect and the field effect are influenced in the same direction by structural changes in the molecule and the distinction between them is not clear. This situation has led many authors to include the field effect in the term 'inductive effect'*. The theoretical models (Scheme 2.4) brings out a clear distinction between the TB and TS effects. Our results support the view that the so-called 'inductive effect' reflects largely a field effect rather than pure through-bond electronic effect. In Figure 2.14, the correlation between the ΔV_{min}(**1a**) and ΔV_{min}(**1b**) clearly shows that the TS effects contribute to 79.6%, while the TB effects are only upto 20.4% of the total substituent effect in **1a**. In general all the substituents show the TS effect as evidenced by the ΔV_{min}(**1b**) values and among them the 'F' substituent has the highest (85.9%) TS effect.

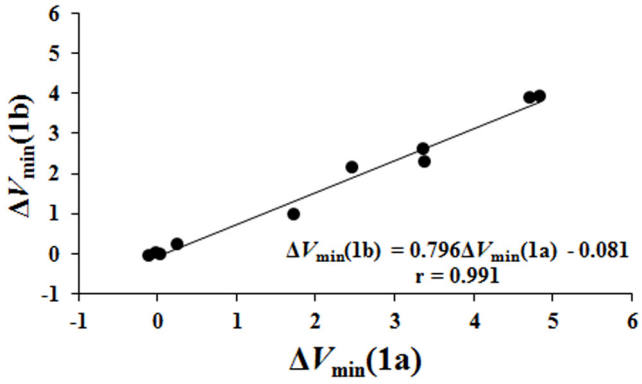

Figure 2.14 Correlation between ΔV_{min}(**1a**) and ΔV_{min}(**1b**).

Further, in order to quantify the transmission of substituent effect through double and triple bonds, **2a** and **3a** systems are examined using V_{min}. In **2a**, the total substituent effect is a combination of both through bond inductive, resonance effect as well as TS effect whereas in **1a**, it is only inductive/field effect [Hansch *et al*. 1991]. The V_{min} values for **2a** are reported in Table 2.7. The electron-donating and withdrawing ability of substituent is remarkable in **2a** compared to that of **1a**. For instance in **2a**, NH_2 shows a ΔV_{min} of -6.89 kcal/mol and NO_2 shows ΔV_{min} of 10.94 kcal/mol whereas in **1a**, the ΔV_{min} values of NH_2 and NO_2 are 0.05, and

4.86 kcal/mol, respectively. In Figure 2.15, the correlation between the V_{min}(**2a**) and the σ_p values strongly suggests that the electron donating and withdrawing nature of substituent is well-represented by the MESP topographical feature over the aromatic ring.

Table 2.7. The V_{min} (in kcal/mol) over the phenyl ring of systems **2a** and **2b**.

X	V_{min}(**2a**)	V_{min}(**2b**)	ΔV_{min}(**2a**)	ΔV_{min}(**2b**)	$\Delta\Delta V_{min}$(**2**)
$N(CH_3)_2$	-23.54	-19.90	-7.81	-2.54	-5.27
NH_2	-22.62	-19.79	-6.89	-2.43	-4.46
OCH_3	-19.90	-18.45	-4.17	-1.09	-3.08
CH_3	-17.45	-18.04	-1.72	-0.68	-1.04
H	-15.73	-17.36	0.00	0.00	0.00
F	-15.14	-15.86	0.59	1.50	-0.91
Cl	-13.04	-15.07	2.69	2.29	0.40
CF_3	-10.21	-14.11	5.52	3.25	2.27
CN	-7.18	-12.64	8.55	4.72	3.83
NO_2	-4.79	-11.95	10.94	5.41	5.53

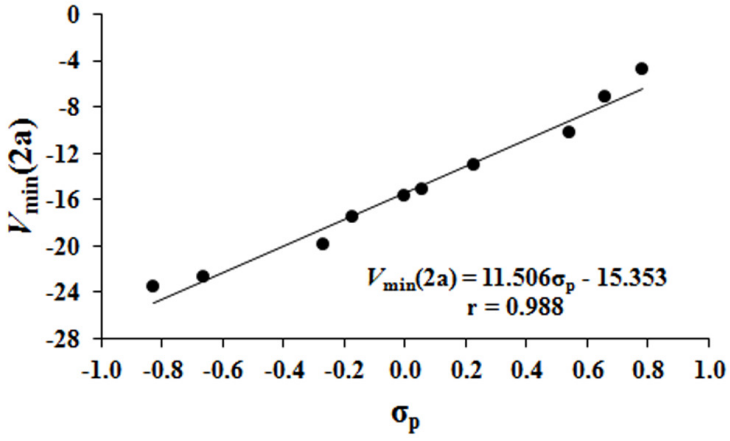

Figure 2.15 Correlation between the V_{min} values of **2a** and the σ_p.

In **2b**, through bond connection between 'X' and the probe phenyl ring is absent. Though V_{min}(**2a**) and V_{min}(**2b**) values show a parallel trend, a large variation in ΔV_{min} is noticed in case of **2a** over **2b**, indicating that the substituent effect transmitted through double bonds is much more effective than the corresponding through-space transmission. This observation can be readily understood from the comparison of ΔV_{min}(**2b**)and $\Delta\Delta V_{min}$(**2**) values. An electron donating TB effect dominates in the case of substituents $N(CH_3)_2$, NH_2, OCH_3 and CH_3. Similarly, NO_2, CN, and CF_3 substituents are noticeable for powerful electron withdrawing TB effect (Table 2.7). Interestingly, when X = F, the ΔV_{min}(**2a**) is 0.59 kcal/mol and ΔV_{min}(**2b**) is 1.50 kcal/mol indicating the dominance of through-space electron withdrawing effect in the latter than the through bond electron withdrawing effect in the former. A striking evidence in favor of this fact was brought out from Figure 2.16; the TS effect is only 44.9% of the total substituent effect for **2a** systems. It may be noted that in the case of **1a**, TS effect is 79.6% of the total substituent effect while it is only 44.9% in the case of **2a** which strongly suggests that TS effect in **1a** is nearly twice to that of **2a**. To summarize, TS effect is more dominant in **1a** than TB effect whereas in **2a** TB as well as TS effects operates in 1.00: 0.81 ratio.

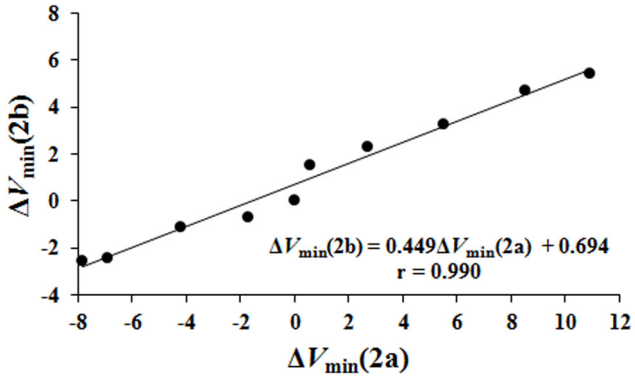

Figure 2.16 Correlation between ΔV_{min}(**2a**) and ΔV_{min}(**2b**).

V_{min} values of the triple-bonded systems **3a** and **3b** are reported in Table 2.8. When X = H, the V_{min}(**3a**) is -10.37 kcal/mol while the V_{min}(**2a**) is -15.73 kcal/mol, clearly showing

the inherent electron seeking power of the triple bonded moiety. Thus, as expected, the V_{min}(**3a**) shows a less negative value than the V_{min}(**2a**). Figure 2.17 shows the correlation between V_{min} of **3a** systems with the σ_p values. Most importantly, a similar magnitude of substituent effect is transmitted in **2a** and **3a** as evidenced from the slopes of the plots of V_{min} and σ_p (slope for **2a** is 11.506 and slope of **3a** is 11.283, *cf.* Figures 2.15 and 2.17). The V_{min}

Table 2.8. V_{min} (in kcal/mol) obtained over the phenyl ring of systems **3a** and **3b**.

X	V_{min}(**3a**)	V_{min}(**3b**)	ΔV_{min}(**3a**)	ΔV_{min}(**3b**)	$\Delta\Delta V_{min}$(**3**)
$N(CH_3)_2$	-18.39	-18.46	-8.02	-2.90	-5.12
NH_2	-17.21	-18.59	-6.84	-3.03	-3.81
OCH_3	-15.58	-17.46	-5.21	-1.90	-3.31
CH_3	-13.20	-16.90	-2.83	-1.34	-1.49
H	-10.37	-15.56	0.00	0.00	0.00
F	-10.93	-15.17	-0.56	0.39	-0.95
Cl	-10.00	-14.82	0.37	0.74	-0.37
CF_3	-4.91	-12.59	5.46	2.97	2.49
CN	-1.79	-11.06	8.58	4.50	4.08
NO_2	-0.46	-10.82	9.91	4.74	5.17

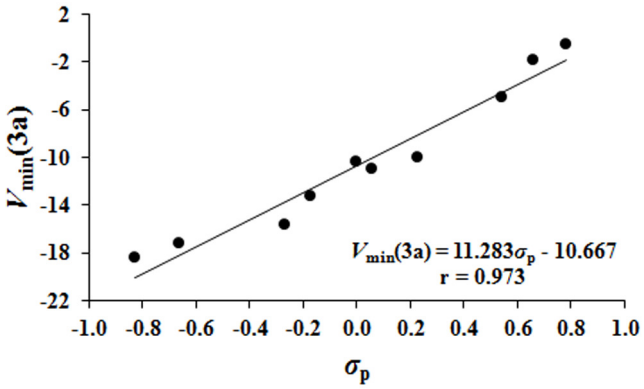

Figure 2.17 Correlation between the V_{min} of **3a** and the corresponding σ_p values.

of **3b** shows a trend similar to that of their counterparts in **3a**, except for the case of 'F'. Interestingly, 'F' shows electron donating nature in **3a** and electron withdrawing nature in **3b**; which may be due to the fact that in the former, fluorine lone pair is in direct conjugation with the phenyl ring through triple bond favoring the electron donation whereas in the latter through-space electron withdrawal effect dominate the TB effect. This fact is reflected by the ΔV_{min} values of 'F' substituent, *viz*. ΔV_{min}(**3a**) is -0.56 kcal/mol and ΔV_{min}(**3b**) is 0.39 kcal/mol. The correlation between ΔV_{min} of **3a** and **3b** systems is shown in Figure 2.18, bringing out that TB effect contributes about 54.3% while TS effect contributes about 45.7% of the total substituent effect in **3a**.

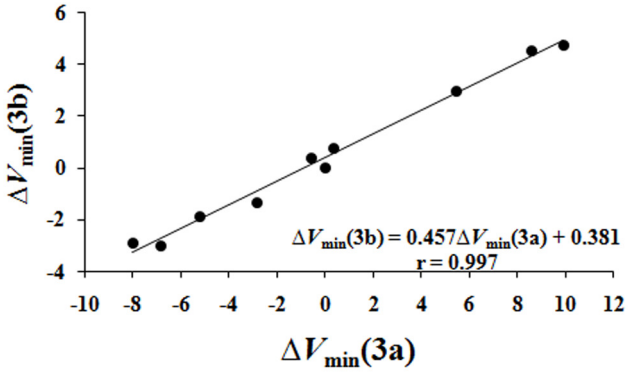

Figure 2.18 Correlation between ΔV_{min}(**3a**) and ΔV_{min} (**3b**).

Therefore, we can conclude that TS effects dominate substantially over the TB effects in **1a** systems and the TB effects slightly dominate the TS effects in **2a** and **3a** systems. Further, the slope for the V_{min} versus σ_p correlation for **2b** systems is 5.171 and the slope for a similar correlation for **3b** systems is 5.162, suggesting that the TB and TS effects in **2b** and **3b** systems are also of similar magnitude. In Table 2.9, the quantified TB and TS effects for the systems studied in this work is summarized. Thus, this work introduces a new and simple

V_{min} methodology for the quantification of TB and TS effects for prototypical systems wherein the substituent effect transmitted through single, double and triple bonds.

Table 2.9 Quantified proportions of TB and TS effects for the systems **1a**, **2a** and **3a.**[a]

System	TB effect	TS effect[a]
1a	20.4%	79.6%
2a	55.1%	44.9%
3a	54.3%	45.7%

[a] Total substituent effect is approximated as a combination of TB and TS effects.

2.11 Conclusions

In part A of this chapter, MESP minimum (V_{min}) at the lone-pair region of OH on the functional group COOH of substituted benzoic acids was proved to be an excellent descriptor to study the substituent effects. The V_{min} can be used as an alternate measure for Hammett substituent constants, σ_m, σ_p. Further, we have provided a molecular fragment approach (Figure 2.5) in conjunctional with a free rotation of COOH group on the benzoic acid to quantify the *ortho* proximity effect. The total proximity effect has been separated into electronic and steric contributions, the steric effects of the substituents are in accord with the Taft's steric substituent constants. The V_{min} approach provided a way to understand the substituent effects without categorizing the substituents in to different classes [Exner and Böhm 2002, Pytela 1996] and also offered mutual relationships among the *ortho*, *meta*, and *para* systems where the order of substituent effect is *para* > *ortho* > *meta*. Multiple substituted systems can also be studied using the V_{min} approach and it is found that substituent effects follow largely (86.3 %) an additive rule. Further, in part B of this chapter, an efficient way for evaluating the substituent resonance effect using MESP is provided.

In part C of this chapter, a proposal for the separation and quantification of TB and TS effects is introduced and tested employing the MESP topography. The deepest MESP minimum on the aromatic ring (V_{min}) is used as a probe for monitoring these effects for a variety of substituents. It is clearly demonstrated that when a substituent is attached to saturated alkyl chain, TS effect (estimated to be typically 79.6%) clearly dominates TB effect (20.4%). On the other hand, in the case of unsaturated side chains, TB effect is ~55% and TS effect is only ~45%. The present approach based on V_{min} for quantifying the TB and TS effects, provides a new way of understanding substituent effects and is expected to be highly useful for a variety of chemical phenomenon.

Chapter 3

Quantification and Characterization of Substituent Effects in Cation-π Interactions

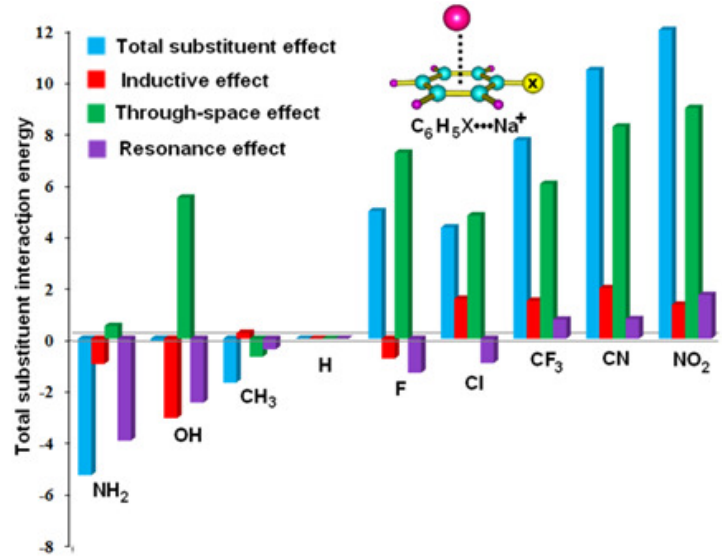

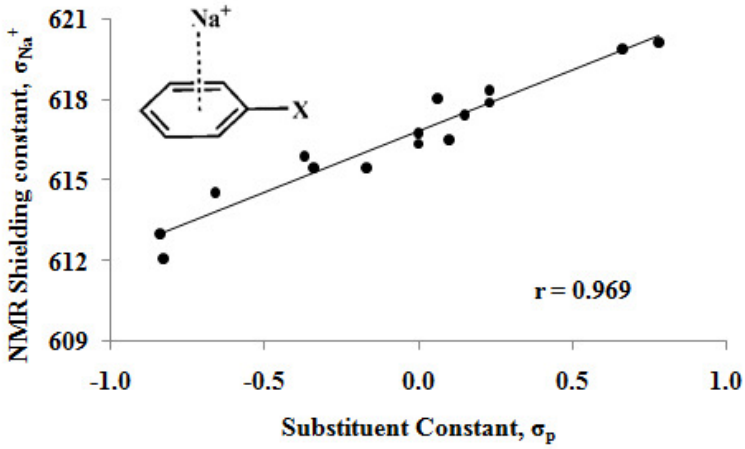

Chapter 3

3.1 Abstract

*The quantification of inductive (I), resonance (R) and through-space (TS) effects of a variety of substituents (X) in cation-π complexes of the type $C_6H_5X\cdots Na^+$ is achieved by modeling $C_6H_5\text{-}(\Phi_1)_n\text{-}X\cdots Na^+$ (**1**), $C_6H_5\text{-}(\Phi_2)_n\text{-}X\cdots Na^+$ (**2**), $C_6H_5\text{-}(\Phi_{2\perp})_n\text{-}X\cdots Na^+$ (**2'**) and $C_6H_6\cdots HX\cdots Na^+$ (**3**), where Φ_1 = -CH_2CH_2-, Φ_2 = -CHCH-, $\Phi_{2\perp}$ indicates that Φ_2 is perpendicular to the plane of C_6H_5, and n = 1–5. The cation-π interaction energies of **1**, **2**, **2'**, and **3**, relative to X = H are fitted to polynomial equations in n have been used to extract the substituent effect E_0^1, E_0^2, $E_0^{2'}$ and E_0^3 for n = 0, the $C_6H_5X\cdots Na^+$ systems. E_0^1 is the combination of inductive (E_I) and through-space (E_{TS}) effects while the difference (E_0^2–$E_0^{2'}$) is purely resonance (E_R) and E_0^3 is attributed to the TS contribution (E_{TS}) of the X. The total interaction energy of $C_6H_5X\cdots Na^+$ is nearly equal to the sum of E_I, E_R and E_{TS} which brings out the unified view of cation-π interaction in terms of I, R and TS effects. The electron withdrawing substituents contribute largely by TS effect whereas the electron donating substituents contribute mainly by resonance effect to the total cation-π interaction energy.*

Further, to identify cation-π interactions in terms of NMR parameters, a detailed NMR analysis has been carried out on the cation-π complexes, $C_6H_5X\cdots M^+$ (M^+ = Li^+, Na^+, K^+, NH_4^+). Good linear relationship between the calculated isotropic nuclear magnetic shielding constants (σ) and the Hammett substituent constant σ_p is established. This correlation suggests that the substituent effects in cation-π interactions can be quantified by NMR experiments. Irrespective of the electron donating and withdrawing nature of X, meta carbons and all the hydrogens attached to the phenyl ring are always deshielded and this property is useful for detecting cation-π interaction through NMR experiments. The σ-scan plots revealed that the deshielding effect of the cation on the aromatic ring is significant even at large cation-π distance (~ 4.5 Å).

Chapter 3

Part A: Quantification Substituent Effects in Cation-π Interactions

3.2 Introduction

Cation-π interaction is recognized as an important noncovalent binding force in structural biology [Ma and Dougherty 1997]. The use of cation-π interactions is significantly growing in the design of molecular materials [Mo and Yip 2009], supramolecular assembly [Hamada *et al.* 2006], stereoselective synthesis [Yamada 2007], and synthetic receptors [Meadows *et al.* 2001]. The interaction of a cation with π-system can be greatly affected by the nature of attached substituent (X) due to inductive (I), resonance (R) and through-space (TS) effects. Therefore, quantification of such effects in cation-π interactions is highly important to fine tune the interactive behavior between π-system and cation. Hunter *et al*. constructed a chemical double mutant cycle to quantify free energy change associated with the interaction between pyridinium cation and substituted aromatic ring and showed that the cation-π binding is very sensitive to electronic nature of the substituent (X) [Hunter *et al.* 2002]. Based on the correlation between interaction energy of $C_6H_5X\cdots Na^+$ systems and Hammett's σ_m constants, Dougherty and co-workers [Mecozzi *et al.* 1996[a]] reported that the inductive effects are much more relevant than the resonance effects. Recently, Wheeler and Houk [Wheeler and Houk 2009[a]] argued that the substituent effects in $C_6H_5X\cdots Na^+$ are largely due to through-space interactions between the X and Na^+. Though the recent and prior reports [Mecozzi *et al.* 1996[a], Wheeler and Houk 2009[a]] diversified the concept of substituent effects in cation-π interactions, a challenge still remains to identify the most governing factor among I, R and TS effects.

Since I, R and TS effects of X operate simultaneously in the $C_6H_5X\cdots Na^+$, separating individual contribution of these effects is almost impossible. Energy decomposition analysis

(EDA) is often used to extract various energy terms such as electrostatic, induction and dispersion effects etc. that contribute to the binding of interacting molecules [Frenking and Frohlich 2000, Soteras *et al.* 2008, Yanai *et al.* 2004]. However, EDA alone is not sufficient to extract simultaneously the substituent contributions of I, R and TS effects because for each of these effects, varying amounts of the various energy terms may contribute. Very often chemical models have been developed for the characterization and quantification I, R and TS effects. Among them, Hammett [Hammett 1937] constants (σ_p and σ_m) developed from benzoic acid derivatives in the 1937 are the most widely used measure of substituent effects. Later, for a thorough understanding of substituent effects in a variety of chemical structures, inductive (through-bond), resonance and TS (sometimes called as field effect, F) effects have been quantified in terms of the substituent constants σ_I, σ_R and σ_F, respectively [Hansch *et al*. 1991], [Sayyed and Suresh 2009[a], Suresh *et al*. 2008]. Quantum chemically derived structural, electronic and thermodynamic parameters have also been employed in the study of substituent effects [Exner and Böhm 2007, Suresh and Gadre 1998]. However, to the best of our knowledge, I, R and TS effect of X in cation-π interactions are not yet separated and quantified. The first part of this chapter, demonstrates a methodology to separate I, R and TS effect in $C_6H_5X\cdots Na^+$ systems.

3.3 Computational Details

The structures of all the cation-π complexes involved in part A of this chapter are optimized using B3LYP method with triple zeta quality 6-311+G(d,p) basis set. The interaction energies of cation-π complexes are calculated by subtracting the energy of the isolated monomers from its complex. Several substituents, *viz*. NH_2, OH, CH_3, H, F, Cl, CF_3, CN, and NO_2 which covers electron-donating, electron-withdrawing, and hyperconjugative effects are selected. All the interaction energies obtained at B3LYP/6-311+G(d,p) level are

counterpoise corrected [Boys and Bernardi 1970]. Further, to examine the effect of different density functional methods on the cation-π interaction energies, C_6H_5-CHCH-X$\cdots Na^+$ complexes (X = NH_2, OH, CH_3, H, F, CN, and NO_2) have been studied using B97-D [Grimme 2006], M06-2X [Zhao and Truhlar 2008], and CAM-B3LYP [Yanai et al. 2004] methods with 6-311+G(d,p) basis set. Moreover, the *ab initio* MP2/6-311+G(d,p) method is used to evaluate the cation-π interaction energies in C_6H_5-CHCH-X$\cdots Na^+$ complexes. B97-D functional was developed by Grimme [Grimme 2006] based on the generalized gradient approximation (GGA) which includes damped atom-pair wise dispersion corrections and M06-2X is a hybrid meta exchange correlation functional developed by Truhlar [Zhao and Truhlar 2008]. CAM-B3LYP is a hybrid-exchange correlation functional based on the Coulomb-attenuating method. All the computational calculations were carried out with Gaussian03/09 suite of programs [Frisch *et al*.].

3.4 Results and Discussion

The systems of the type $C_6H_5X\cdots Na^+$ are prototypical for the study of cation-π interactions [Mecozzi *et al*. 1996[a], Reddy and Sastry 2005]. The notation E_0 is used to indicate the cation-π interaction energy of all $C_6H_5X\cdots Na^+$ systems while the relative E_0 with respect to X = H is denoted as ΔE_0. For instance, in the case of benzene, aniline, and nitrobenzene, the E_0 values are -23.43, -28.74 and -10.93 kcal/mol, respectively. It means that compared to X = H, NH_2 group can increase the strength of cation-π binding by -5.31 kcal/mol while NO_2 group will decrease it by 12.50 kcal/mol. The increase or decrease in the interaction energy (ΔE_0) relative to the unsubstituted system can be attributed solely due to the substituent effect. For all the substituents, E_0 and ΔE_0 values are presented in Table 3.1. In the case of electron donating (NH_2, OH, CH_3) groups, ΔE_0 is negative in the range of -5.31 to -0.10 kcal/mol, suggesting enhancement in the cation-π interaction while ΔE_0 is positive for electron

withdrawing groups (F, Cl, CF_3, CN, and NO_2), in the range 4.33 to 12.50 kcal/mol, indicating substantial reduction in the cation-π interaction binding. Thus, it is clear that the cation-π interaction is highly sensitive to the electronic nature of X. Since electron donation/withdrawal mechanism of X depends on the I, R and TS effects, the quantification of these effects are essential for a comprehensive understanding of the nature of cation-π interactions in chemistry and biology.

Table 3.1 E_0 and ΔE_0 (in kcal/mol) of $C_6H_5X\cdots Na^+$ systems obtained at B3LYP/6-311+G(d,p) level.

X	E_0	ΔE_0
NH_2	-28.74	-5.31
OH	-23.54	-0.10
CH_3	-25.14	-1.71
H	-23.43	0.00
F	-18.47	4.96
Cl	-19.11	4.33
CF_3	-15.72	7.72
CN	-12.99	10.44
NO_2	-10.93	12.50

Four different chemical models *viz.* **1**, **2**, **2′**, and **3** that are appealing to the intuitive definitions of the I, R and TS effects for the study of cation-π interactions are presented in Scheme 3.1. Model **1** is C_6H_5-$(\Phi_1)_n$-$X\cdots Na^+$ (n = 1–5) wherein Φ_1 is -CH_2CH_2- moiety. In **1**, the CC single bond of Φ_1 ensures that only the I and TS effects of the X is transmitted to the π-ring [Hansch et al. 1991, Nolan and Linck 2000]. Therefore, the cation-π interaction energy of **1** ($E_n^{\mathbf{1}}$) for a given X relative to X = H can be attributed to sum of I and TS effects

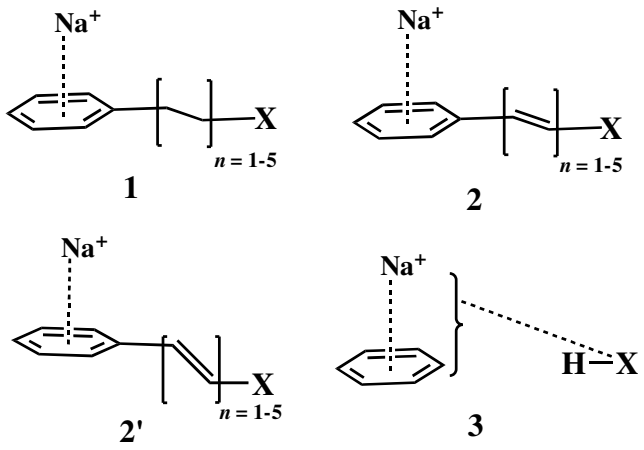

Scheme 3.1 Cation-π complexes designed for the quantification of inductive (**1**), resonance (**2, 2′**), and TS (**3**) substituent effects.

of that X for the corresponding *n*. For **1**,the dihedral angle joining the plane of the phenyl ring and the substituted alkyl chain is kept to zero to restrict the movement of Na^+ within the π-region. In the case of X = NH_2, E_1^1 = -0.29, E_2^1 = -0.11, E_3^1 = 0.06, E_4^1 = 0.01 and E_5^1 = 0.14 kcal/mol while for X = NO_2, E_1^1 = 7.42, E_2^1 = 4.81, E_3^1 = 3.50, E_4^1 = 2.05 and E_5^1 = 1.61 kcal/mol (Table 3.2) indicating that substituent effect progressively falls off with the increase in *n*. For instance, in the case of NO_2, 78.3% of reduction of its contribution to the cation-π

Table 3.2 E_n^1 and ΔE_n^1 (in kcal/mol) of $C_6H_5(\Phi_1)_{n=1-5}X\cdots Na^+$ systems obtained at B3LYP/6-311+G(d,p) level.

X	E_1^1	E_2^1	E_3^1	E_4^1	E_5^1	ΔE_1^1	ΔE_2^1	ΔE_3^1	ΔE_4^1	ΔE_5^1
NH_2	-25.99	-26.42	-26.54	-26.68	-26.65	-0.29	-0.11	0.06	0.01	0.15
OH	-23.81	-24.95	-25.63	-25.99	-26.50	1.89	1.36	0.97	0.70	0.30
CH_3	-26.06	-26.48	-26.74	-26.72	-26.72	-0.36	-0.17	-0.14	-0.03	0.08
H	-25.70	-26.31	-26.60	-26.69	-26.80	0.00	0.00	0.00	0.00	0.00
F	-21.20	-23.55	-24.84	-25.51	-25.99	4.50	2.76	1.76	1.18	0.81
Cl	-21.24	-23.46	-24.71	-25.42	-25.83	4.46	2.85	1.89	1.27	0.97
CF_3	-20.49	-23.07	-24.48	-25.25	-25.66	5.21	3.24	2.12	1.44	1.14
CN	-18.56	-21.84	-23.67	-24.69	-25.31	7.14	4.47	2.93	2.00	1.49
NO_2	-18.28	-21.49	-23.10	-24.64	-25.18	7.42	4.82	3.50	2.05	1.62

interaction can be seen from n = 1 to n = 5. For any X, a plot of E_n[1] against n can be fitted almost perfectly by a 2nd order polynomial equation. Since n = 0 for $C_6H_5X\cdots Na^+$, the polynomial equation can be extrapolated to n = 0 to obtain the substituent effect which is the sum of I and TS contributions (abbreviated as E_{I+TS}). E_{I+TS} values for all the systems are presented in Table 3.3.

Table 3.3 Relative contributions of inductive (E_I), through-space (E_{TS}), and resonance effects (E_R) of $C_6H_5X\cdots Na^+$ systems. All values in kcal/mol.

X	E_{I+TS}	E_I	E_{TS}	E_R	E_{Total} [a]
NH_2	-0.49	-0.98	0.49	-3.96	-4.45
OH	2.39	-3.09	5.48	-2.49	-0.10
CH_3	-0.48	0.22	-0.70	-0.41	-0.89
H	0.00	0.00	0.00	0.00	0.00
F	6.46	-0.77	7.24	-1.32	5.14
Cl	6.34	1.55	4.79	-0.95	5.39
CF_3	7.49	1.47	6.02	0.74	8.23
CN	10.21	1.97	8.24	0.76	10.97
NO_2	10.29	1.32	8.97	1.70	11.99

[a] $E_{Total} = E_I + E_{TS} + E_R$

Model **2** is C_6H_5-$(\Phi_2)_{n=1\text{-}5}$-$X\cdots Na^+$ wherein Φ_2 is -CHCH- group (Scheme 3.1). The conjugated alkenyl chain ensures the transmission of resonance effect of X to the π-system along with inductive and TS effects. Model **2′** (abbreviated as C_6H_5-$(\Phi_{2\perp})_n$-$X\cdots Na^+$) is derived from **2** by restricting the orientation of plane of the phenyl group in a position orthogonal to plane of the substituted alkenyl unit and this will prohibit the resonance between Φ_2-X and C_6H_5 [Silva 2009]. For a given n, distance between the X and Na^+ (through-space distance) in **2** is ~0.686 Å lower than that of **2′**. Further, for a given n, the

total CC bond distance of Φ_2 in **2** (through-bond distance) is ~0.035 Å higher than CC bond distance of $\Phi_{2\perp}$ in **2′**. Therefore, the inductive and TS contributions of X in **2** and **2′** are nearly identical [Silva 2009]. In other words, for a given *n*, the quantity ($E_n^{\mathbf{2}}$–$E_n^{\mathbf{2'}}$) brings out the pure resonance effect of X in the cation-π interaction. By plotting ($E_n^{\mathbf{2}}$–$E_n^{\mathbf{2'}}$) against *n*, for *n* = 1–5 and extrapolating to *n* = 0 via a 2nd order polynomial equation, the resonance contribution of X in $C_6H_5X\cdots Na^+$ (designated as E_R) can be obtained. The values of E_R with respect to the X = H are presented in Table 3.3.

The model **3** is used for the quantification of TS effect which is derived from **2** by chopping off the spacer unit between phenyl ring and X, and subsequently adding 'H' atom to the free valency created on the phenyl carbon and the X. The positions of the newly added hydrogens are optimized by freezing all other atoms. The procedure used herein to develop **3** is similar to a model recently introduced by Wheeler and Houk [Wheeler and Houk 2009[a]] for the determination of TS effect of substituents in cation-π interactions. In their model, the X is connected directly on the aromatic ring while in our case we use the spacer Φ_2 to include distance dependency. Since through-bond interaction between X and phenyl ring is absent in **3**, cation-π interaction energy for **3** ($E_n^{\mathbf{3}}$) will be affected only by TS effect of X [Sayyed *et al.* 2010]. $E_n^{\mathbf{3}}$ can be fitted using a polynomial equation in *n*, which upon extrapolation to *n* = 0 will yield TS effect of X, E_{TS} (Table 3.3). By subtracting E_{TS} from E_{I+TS}, through-bond inductive contribution, E_I can be obtained (Table 3.3).

Figure 3.1 depicts the correlation plots of (E_{I+TS}, σ_I), (E_R, σ_R) and (E_{TS}, σ_F). It is gratifying that all these plots are linear which means that the computed energy terms serve as good measure of the I, R and TS substituent effects in $C_6H_5X\cdots Na^+$. It may be noted that in the original definition of σ_I, inductive and TS effects are combined and therefore only E_{I+TS} can be correlated with σ_I and not E_I [Hansch *et al.* 1991, Sayyed *et al.* 2010]. According to IUPAC, "*the field effect symbolized by F is an experimentally observable effect (on reaction*

rates, etc.) of intramolecular coulombic interaction between the centre of interest and a remote unipole or dipole, by direct action through space rather than through bonds". Hence, σ_F, the substituent field effect constant is the right choice to understand the use of E_{TS} in measuring the TS effect (Figure 3.1c).

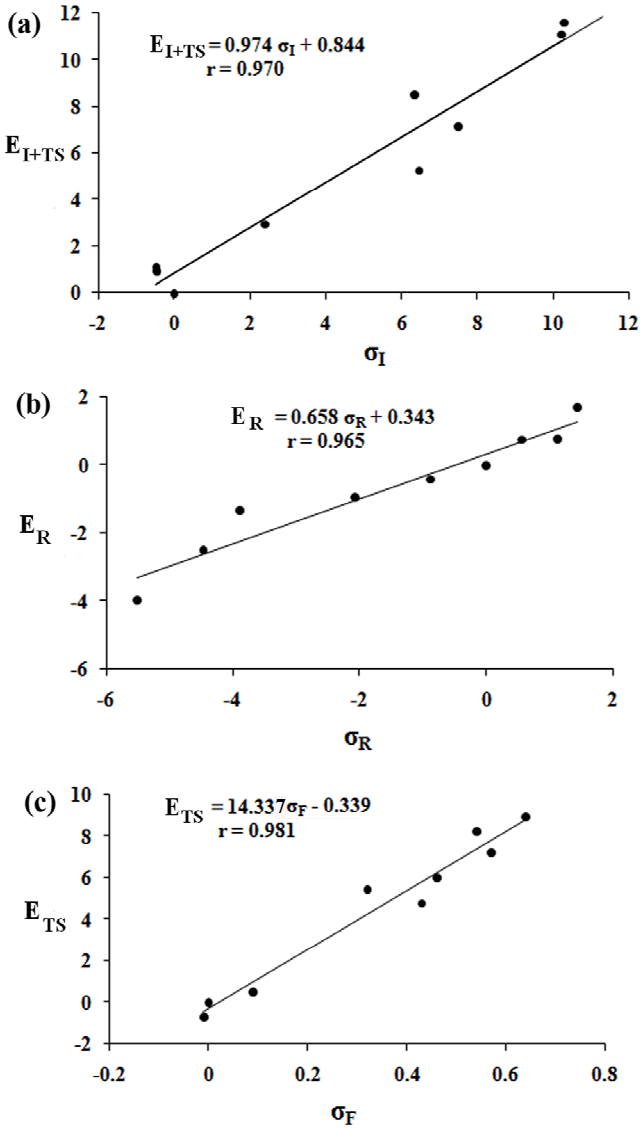

Figure 3.1 Correlation between the inductive, resonance and TS contributions of total cation-π interaction energy of $C_6H_5X\cdots Na^+$ with substituent constants. (a) E_{I+TS} vs σ_I (b) E_R vs σ_R (c) E_{TS} vs σ_F.

The data presented in Table 3.3 allow a comprehensive understanding of the substituent effects in cation-π interactions through the quantification of chemically intuitive I, R and TS concepts. OH group shows the highest inductive effect, E_I of -3.09 kcal/mol and the rest can be grouped in the range of -0.98 to 1.97 kcal/mol. CH_3 showed an enhancement in cation-π interaction energy due to TS effect while all other substituents decrease the interaction energy through TS effect. TS effect of NH_2 is only 0.49 kcal/mol whereas OH group has a high value of 5.48 kcal/mol. All the electron withdrawing groups showed high values of TS effect in the range of 4.79 to 8.97 kcal/mol. In fact, TS contribution to the total effect is 78.0, 78.9, and 71.8% for CF_3, CN and NO_2 substituted systems, respectively. From E_R values, it can be seen that the substituents bearing lonepair of electrons, viz. NH_2, OH, F, Cl and hyperconjugative CH_3 will enhance the cation-π interaction through resonance effect. The electron withdrawing groups CF_3, CN and NO_2 can decrease the interaction energy through resonance by a small amount in the range 0.74 to 1.70 kcal/mol. In the case of NH_2, a remarkable resonance effect of 74.6% accounts to the total cation-π interaction while TS effect accounts only 9.2%. Interestingly, electron-donating OH has negligible influence on the cation-π interaction when compared to benzene; [Ma and Dougherty 1997] the reason can be attributed to the near cancellation of the destabilizing TS effect (5.48 kcal/mol) and stabilizing resonance and inductive effects (total 5.58 kcal/mol) (Table 3.3). In the case of electron-withdrawing CF_3, CN and NO_2 substituted systems, decrease in the E_0 due to resonance is only 9.6, 7.3 and 13.6 %, respectively. Thus, models shown in Scheme 3.1 satisfy the criteria not only for the accurate quantification of inductive, resonance and TS effects but also allow to understand the most intriguing interplay of electronic features of X in cation-π interactions.

Further, a quantity E_{Total}, is defined (sum of E_I, E_R and E_{TS}) (Table 3.3) to show the merit of proposed approach of factoring total cation-π interaction energy into I, R and TS contributions. Surprisingly, E_{Total} is nearly equal to E_0 and the correlation plot of (E_{Total}, ΔE_0)

shown in Figure 3.2 indeed proves it (slope = 1.01). Hence, it can be concluded that the substituent effects in cation-π interactions are primarily due to the interplay of I, R and TS effects of the substituent.

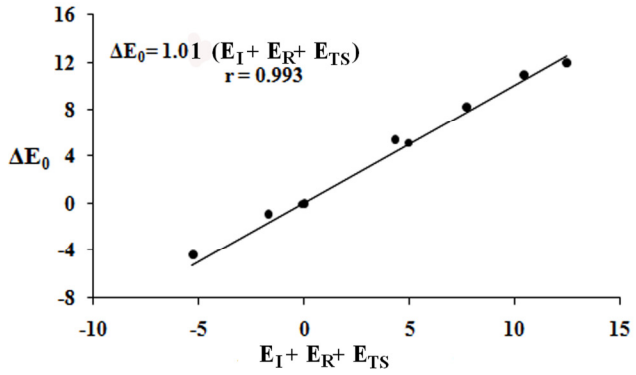

Figure 3.2 Correlation between the total substituent effect and the sum of the inductive, TS, and resonance contributions.

In order to assess the performance of various DFT methods and also the MP2 method in deriving the substituent effect, cation-π interaction energies of **2** and **2′** for n = 1 are calculated at B3LYP, CAM-B3LYP, M06-2X, B97-D and MP2 levels (Table 3.4). In many computational studies, MP2 is used as an affordable *ab initio* method to assess the quality of a DFT result. For the ordered pair ($E_I^{\mathbf{2}}$, $E_I^{\mathbf{2'}}$), using the MP2 data as standard, the mean deviation in kcal/mol is found to be (-0.38, -0.54) for B3LYP, (-1.61, -1.88) for CAM-B3LYP, (-2.84, -2.98) for M06-2X and (-9.18, -9.14) for B97-D. It means that B3LYP showed the best agreement to the MP2 data. Compared to MP2, DFT methods over estimate both $E_I^{\mathbf{2}}$ and $E_I^{\mathbf{2'}}$ which is ~2.6%, ~8.0%, ~12.9% and ~39.1%, respectively for B3LYP, CAM-B3LYP, M06-2X and B97-D. The substantially high value of the cation-π interaction energy at B97-D method is noteworthy because dispersion effect is expected to play only a minor (6%) role while the major contribution is due to the electrostatic interaction (~67%) [Soteras *et al*. 2008].

Table 3.4 Cation-π interaction energies of $C_6H_5(\Phi_2)_1X\cdots Na^+$ ($E_1^{\mathbf{2}}$) and $C_6H_5(\Phi_{2\perp})_1X\cdots Na^+$ ($E_1^{\mathbf{2'}}$) systems. All values in kcal/mol.

	$E_1^{\mathbf{2}}$					$E_1^{\mathbf{2'}}$				
X	A[a]	B[b]	C[c]	D[d]	E[e]	A[a]	B[b]	C[c]	D[d]	E[e]
NH_2	-33.00	-33.90	-35.06	-42.05	-30.56	-29.19	-30.61	-31.58	-37.78	-27.66
OH	-27.40	-28.40	-29.57	-36.42	-26.01	-25.00	-26.31	-27.44	-33.64	-24.09
CH_3	-27.61	-28.89	-30.16	-36.32	-26.65	-26.67	-28.06	-29.20	-35.17	-25.70
H	-25.29	-26.68	-27.99	-33.85	-24.96	-24.88	-26.30	-27.47	-33.32	-24.23
F	-23.10	-24.27	-25.56	-32.00	-22.64	-21.90	-23.24	-24.43	-30.54	-21.52
CN	-17.00	-18.32	-19.55	-25.69	-17.68	-17.54	-18.79	-19.88	-26.11	-17.55
NO_2	-14.81	-16.40	-17.60	-23.51	-17.08	-16.02	-17.29	-18.31	-24.83	-16.69

[a] B3LYP, [b]CAM-B3LYP, [c] M06-2X, [d] B97-D, and [e] MP2 results

Further, in Table 3.5, relative interaction energies, $\Delta E_1^{\mathbf{2}}$ and $\Delta E_1^{\mathbf{2'}}$ of **2** and **2′** systems with respect to X = H are shown. These values correspond to the total substituent effect of X and show that all DFT methods show nearly same values of substituent effect. MP2 results also show good agreement with the DFT results, but the variation is slightly larger than that between any two DFT methods. For example, the contributions of (NH_2, NO_2) in kcal/mol towards $E_1^{\mathbf{2}}$ are (-7.71, 10.48) at B3LYP, (-7.22, 10.28) at CAM-B3LYP, (-7.07, 10.39) at M06-2X, (-8.20, 10.34) at B97-D, and (-5.60, 7.88) at MP2. Moreover, the correlation matrix obtained (Table 3.6) for all these methods suggest a correlation coefficient in the range of 0.995 to 1.000 for the data of any two methods. Thus, we can conclude that individual substituent effect obtained using any of the DFT method or MP2 method is accurate as they do not vary significantly with respect to the applied methodology. Hence, we believe that the relationship given in Figure 3.2, $\Delta E_0 \approx E_I + E_R + E_{TS}$ is reliable.

Table 3.5 Cation-π interaction energies of $C_6H_5(\Phi_2)_1X\cdots Na^+$ (ΔE_1^{2}) and $C_6H_5(\Phi_{2\perp})_1X\cdots Na^+$ ($\Delta E_1^{2'}$) systems relative to X = H system. All values in kcal/mol.

	ΔE_1^{2}					$\Delta E_1^{2'}$				
X	A[a]	B[b]	C[c]	D[d]	E[e]	A[a]	B[b]	C[c]	D[d]	E[e]
NH_2	-7.71	-7.22	-7.07	-8.20	-5.60	-4.11	-4.31	-4.31	-4.46	-3.43
OH	-2.11	-1.72	-1.58	-2.57	-1.05	0.03	-0.12	-0.01	-0.32	0.14
CH_3	-2.32	-2.21	-2.17	-2.47	-1.69	-1.73	-1.79	-1.76	-1.85	-1.47
H	0.00	0.00	0.00	0.00	0.00	0.00	0.00	0.00	0.00	0.00
F	2.19	2.41	2.43	1.85	2.32	3.04	2.98	3.06	2.78	2.71
CN	8.29	8.36	8.44	8.16	7.28	7.59	7.34	7.51	7.21	6.68
NO_2	10.48	10.28	10.39	10.34	7.88	9.16	8.86	9.01	8.49	7.54

[a]B3LYP, [b]CAM-B3LYP, [c] M06-2X, [d] B97-D, and [e] MP2 results.

Table 3.6 Correlation matrix obtained for various quantum chemical methods from the interaction energies of $C_6H_5(\Phi_2)_1X\cdots Na^+$ and $C_6H_5(\Phi_{2\perp})_1X\cdots Na^+$ systems.[a]

	B3LYP	CAM-B3LYP	M06-2X	B97-D	MP2
B3LYP	1				
CAM-B3LYP	1.000	1			
M06-2X	0.999	1.000	1		
B97-D	0.999	0.998	0.998	1	
MP2	0.996	0.997	0.997	0.995	1

[a] E_1^{2} and $E_1^{2'}$ are placed under one column for obtaining the correlation matrix.

Part B: NMR Characterization of Substituent Effects in Cation-π Interactions

3.5 Introduction

NMR spectroscopy is a powerful tool for the structural interpretation of molecules using the information of nuclear magnetic shielding constants (σ), as 'σ' is directly related to chemical shift *via* the equation $\delta_k = \sigma_{ref} - \sigma_A$ (for nucleus A) [Vaara 2007, Willans and Schurko 2003]. The identification and characterization of noncovalent interactions using NMR technique has shown a new way of understanding molecular structures at the atomic level [Bagno *et al.* 2001, 2002, Platts and Gkionis 2009, Wong *et al.* 2004, Wu and Terskikh 2008]. The strength of the cation-π interaction depends upon the type of the π-system as well as the type of interacting cation [Mecozzi et al. 1996[b], Meyer *et al*. 2003]. For a given cation-π complex, the substituent (X) can tune the strength of the cation-π interaction significantly. For instance, in the case of $C_6H_5X\cdots Na^+$ complexes, compared to X = H, larger interaction energy is observed when X is an electron-donating (ED) substituent and smaller interaction energy is observed when X is an electron-withdrawing (EW) substituent. Solid-state NMR study of cation-π complexes of sodium and potassium tetraphenylborates by Wu and co-workers revealed the existence of highly shielded environment at the metal cation as well as deshielded environment on the π-system [Wong et al. 2004, Wu and Terskikh 2008]. Further, they suggested that theoretically derived 'σ' values are useful quantities for the study of alkali metal cation-π complexes. Recently, He *et al*. showed the importance of NMR experiments in identifying the cation-π interactions between the cyclooctatetraene and alkaline earth metals [He *et al.* 2008]. However, the substituent effect in cation-π interactions on the NMR properties is not yet known and this problem was discussed by studying the substituent

effects in the cation-π complexes of $C_6H_5X\cdots M^+$ ($M^+ = Li^+$, Na^+, K^+, and NH_4^+) using NMR isotropic shielding constants in part B of this chapter.

3.6 Computational details

All the cation-π complexes of substituted benzenes (C_6H_5X) with cations (M^+; $M^+ = Li^+$, Na^+, K^+, and NH_4^+) are optimized at B3LYP/6-311+G(d,p) level [Becke 1993]. In part A of this chapter, it was shown that B3LYP method accurately represents the substituent effects in cation-π interactions and the trend obtained for the substituent effects is almost identical irrespective of the method used. The isotropic nuclear shielding constants (σ) of $C_6H_5X\cdots M^+$ complexes as well as the corresponding C_6H_5X systems are calculated using gauge invariant atomic orbital (GIAO) [Ditchfield 1974] method at B3LYP/6-311+G(d,p) level for a variety of 15 substituents, *viz*. $N(CH_3)_2$, $NHCH_3$, NH_2, NHOH, CH_3, OH, H, SCH_3, SH, SiH_3, CCH, F, Cl, CN, and NO_2. Helgaker and co-workers demonstrated that NMR shielding constants can be accurately obtained using a valence triple-ζ basis set with a set of polarization functions [Helgaker *et al.* 1999]. Therefore, 6-311+G(d,p) basis set is adequate for a reliable representation of 'σ' values. However, to test the validity of the results obtained using B3LYP method, σ values are computed for five $C_6H_5X\cdots Na^+$ (X = NH_2, CH_3, H, F, CN) complexes at other DFT methods *viz*. PBE1PBE [Adamo and Barone 1999], CAM-B3LYP [Yanai *et al*. 2004], wB97X-D [Chai and Head-Gordon 2008] and M06-2X [Zhao and Truhlar 2008] as well as the *ab initio* MP2 [Møller and Plesset 1934] method. In the case of Li^+, Na^+, and K^+ complexes, σ is taken directly at the cationic nucleus whereas for NH_4^+ system, σ of the proton oriented towards the π-systems is taken. All the computational calculations have been carried out using Gaussin09 suite of programs [Frisch *et al*.].

3.7 Results and Discussion

The isotropic nuclear magnetic shielding constants, $\sigma_M{}^+$ obtained for the M^+ nucleus of $C_6H_5X\cdots M^+$ complexes ($M^+ = Li^+$, Na^+, K^+, or $NH_4{}^+$) at B3LYP/6-311+G(d,p) method are reported in Table 3.7. For the unsubstituted reference system, $C_6H_6\cdots M^+$, $\sigma_M{}^+$ values are 99.9, 616.4, 1319.9, and 27.5 ppm for $M^+ = Li^+$, Na^+, K^+ and $NH_4{}^+$, respectively. In general,

Table 3.7 Isotropic nuclear magnetic shielding constants of M^+ ($\sigma_M{}^+$) in $C_6H_5X\cdots M^+$ ($M^+ = Li^+$, Na^+, K^+, $NH_4{}^+$) complexes.[a]

X	$\sigma_{Li}{}^{+b}$	$\sigma_{Na}{}^{+b}$	$\sigma_K{}^{+b}$	$\sigma_{NH4}{}^+$	σ_p
$N(CH_3)_2$	98.3	612.1	1317.6	26.8	-0.83
$NHCH_3$	98.2	613.0	1318.7	26.7	-0.84
NH_2	98.3	614.6	1320.1	26.9	-0.66
NHOH	98.7	615.5	1321.9	27.0	-0.34
CH_3	99.6	615.5	1319.7	27.4	-0.17
OH	99.1	615.9	1320.4	27.2	-0.37
H	99.9	616.4	1319.9	27.5	0.00
SCH_3	98.9	616.8	1322.5	27.3	0.00
SH	99.0	617.5	1323.4	27.5	0.15
SiH_3	99.8	616.5	1321.1	27.6	0.10
CCH	99.5	617.9	1325.2	27.7	0.23
F	99.6	618.1	1322.7	27.5	0.06
Cl	99.5	618.4	1324.1	27.8	0.23
CN	99.8	619.9	1326.7	28.0	0.66
NO_2	100.0	620.2	1326.0	28.3	0.78

[a] All the $\sigma_M{}^+$ values are in ppm.

[b] σ_{ref} values are 91.9 ppm for $[Li(H_2O)_4]^+$, 568.4 ppm for $[Na(H_2O)_6]^+$ and 1237.3ppm for $[K(H_2O)_6]^+$.

the presence of an electron-donating substituent decreases σ_M^+ values while an electron-withdrawing substituent increases it. For instance, $N(CH_3)_2$ decreases σ_M^+ by 1.6, 4.3, 2.3, and 0.7 ppm for $M^+ = Li^+$, Na^+, K^+ and NH_4^+, respectively whereas NO_2 increases it by 0.1, 3.8, 6.1, and 0.8 ppm for $M^+ = Li^+$, Na^+, K^+ and NH_4^+, respectively. The increase or decrease in σ_M^+ is found to be proportional to the Hammett substituent parameter, σ_p (Figure 3.3). The linear correlation between σ_M^+ and σ_p clearly suggests that the substituent effects in cation-π complexes can be easily quantified by measuring the nuclear magnetic shielding constants on the cation and such studies should be amenable to experiments.

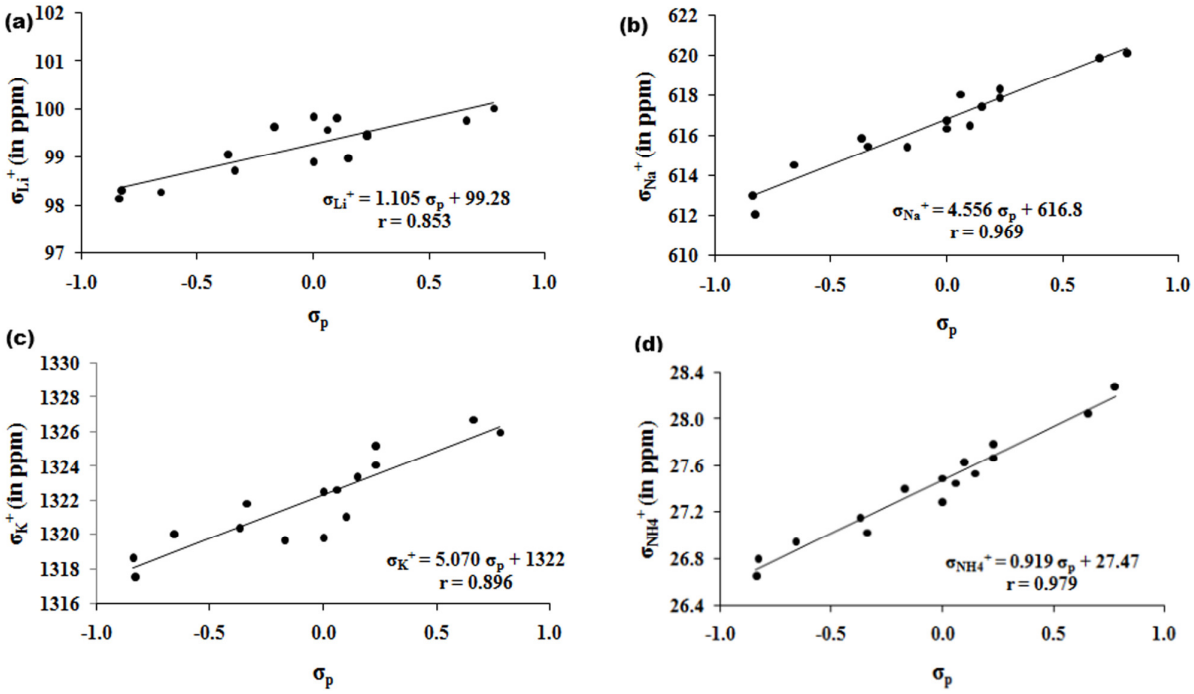

Figure 3.3 Correlation between the NMR isotropic shielding constants of M^+ in $C_6H_5X\cdots M^+$ and Hammett σ_p values. (a) $M^+ = Li^+$ (b) $M^+ = Na^+$ (c) $M^+ = K^+$ (d) $M^+ = NH_4^+$.

To test the reliability of B3LYP method to compute σ_M^+, the σ_{Na}^+ for a test set of five systems, *viz.* $C_6H_5X\cdots Na^+$ (X = NH_2, CH_3, H, F, CN) are calculated with *ab initio* MP2

method as well as PBE1PBE, CAM-B3LYP, M06-2X and wB97X-D density functional methods (Table 3.8). σ_{Na}^{+} at B3LYP is lower than MP2, PBE1PBE and wB97X-D values and slightly higher than that at M06-2X level. However, compared to MP2 data, average mean deviation of σ_{Na}^{+} between substituted and unsubstituted complexes is 0.1, -0.1, 0.6, 0.1, and -0.2 ppm for B3LYP, PBE1PBE, M06-2X, CAM-B3LYP, and wB97X-D, respectively. The correlation matrix shown in Table 3.9 with correlation coefficients ranging from 0.963

Table 3.8 σ_{Na}^{+} (in ppm) of $C_6H_5X\cdots Na^+$ (X = NH_2, CH_3, H, F, CN) complexes obtained at various methods.

X	MP2	B3LYP	PBE1PBE	M06-2X	CAM-B3LYP	wB97X-D
NH_2	622.7	614.6	615.2	612.5	614.7	621.4
CH_3	622.5	615.5	616.2	612.5	615.4	621.8
H	623.2	616.4	617.2	613.5	616.5	622.5
F	624.5	618.1	618.6	615.7	618.1	623.4
CN	625.4	619.9	620.4	618.1	620.2	624.6

Table 3.9 Correlation matrix of σ_{Na}^{+} between various methods.

	MP2	B3LYP	PBE1PBE	M06-2X	CAM-B3LYP	wB97X-D
MP2	1					
B3LYP	0.976	1				
PBE1PBE	0.967	0.999	1			
M06-2X	0.993	0.982	0.973	1		
CAM-B3LYP	0.981	0.999	0.997	0.987	1	
wB97X-D	0.979	0.999	0.998	0.986	1.000	1

to 1.000 strongly suggests that the trend obtained for σ_{Na}^{+} with respect to the electronic nature of the X is almost identical irrespective of the method used. Therefore, the results obtained from the B3LYP method are sufficient to represent the σ values and hereafter only B3LYP results will be discussed.

To understand the trend of substituent effects that reflected in the σ_M^{+} , σ_M^{+} of the cation without the aromatic ring (designated as $\sigma_M^{+\prime}$, the σ_M^{+} bare cation) is also computed. The difference between the σ_M^{+} and $\sigma_M^{+\prime}$ ($\Delta\sigma_M^{+}$) exclusively represents the change in isotropic NMR shielding constant due to cation-π complex formation. Further, in the equilibrium geometry of $C_6H_5X\cdots M^{+}$, a ghost atom is used in place of M^{+} to evaluate the isotropic NMR shielding constant. This quantity designated as σ_g exclusively represents the isotropic shielding density that would be induced by the substituted π-system in the absence of M^{+}. Therefore, the difference between $\Delta\sigma_M^{+}$ and σ_g ($\Delta\Delta\sigma_M^{+}$) will give the contribution of the charge transfer, polarization, through-space effects *etc*. A similar procedure was previously employed by Platts and Gkionis in the case of benzene-methane complex [Platts and Gkionis 2009].

For $C_6H_5X\cdots Na^{+}$ systems, $\Delta\sigma_{Na}^{+}$, σ_g and $\Delta\Delta\sigma_{Na}^{+}$ values are reported in Table 3.10. A good linear correlation is observed between $\Delta\Delta\sigma_M^{+}$ and σ_p (Figure 3.4) which suggests that the magnitude of $\Delta\Delta\sigma_M^{+}$ is proportional to electron-donating or electron-withdrawing ability of X. These correlations suggest that factors influencing the substituent effect, *viz.* charge transfer interactions between π-system and cation, polarization due to charge separation, and through-space effects from the substituent are also responsible for the changes in the isotropic nuclear magnetic shielding at the cation [Cheng *et al.* 2006, Martin *et al.* 2008]. Previous studies by Wong *et al.* showed that the diamagnetic ring current is insignificant in cation-π interaction [Wong *et al.* 2004]. Even in the case of substituted benzenes, Krygowski *et al.* observed that the substituent has only a weak influence on the ring current [Krygowski *et al.*

2004]. Our data on σ_g showed poor correlation with σ_p suggesting that ring current has no significant role in transmitting the substituent effect to the M^+ (Figure 3.5).

Table 3.10. σ_g, $\Delta\sigma_M{}^+$ and $\Delta\Delta\sigma_M{}^+$ (in ppm) values of $C_6H_5X\cdots M^+$ ($M^+ = Li^+, Na^+, K^+, NH_4{}^+$) systems obtained at the B3LYP/6-311+G(d,p) level.

	Li^+			Na^+			K^+			$NH_4{}^+$		
X	σ_g	$\Delta\sigma_{Li}{}^+$	$\Delta\Delta\sigma_{Li}{}^+$	σ_g	$\Delta\sigma_{Na}{}^{+\,a}$	$\Delta\Delta\sigma_{Na}{}^+$	σ_g	$\Delta\sigma_K{}^+$	$\Delta\Delta\sigma_K{}^+$	σ_g	$\Delta\sigma_{NH4}{}^+$	$\Delta\Delta\sigma_{NH4}{}^+$
$N(CH_3)_2$	-5.1	3.0	-8.1	-3.0	-11.5	8.5	-2.1	-7.8	5.7	-2.9	-0.3	-2.7
$NHCH_3$	-4.9	2.9	-7.8	-2.8	-10.6	7.7	-1.9	-6.7	4.8	-2.7	-0.4	-2.3
NH_2	-4.8	3.0	-7.7	-2.8	-9.0	6.2	-1.8	-5.3	3.5	-2.6	-0.2	-2.4
NHOH	-5.1	3.4	-8.4	-2.9	-8.1	5.2	-1.8	-3.5	1.7	-2.7	-0.1	-2.6
CH_3	-5.5	4.3	-9.8	-3.3	-8.1	4.8	-2.1	-5.7	3.6	-2.9	0.3	-3.3
OH	-5.1	3.8	-8.9	-3.0	-7.7	4.7	-1.9	-5.0	3.1	-2.7	0.1	-2.8
H	-5.6	4.6	-10.2	-3.3	-7.2	3.9	-2.1	-5.5	3.3	-3.1	0.4	-3.5
SCH_3	-5.2	3.6	-8.8	-3.0	-6.8	3.8	-1.9	-2.9	1.0	-2.6	0.2	-2.9
SH	-5.1	3.7	-8.7	-2.9	-6.1	3.2	-1.9	-2.0	0.1	-2.6	0.4	-3.0
SiH_3	-5.5	4.5	-10.0	-3.3	-7.1	3.8	-2.2	-4.3	2.0	-3.0	0.5	-3.5
CCH	-5.4	4.2	-9.6	-3.1	-5.7	2.6	-2.0	-0.2	-1.9	-2.7	0.6	-3.4
F	-5.3	4.3	-9.6	-3.1	-5.5	2.4	-1.9	-2.7	0.7	-2.9	0.4	-3.3
Cl	-5.2	4.2	-9.4	-3.1	-5.2	2.1	-1.9	-1.3	-0.6	-2.6	0.7	-3.4
CN	-5.3	4.5	-9.8	-3.3	-3.7	0.4	-1.8	1.3	-3.2	-2.5	0.9	-3.4
NO_2	-5.3	4.7	-10.0	-3.0	-3.4	0.3	-2.0	0.6	-2.6	-2.5	1.2	-3.7

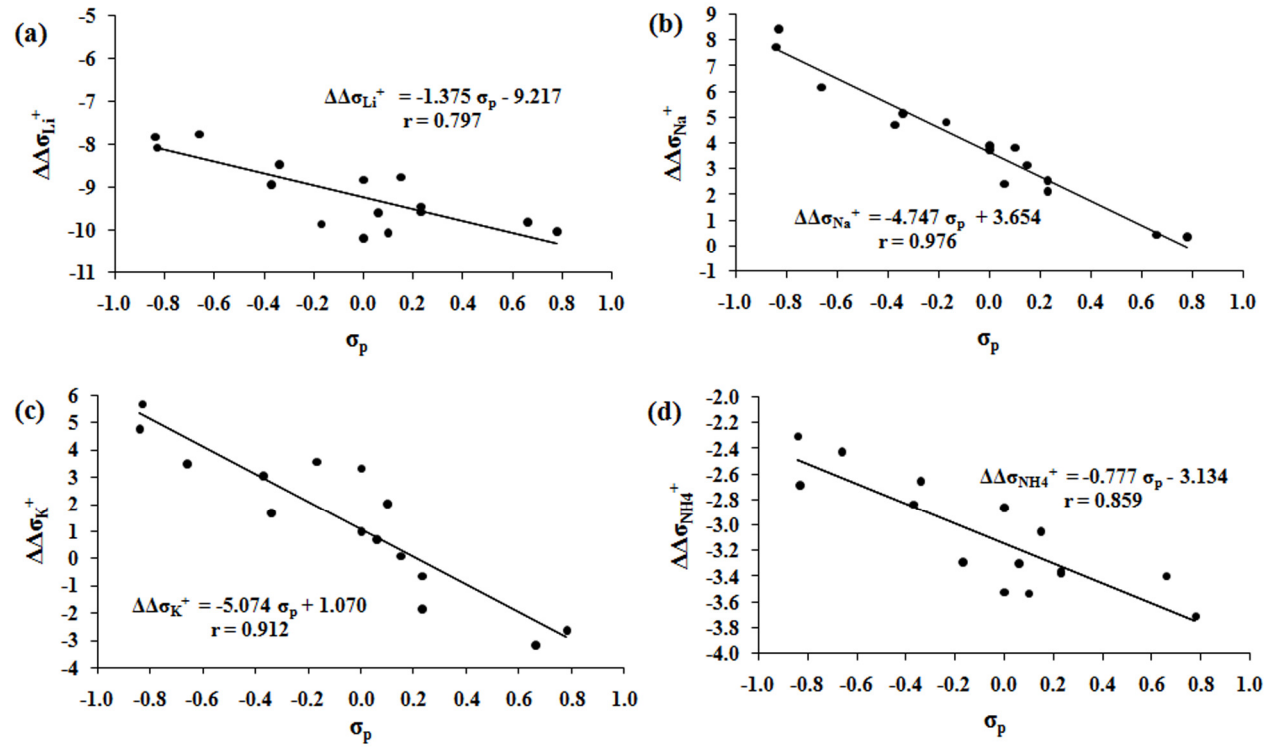

Figure 3.4 Correlation between $\Delta\Delta\sigma_M^+$ ($M^+ = Li^+$, Na^+, K^+, NH_4^+) and σ_p values. (a) $M^+ = Li^+$ (b) $M^+ = Na^+$(c) $M^+ = K^+$,(d) $M^+ = NH_4^+$.

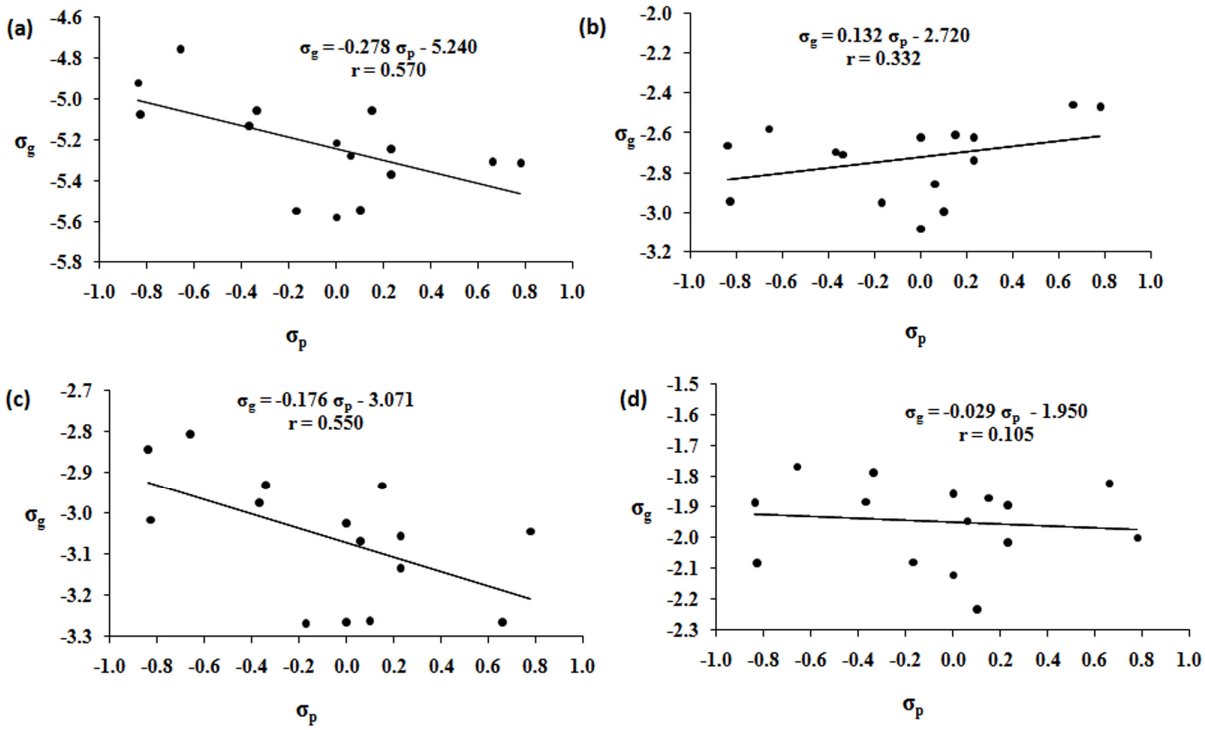

Figure 3.5 Correlation between the σ_g (in ppm) and the σ_p constants for $C_6H_5X\cdots M^+$systems. (a) $M^+ = Li^+$ (b) $M^+ = Na^+$ (c) $M^+ = K^+$, (d) $M^+ = NH_4^+$.

Further, the isotropic nuclear shielding constant (σ) is calculated for all the carbon and hydrogen atoms in both $C_6H_5X\cdots M^+$ and C_6H_5X and evaluated the change in σ ($\Delta\sigma$) due to cation-π interaction. The $\Delta\sigma$ data for all the 60 cation-π complexes, obtained at the B3LYP/6-311+G(d,p) level are summarized in Table 3.11, Table 3.12, Table 3.13, and Table 3.14 for $M^+ = Li^+$, Na^+, K^+ and NH_4^+, respectively. The notation used to represent the isotropic nuclear magnetic shielding constants for the $C_6H_5X\cdots M^+$ complex is shown in Scheme 3.2.

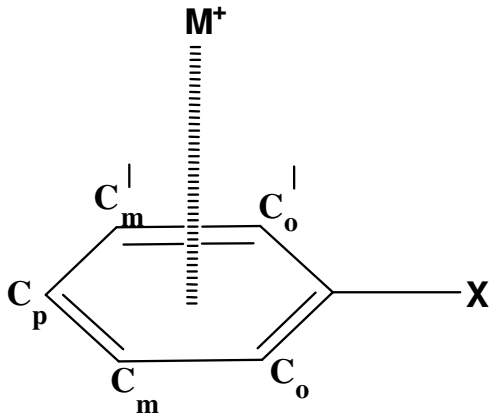

Scheme 3.2 Notation used to represent the isotropic nuclear magnetic shielding constants for the $C_6H_5X\cdots M^+$ complex. The hydrogens attached to the C_o, C_m, C_p, C_m', and C_o', are denoted as H_o, H_m, H_p, H_m', and H_o', respectively.

A positive value of $\Delta\sigma$ indicated shielding while a negative value indicated deshielding of a particular nucleus due to the cation-π interaction [Martin *et al.* 2001, Platts and Gkionis 2009]. In $C_6H_6\cdots M^+$, the carbon nuclei are highly deshielded by 4.92, 3.36, 3.49 and 4.24 ppm while the hydrogen atoms are slightly deshielded by 0.89, 0.68, 0.54 and 0.57 for $M^+ = Li^+$, Na^+, K^+ and NH_4^+, respectively. Further, irrespective of the electronic nature of the substituent, all $C_6H_5X\cdots M^+$ systems showed deshielding at hydrogen nuclei. In the case of π-carbons, the *meta* carbons (C_m) always showed deshielding irrespective of electron donating or electron withdrawing nature of the substituent. Deshielding is also noted for *ortho* (C_o) and

para (C_p) carbons except the cases of $N(CH_3)_2$, $NHCH_3$ and NH_2 substituted systems. The observed shielding at the C_o and C_p carbons of some systems can be attributed strong resonance effect from the substituent. In summary, the presence of a cation over the π-ring always causes deshielding at the hydrogen nuclei as well as deshielding at *meta* carbon atoms regardless of the electron donating or electron withdrawing nature of X and this feature can be taken as a signature of cation-π interaction.

Table 3.11 Change in NMR isotropic shielding constants, $\Delta\sigma$ (in ppm) of $C_6H_5X\cdots Li^+$ complexes.

$C_6H_5X\cdots Li^+$ systems										
X	H_o	H_m	H_p	H_m'	H_o'	C_o	C_m	C_p	C_m'	C_o'
$N(CH_3)_2$	-0.59	-0.73	-0.40	-0.73	-0.59	-1.47	-4.36	2.44	-4.36	-1.47
$NHCH_3$	-0.40	-0.63	-0.36	-0.63	-0.41	1.34	-3.03	4.04	-3.20	1.59
NH_2	-0.60	-0.80	-0.62	-0.80	-0.60	-1.41	-4.71	0.00	-4.71	-1.41
NHOH	-0.71	-0.68	-0.47	-0.68	-0.56	0.16	-3.26	2.24	-3.17	-0.67
CH_3	-0.82	-0.87	-0.81	-0.87	-0.82	-3.91	-4.53	-3.50	-4.53	-3.91
OH	-0.82	-0.85	-0.76	-0.85	-0.75	-4.95	-4.71	-2.06	-4.96	-3.52
H	-0.89	-0.89	-0.89	-0.89	-0.89	-4.92	-4.92	-4.92	-4.92	-4.92
SCH_3	-0.62	-0.61	-0.48	-0.65	-0.61	-1.51	-2.71	1.50	-2.55	-1.39
SH	-0.66	-0.69	-0.54	-0.67	-0.59	-1.34	-2.91	0.55	-2.92	-0.79
SiH_3	-0.67	-0.73	-0.65	-0.73	-0.67	-2.46	-2.94	-1.55	-2.94	-2.45
CCH	-0.56	-0.72	-0.59	-0.72	-0.56	-0.47	-3.22	0.46	-3.22	-0.47
F	-0.85	-0.86	-0.82	-0.86	-0.85	-5.32	-5.00	-3.16	-5.00	-5.32
Cl	-0.79	-0.84	-0.76	-0.84	-0.79	-3.98	-4.37	-2.39	-4.37	-3.98
CN	-0.72	-0.84	-0.75	-0.84	-0.72	-2.04	-4.97	-2.08	-4.97	-2.06
NO_2	-0.44	-0.86	-0.78	-0.83	-0.44	-3.14	-5.15	-1.66	-4.93	-3.34

Table 3.12 Change in NMR isotropic shielding constants, $\Delta\sigma$ (in ppm) of $C_6H_5X\cdots Na^+$ complexes.

$C_6H_5X\cdots Na^+$ systems										
X	H_o	H_m	H_p	H_m'	H_o'	C_o	C_m	C_p	C_m'	C_o'
$N(CH_3)_2$	-0.36	-0.61	-0.27	-0.61	-0.36	0.01	-3.36	3.06	-3.36	0.01
$NHCH_3$	-0.37	-0.60	-0.33	-0.62	-0.39	0.49	-3.49	2.40	-3.62	1.17
NH_2	-0.42	-0.64	-0.40	-0.64	-0.42	0.17	-3.83	0.96	-3.83	0.17
NHOH	-0.66	-0.62	-0.42	-0.61	-0.51	-0.24	-3.45	0.82	-3.40	-0.85
CH_3	-0.66	-0.68	-0.61	-0.68	-0.66	-2.71	-3.14	-2.14	-3.14	-2.71
OH	-0.60	-0.67	-0.57	-0.68	-0.61	-2.88	-3.34	-1.05	-4.09	-2.48
H	-0.68	-0.68	-0.68	-0.68	-0.68	-3.36	-3.36	-3.36	-3.36	-3.36
SCH_3	-0.55	-0.58	-0.46	-0.58	-0.59	-1.90	-3.34	-0.24	-2.93	-1.31
SH	-0.63	-0.65	-0.53	-0.60	-0.54	-1.27	-3.24	-0.95	-3.44	-1.01
SiH_3	-0.58	-0.64	-0.58	-0.64	-0.58	-2.46	-3.00	-2.04	-3.00	-2.45
CCH	-0.49	-0.64	-0.53	-0.64	-0.49	-0.59	-3.38	-0.73	-3.38	-0.59
F	-0.65	-0.67	-0.61	-0.67	-0.65	-3.42	-3.65	-1.90	-3.65	-3.42
Cl	-0.64	-0.66	-0.60	-0.66	-0.64	-2.51	-3.07	-1.84	-3.05	-2.49
CN	-0.52	-0.64	-0.57	-0.64	-0.52	-1.01	-3.31	-1.50	-3.31	-1.03
NO_2	-0.58	-0.65	-0.60	-0.65	-0.58	-1.80	-3.02	-1.20	-3.02	-1.80

Table 3.13 Change in NMR isotropic shielding constants, $\Delta\sigma$ (in ppm) of $C_6H_5X\cdots K^+$ complexes.

$C_6H_5X\cdots K^+$ systems										
X	H_o	H_m	H_p	H_m'	H_o'	C_o	C_m	C_p	C_m'	C_o'
$N(CH_3)_2$	-0.34	-0.43	-0.24	-0.44	-0.35	-2.20	-3.76	0.80	-3.77	-2.27
$NHCH_3$	-0.31	-0.50	-0.26	-0.46	-0.36	-1.12	-3.96	0.30	-4.11	-1.08
NH_2	-0.35	-0.49	-0.40	-0.49	-0.35	-0.90	-4.08	-0.91	-4.08	-0.91
NHOH	-0.06	-0.42	-0.34	-0.52	-0.28	3.46	-4.08	-0.53	-4.83	0.70
CH_3	-0.51	-0.54	-0.50	-0.54	-0.51	-2.82	-3.36	-2.52	-3.36	-2.82
OH	-0.48	-0.49	-0.48	-0.55	-0.51	-3.07	-3.59	-1.97	-4.13	-2.75
H	-0.54	-0.54	-0.54	-0.54	-0.54	-3.49	-3.49	-3.49	-3.49	-3.49
SCH_3	-0.49	-0.48	-0.44	-0.48	-0.46	-2.90	-3.78	-1.92	-3.57	-1.59
SH	-0.49	-0.51	-0.48	-0.49	-0.38	-1.56	-3.87	-2.56	-3.96	-1.82
SiH_3	-0.46	-0.48	-0.42	-0.48	-0.46	-3.22	-3.23	-2.49	-3.23	-3.21
CCH	-0.38	-0.52	-0.43	-0.52	-0.38	-0.94	-3.60	-1.88	-3.60	-0.94
F	-0.50	-0.52	-0.49	-0.52	-0.50	-3.04	-3.75	-2.55	-3.75	-3.04
Cl	-0.46	-0.51	-0.50	-0.51	-0.46	-2.24	-3.38	-2.61	-3.38	-2.24
CN	-0.35	-0.51	-0.51	-0.51	-0.35	-0.54	-3.50	-2.61	-3.50	-0.57
NO_2	-0.42	-0.48	-0.51	-0.47	-0.41	-1.72	-3.24	-2.37	-3.10	-1.53

Table 3.14 Change in NMR isotropic shielding constants, $\Delta\sigma$ (in ppm) of $C_6H_5X\cdots NH_4^+$ complexes.

$C_6H_5X\cdots NH_4^+$ systems										
X	H_o	H_m	H_p	H_m'	H_o'	C_o	C_m	C_p	C_m'	C_o'
$N(CH_3)_2$	-0.27	-0.46	-0.31	-0.47	-0.31	0.01	-4.35	-0.87	-4.37	-0.97
$NHCH_3$	-0.29	-0.51	-0.34	-0.47	-0.33	-0.21	-4.30	-1.36	-4.63	0.79
NH_2	-0.31	-0.54	-0.46	-0.51	-0.34	0.06	-5.05	-2.79	-4.31	-1.43
NHOH	-0.57	-0.46	-0.40	-0.52	-0.39	-1.25	-3.85	-2.30	-3.89	-0.91
CH_3	-0.48	-0.54	-0.52	-0.49	-0.53	-2.34	-3.76	-4.39	-2.79	-3.49
OH	-0.51	-0.52	-0.55	-0.55	-0.43	-3.56	-3.31	-4.06	-4.63	-2.18
H	-0.53	-0.62	-0.56	-0.53	-0.62	-3.11	-5.49	-4.14	-3.12	-5.49
SCH_3	-0.48	-0.47	-0.46	-0.47	-0.44	-1.80	-4.41	-3.29	-3.46	-1.81
SH	-0.59	-0.57	-0.53	-0.46	-0.27	-0.79	-3.56	-3.69	-4.54	-1.69
SiH_3	-0.42	-0.50	-0.52	-0.51	-0.43	-2.17	-3.36	-4.00	-3.57	-2.55
CCH	-0.34	-0.53	-0.50	-0.51	-0.36	-0.01	-4.21	-3.15	-3.45	-1.01
F	-0.39	-0.60	-0.61	-0.53	-0.57	-2.24	-3.94	-5.28	-3.08	-6.92
Cl	-0.49	-0.56	-0.57	-0.53	-0.52	-1.61	-3.92	-4.02	-3.11	-2.57
CN	-0.33	-0.52	-0.53	-0.49	-0.34	0.14	-4.01	-3.56	-3.53	-0.19
NO_2	-0.33	-0.48	-0.53	-0.45	-0.31	-0.44	-3.24	-3.28	-2.47	-1.24

In order to understand the effect of intermolecular distance (R) on σ values, NMR shielding constants are computed for R values in the range 1.5 Å to 7.0 Å and taken in steps of 0.5 Å for $C_6H_5X\cdots M^+$ (M^+ = Li^+, Na^+, K^+, NH_4^+ and X = H, CH_3, NH_2, and CN). These σ-scan plots for $C_6H_5X\cdots M^+$ (M^+ = Li^+, Na^+, K^+, NH_4^+) complexes are shown in Figure 3.6, 3.7, 3.8 and 3.9 for Li^+, Na^+, K^+, and NH_4^+ respectively. In all the cases of $C_6H_6\cdots M^+$, σ-scan plot indicates that the magnitude of deshielding decreases as M^+ moves away from the

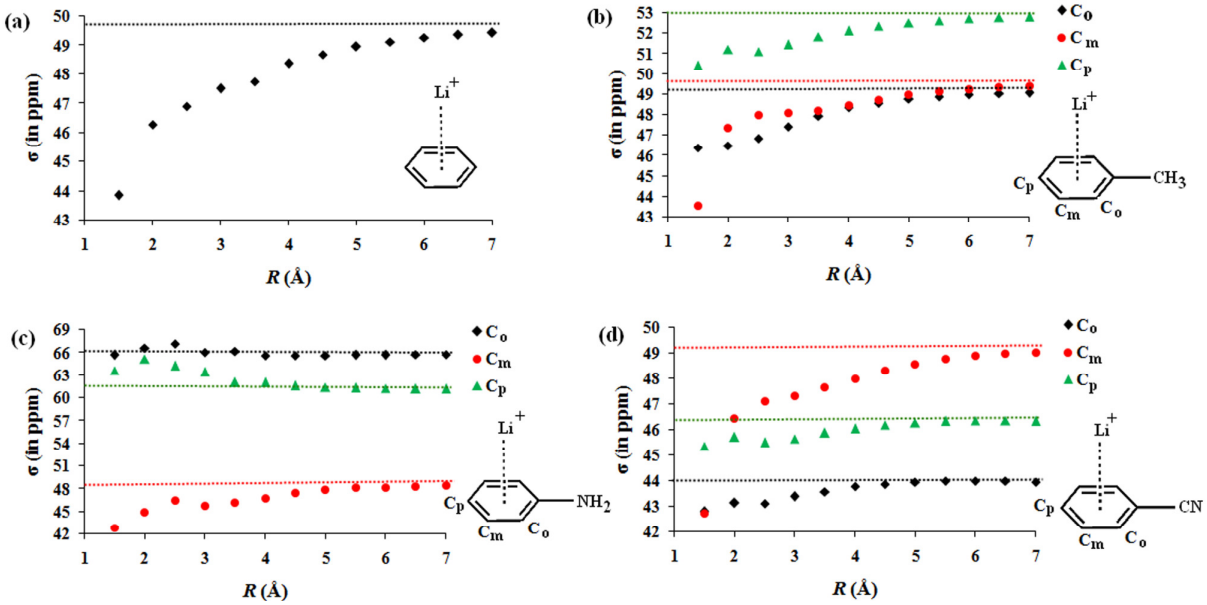

Figure 3.6 Dependence of σ at the C nuclei of $C_6H_5X\cdots Li^+$ with the intermolecular distance, R (Å). The dotted horizontal lines represent the C_m (red), C_o (black), and C_p (green) σ-values of C_6H_5X. (a) X = H (b) X = CH_3 (c) X = NH_2 (d) X = CN.

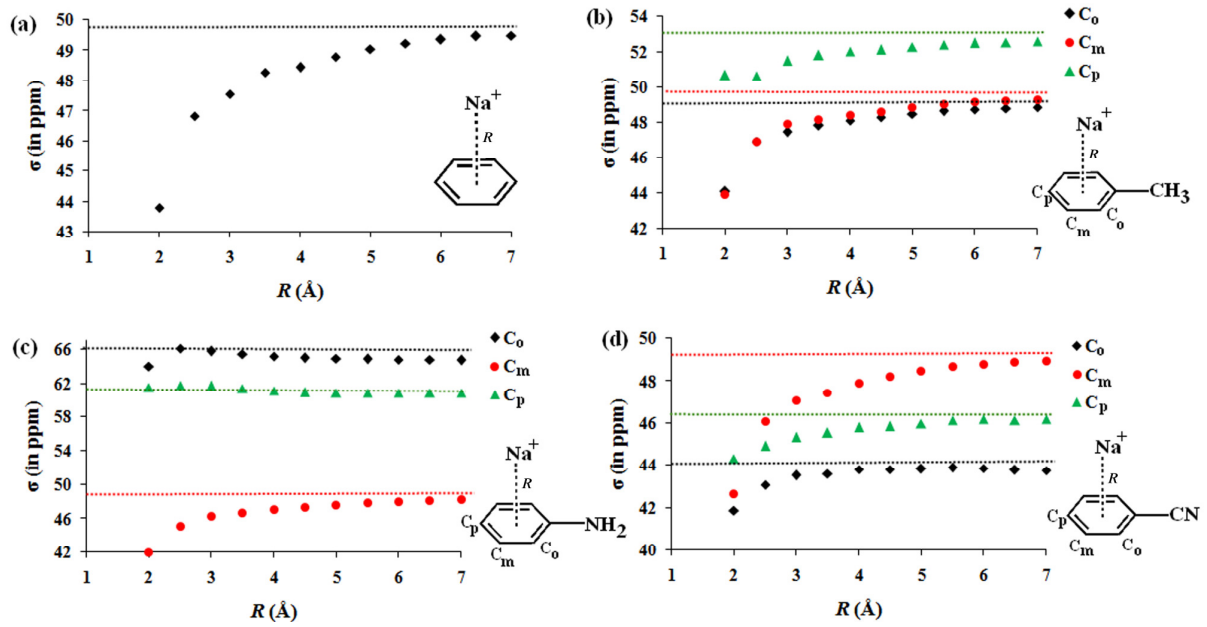

Figure 3.7 Dependence of σ at the C nuclei of $C_6H_5X\cdots Na^+$ with the intermolecular distance, R (Å). The dotted horizontal lines represent the C_m (red), C_o (black), and C_p (green) σ-values of C_6H_5X. (a) X = H (b) X = CH_3 (c) X = NH_2 (d) X = CN.

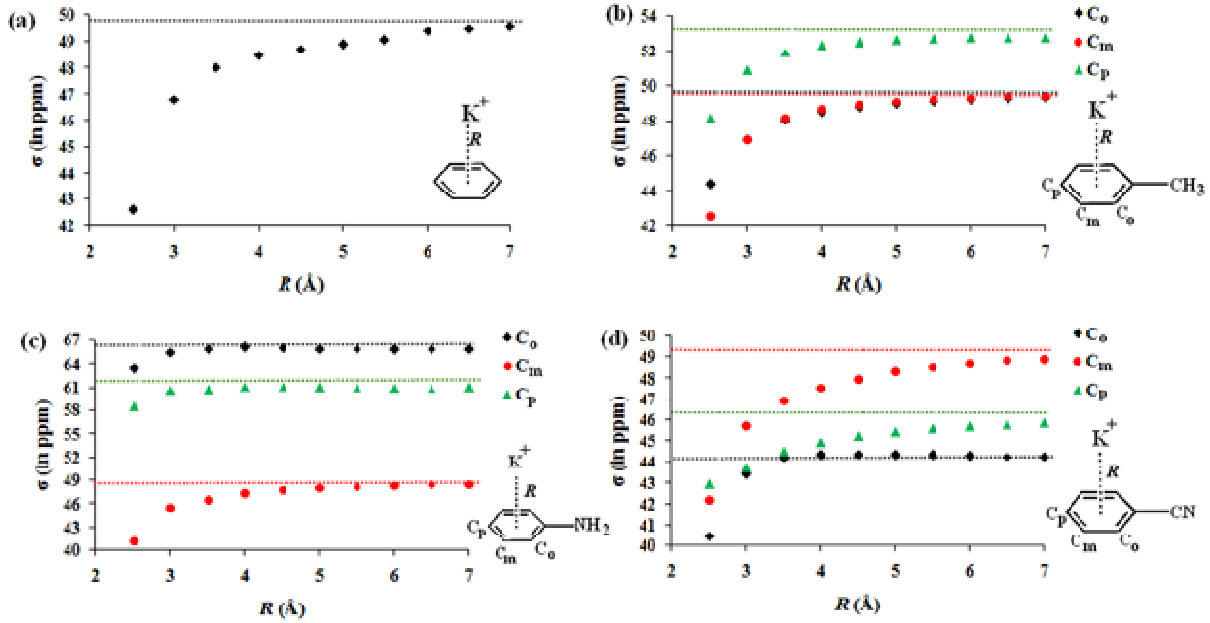

Figure 3.8 Dependence of σ at the C nuclei of $C_6H_5X\cdots K^+$ with the intermolecular distance, *R* (Å). The dotted horizontal lines represent the C_m (red), C_o (black), and C_p (green) σ-values of C_6H_5X. (a) X = H (b) X = CH_3 (c) X = NH_2 (d) X = CN.

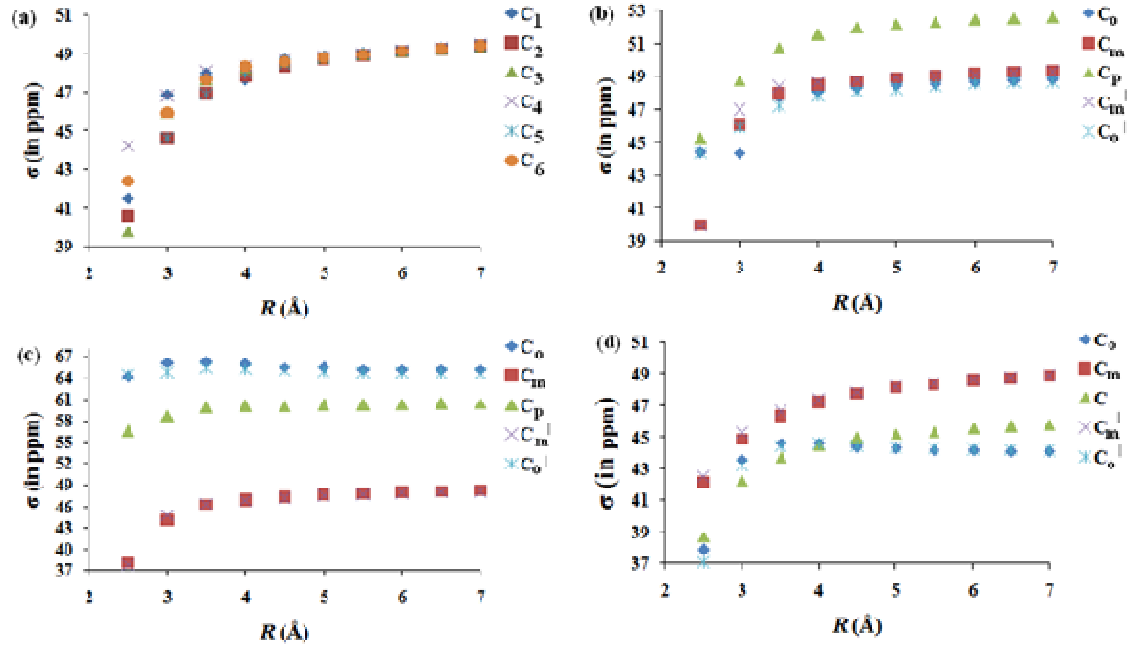

Figure 3.9 Dependence of σ at the C nuclei of $C_6H_5X\cdots NH_4^+$ with the intermolecular distance, *R* (Å). (a) X = H (b) X = CH_3 (c) X = NH_2 (d) X = CN.

benzene. However, even at 4.5 Å, the cation causes a significant deshielding on the π-carbons (~1.0 ppm). For CH_3 and CN substituted complexes, C_o, C_m and C_p atoms are significantly deshielded up to R = 4.5 Å and beyond that distance, σ of $C_6H_5X\cdots M^+$ slowly converges to σ of C_6H_5X. These results strongly suggest that the deshielding effect of a cation is significant up to 4.5 Å.

3.8 Conclusions

In part A of this chapter, a methodology for the quantification of inductive (I), resonance (R) and through-space (TS) effects of a variety of substituents (X) in cation-π interactions of the type $C_6H_5X\cdots Na^+$ can be achieved by modeling **1**, **2**, **2'** and **3** systems and by applying an extrapolation procedure to the corresponding interaction energies was developed. The extrapolation procedure avoids direct interaction of X with aromatic π-system and facilitates the computation of classical effects such as inductive, resonance and through-space effects. The electron-withdrawing substituents contribute largely through TS effect whereas the electron donating substituents give more resonance contribution to the total interaction energy. We have also confirmed that the computed substituent effect show only minor variation with respect to the choice of the method. The most unique result is that the total interaction energy of $C_6H_5X\cdots Na^+$ is a sum of E_I, E_R and E_{TS} which brings out the unified view that the cation-π interactions are controlled by the combined effect of I, R and TS of substituents and not solely by any one of them.

In part B of this chapter, the NMR characterization of substituent effects in $C_6H_5X\cdots M^+$ ($M^+ = Li^+$, Na^+, K^+, NH_4^+) cation-π complexes in terms of the isotropic nuclear magnetic shielding constants (σ), was discussed. A linear relationship between σ_M^+ and σ_p is established which suggests that substituent effects on cation-π interaction can be quantified using NMR parameters. The presence of a cation over benzenoid ring always causes deshielding at the hydrogen as well as all deshielding at *meta* carbon atoms regardless of the electron donating or electron withdrawing nature of X and this property can be used to detect cation-π interaction through NMR experiments. Further, σ-scan plots show that the deshielding persists even at large R values.

Chapter 4

Accurate Prediction of Cation-π Interaction Energy Using Molecular Electrostatic Potential Topography

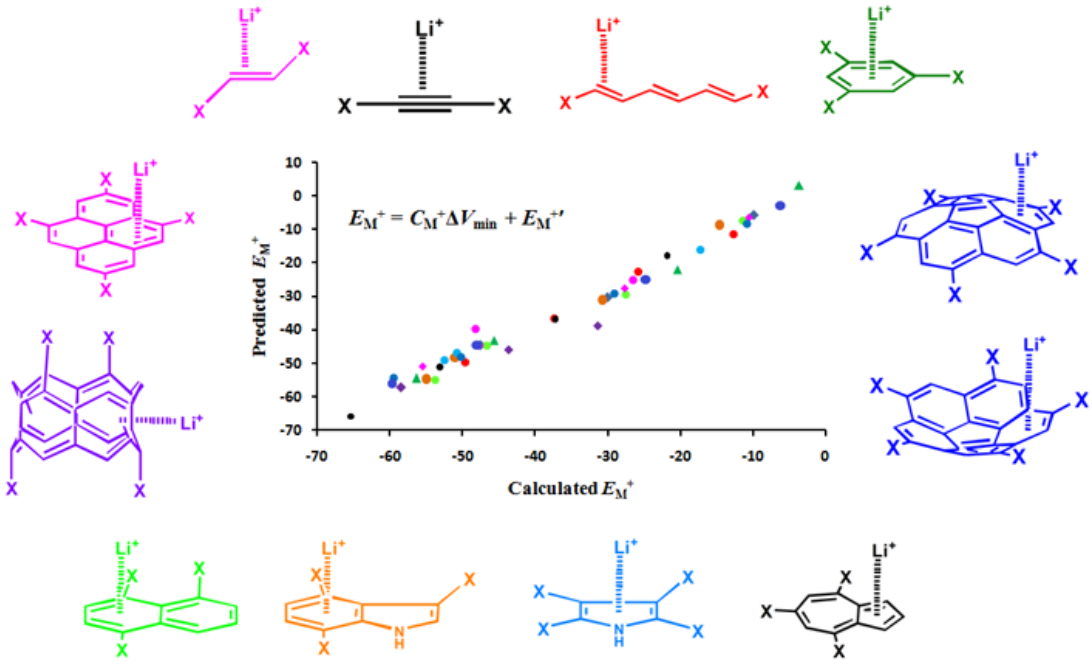

4.1 Abstract

A molecular electrostatic potential (MESP) topography based approach has been proposed to quantify substituent effects on cation-π interactions in Φ-X···M^+ complexes where Φ, X and M^+ are the π-system, substituent and cation, respectively. The cation-π interaction energy, E_M^+ showed a strong linear correlation with the MESP based measure of the substituent effect, ΔV_{min}, (difference between MESP minimum (V_{min}) on the π-region of a substituted system and the corresponding unsubstituted system). The linear relationship is $E_M^+ = C_M^+(\Delta V_{min}) + E_M^{+\prime}$ where C_M^+ is reaction constant and $E_M^{+\prime}$ is cation-π interaction energy of the unsubstituted complex. This relationship is similar to Hammett equation and its first term yields the substituent contribution of the cation-π interaction energy. Further, a linear correlation between C_M^+ and $E_M^{+\prime}$ has been established which facilitates the prediction of C_M^+ for unknown cations. Thus, a prediction of E_M^+ for any Φ-X···M^+ complex is achieved by knowing the values of $E_M^{+\prime}$ and ΔV_{min}. The generality of the equation is tested for a variety of cations (Li^+, Na^+, K^+, Mg^+, $BeCl^+$, $MgCl^+$, $CaCl^+$, $TiCl_3^+$, $CrCl_2^+$, $NiCl^+$, Cu^+, $ZnCl^+$, NH_4^+, $CH_3NH_3^+$, $N(CH_3)_4^+$, $C(NH_2)_3^+$), substituents ($N(CH_3)_2$, NH_2, OCH_3, CH_3, OH, H, SCH_3, SH, CCH, F, Cl, COOH, CHO, CF_3, CN, NO_2) and a large number of π-systems. The tested systems also include multiple substituted π-systems, viz. ethylene, acetylene, hexa-1,3,5-triene, benzene, naphthalene, indole, pyrrole, phenylalanine, tryptophan, tyrosine, azulene, pyrene, [6]-cyclacene, and corannulene and found that E_M^+ follows the additivity of substituent effects. Further, substituent effects on cationic sandwich complexes of the type $C_6H_6\cdots M^+\cdots C_6H_5X$ have been assessed and found that E_M^+ can be predicted with 97.7 % accuracy using the values of $E_M^{+\prime}$ and ΔV_{min}. All the Φ-X···M^+ systems showed good agreement between calculated and predicted E_M^+ values, suggesting that the ΔV_{min} approach to substituent effect is accurate and useful for predicting the interactive behaviour of substituted π-systems with cations.

4.2 Introduction

The cation-π interactions are experimentally observed [De Wall *et al.* 1999, Gokel *et al*. 2000, Meadows *et al*. 2001] noncovalent interactions which play an important role in organic synthesis [Ribelin *et al.* 2008, Yamada 2007, Yamada and Tokugawa 2009, Yamada *et al*. 2007], crystal packing [Busi *et al.* 2008], molecular recognition and in various biological process [Matsumura *et al.* 2008, Orner *et al.* 2002, Salonen *et al.* 2009, Zhong *et al.* 1998]. The importance of these interactions in biology is significantly explored by Dougherty and co-workers [Gallivan and Dougherty 1999, Mecozzi *et al.* 1996a, Xiu *et al.* 2009, Zhong *et al*. 1998]. Several attempts have been made to understand cation-π interactions quantitatively, using various experimental techniques such as High Pressure Mass Spectroscopy, threshold collision-induced dissociation and ^{1}H NMR titrations [Amunugama and Rodgers 2002[a, b, c,] Hunter *et al*. 2002, Wu and McMahon 2008]. Several theoretical works [Engerer and Hanusa 2011, Kim *et al.* 2003, Kim *et al.* 2007, Liu *et al.* 2001, Liu *et al.* 2004, Lucas *et al.* 2009, Marshall *et al.* 2009, Reddy and Sastry 2005, Watt *et al.* 2009, Yi *et al.* 2009] have been devoted to understand the origin of cation-π interactions by decomposing the total interaction energy into electrostatic, induction, charge-transfer, Pauli repulsion and dispersion components. It was shown that these components vary depending on the type of interacting cation. For example, electrostatic effect is mainly responsible for the attraction in the case of $C_6H_6\cdots Na^+/K^+$, whereas the induction effect dominates in $C_6H_6\cdots Li^+$, $C_6H_6\cdots Be^{+2}$, $C_6H_6\cdots Mg^{+2}$, and $C_6H_6\cdots Ca^{+2}$ [Tsuzuki *et al.* 2003]. Dispersion is also shown to be important for cations like NMe_4^+ [Liu *et al*. 2001, Soteras *et al*. 2008].

The knowledge of substituent effect is of fundamental importance in many areas of chemistry for understanding a wide range of chemical problems, including cation-π interaction [Adcock and Trout 1999, Krygowski and Stepień 2005]. In an elegant work, Yamada *et al*. showed that in the photodimerization reaction of *trans*-4-styrylpyridines (SP),

pyridinium-π interaction plays a decisive role for the selective formation of *syn*-SP dimer [Yamada *et al*. 2007]. They observed that the selective formation of *syn*-SP dimer is enhanced to ~95% with the presence of electron-donating OCH_3 group on the π-system while it is reduced to ~27% when electron-withdrawing CF_3 is present on the π-system when compared with the unsubstituted one (~64%). The prominent studies that address the importance of substituent effects in cation-π interactions are by Hunter *et al*.,[Hunter *et al*. 2002] Dougherty and co-workers,[Mecozzi *et al*. 1996[a]] and Wheeler and Houk.[Wheeler and Houk 2009[a]]. Hunter *et al*. quantified the cation-π interaction energies using a chemical double mutant cycle and showed that the interaction energies are very sensitive to the electronic-nature of the substituent [Hunter *et al*. 2002]. Dougherty and co-workers [Mecozzi *et al*. 1996[a]] showed that subtle variations in cation-π interactions due to the substituents can be monitored using electrostatic potential. They also suggested a model that the cation-π interaction energy can be estimated by evaluating the electrostatic potential at a point of equilibrium distance between the cation and the centroid of the π-system. Recently, Wheeler and Houk [Wheeler and Houk 2009[a]] reported that the substituent effects in cation-π interactions are mainly due to through-space interactions. On the other hand, Hallowita *et al*. emphasized the importance of inductive effects in $C_6H_5X\cdots M^+$ complexes ($M^+ = Na^+$, K^+ and X = Cl, Br and I) [Hallowita *et al*. 2009]. However, all the above studies are confined to the monosubstituted systems and the effect of multiple substituents on the cation-π interactions is yet to be explored.

In chapter 2, it was shown that MESP minimum (designated as V_{min}) calculated over the π-region of a molecule provides a convenient way to assess the substituent effect. Further, quantification of *ortho*-effect, through-space effect, and resonance effect using the MESP topography in a variety of substituted systems has promised the use of this electronic descriptor for the prediction of substituent effects. In this chapter, the utility of MESP

topography for the quantification of substituent effects in the cation-π interactions is discussed. For this purpose, Φ-X$\cdots$M$^+$ and Φ$\cdots$M$^+\cdots$Φ-X type systems (Φ = π-system, X = substituent and M$^+$ = cation) are selected. The three π-systems, *viz.* benzene, naphthalene, and indole and four cations, *viz.* Li$^+$, Na$^+$, K$^+$, and NH_4^+ (Figure 4.1) are the main focus in this chapter. Benzene derivatives are widely studied cation-π systems while studies on naphthalene ($C_{10}H_7X\cdots M^+$), and indole ($C_8H_6NX\cdots M^+$) are limited [Amunugnama and Rodgers 2003, Dunbar 1998, Reddy and Sastry 2005, Ruan *et al.* 2007, Zhong *et al*. 1998]. Naphthalene is an extended π-conjugated system to benzene while indole is a model for the

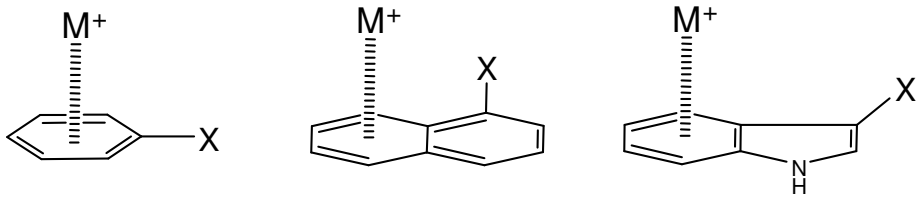

(a) **(b)** **(c)**

M$^+$ = Li$^+$, Na$^+$, K$^+$, and NH_4^+

X = $N(CH_3)_2$, NH_2, OH, CH_3, H, F, Cl, CN and NO_2

Figure 4.1 Cation-π complexes considered for the present study. (a) $C_6H_5X\cdots M^+$ (b) $C_{10}H_7X\cdots M^+$ (c) $C_8H_6NX\cdots M^+$.

tryptophan moiety, the most frequently encountered moiety for cation-π interactions in biological systems [Dougherty 2007, Zhong *et al*. 1998]. Further, to test the generality of the V_{min} approach, cation-π interactions of C_6H_5X, $C_{10}H_7X$, C_8H_6NX, (X = $N(CH_3)_2$, NH_2, OCH_3, CH_3, OH, H, SCH_3, SH, CCH, F, Cl, COOH, CHO, CF_3, CN, NO_2) with a variety of cations, *viz*. alkali metals, organic cations, derivatives of alkaline earth metals, and transition metals are studied. The selected cations are Li$^+$, Na$^+$, K$^+$, $BeCl^+$, $MgCl^+$, $CaCl^+$, $TiCl_3^+$, $CrCl_2^+$, $NiCl^+$, Cu$^+$, $ZnCl^+$, NH_4^+, $CH_3NH_3^+$, $N(CH_3)_4^+$, $C(NH_2)_3^+$. The V_{min} approach is also validated by modeling the cation-π interactions in a variety of Φ-$X_n\cdots Li^+$ systems where Φ = ethylene, acetylene, hexa-1,3,5-triene, benzene, naphthalene, indole, pyrrole, phenylalanine, tryptophan, tyrosine, azulene, pyrene, [6]-cyclacene, and corannulene and X_n corresponds to

multiple substitution. Multiple substitutions are considered to bring out the additivity of substituent effects. The V_{min} approach is also expanded to include the cationic sandwich complexes of the type $C_6H_6\cdots M^+\cdots C_6H_5X$.

4.3 Computational details

In chapter 3, it was shown that the cation-π interaction energy, E_{M^+} of $C_6H_5(CHCH)X\cdots M^+$ ($M^+ = Na^+$) systems showed that B3LYP/6-311+G(d,p) method can provide reliable results comparable to those obtained from the MP2 method. Moreover, the trend of substituent effects on E_{M^+} was nearly independent of the method used. Prior studies also demonstrated that the substituent effects quantified in terms of V_{min} at various basis sets and various methods followed the same trend [Gadre *et al*. 1995, Mathew and Suresh 2010, Suresh *et al*. 2008, Suresh and Gadre 2007]. Hence, the B3LYP/6-311+G(d,p) method is selected for all the calculations. All the cation-π complexes are optimized without any symmetry constraints. However, for a few cases wherein the cation showed strong interaction with the substituent, a restricted optimization has been done to ensure the formation of a cation-π complex. Further, frequency calculation is performed on all the complexes and verified that all the normal modes of vibrations are real. All the computational calculations have been carried out using Gaussian 03 suite of programs [Frisch *et al*.].

The V_{min} is calculated by generating a cube file using the keyword cube=(potential,60) and the exact location of V_{min} point is obtained using prop=(potential,opt) keyword in Gaussian 03. From hereafter, MESP minimum obtained over the substituted π-system is designated as V_{min} and relative V_{min} with respect to X = H is designated as ΔV_{min}. ΔV_{min} is obtained by subtracting V_{min} of unsubstituted system from V_{min} of substituted system ($\Delta V_{min} = V_{min}(X) - V_{min}(H)$) [Sayyed and Suresh 2009[b], Sayyed *et al*. 2010]. ΔV_{min} exclusively represents the

substituent effect [Sayyed and Suresh 2009b, Sayyed *et al*. 2010, Suresh and Gadre 1998]. A positive value of ΔV_{min} characterizes electron withdrawing ability while a negative value indicates electron donating ability of X [Sayyed *et al*. 2010, Suresh and Gadre 1998, 2007].

4.4 Results and Discussion

4.4.1 MESP Topography and Effect of Substituent

In Figure 4.2, MESP isosurfaces of C_6H_5X, $C_{10}H_7X$, C_8H_6NX systems for a representative set of substituents (X = NH_2, CH_3, H, F, and CN) are shown along with the V_{min} values. In Table 4.1, V_{min} and ΔV_{min} values for all the systems are presented. Compared to benzene, V_{min} of aniline and toluene are more negative, indicating the electron donating ability of NH_2 and CH_3 groups whereas V_{min} of fluorobenzene and benzonitrile are less negative than benzene, indicating the electron withdrawing ability of F and CN groups [Gadre and Suresh 1997, Suresh and Gadre 1998, 2007]. V_{min} of naphthalene (-14.8 kcal/mol) is less negative than the V_{min} of benzene (-15.7 kcal/mol) and this behavior is expected because former has ten π-electrons and shared over two 6-membered rings to give five electrons per ring while latter has six π-electrons in one ring. The magnitude of ΔV_{min} is higher in the case of benzene derivatives than naphthalene derivatives, indicating that substituent effect is higher in the former than the latter. In the case of indole systems, all

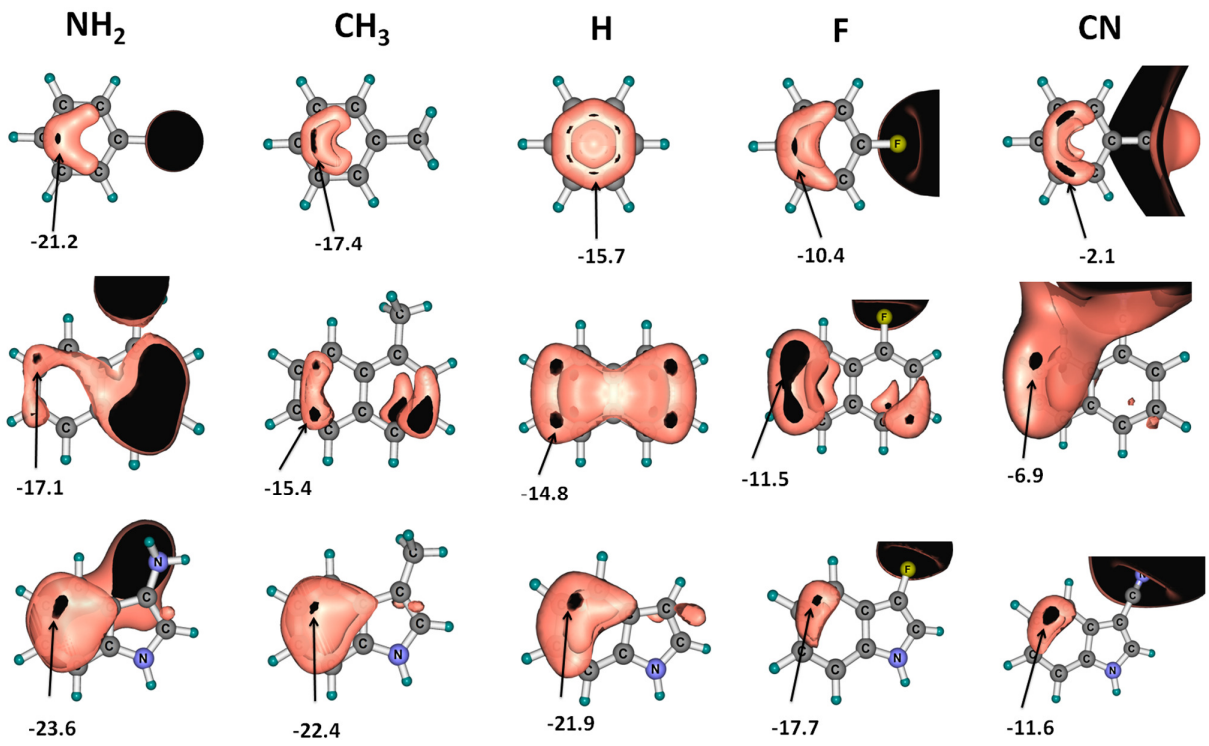

Figure 4.2 Representation of MESP using isosurfaces for substituted π-systems. V_{min} value (in kcal/mol) is indicated with an arrow mark. Benzene, naphthalene, and indole derivatives are shown in the first, second, and third rows, respectively.

Table 4.1 V_{min} and ΔV_{min} values of substituted π-systems. All values are in kcal/mol.

	V_{min}			ΔV_{min}		
X	C_6H_5X	$C_{10}H_7X$	C_8H_6NX	C_6H_5X	$C_{10}H_7X$	C_8H_6NX
$N(CH_3)_2$	-23.0	-17.6	-23.1	-7.3	-2.8	-1.2
NH_2	-21.2	-17.1	-23.6	-5.6	-2.3	-1.7
CH_3	-17.4	-15.4	-22.4	-1.7	-0.6	-0.6
OH	-16.1	-16.3	-22.3	-0.4	-1.5	-0.5
H	-15.7	-14.8	-21.9	0.0	0.0	0.0
F	-10.4	-11.5	-17.7	5.3	3.2	4.2
Cl	-9.5	-11.6	-17.6	6.1	3.2	4.3
CN	-2.1	-6.9	-11.6	13.6	7.9	10.2
NO_2	0.0	-5.7	-10.2	15.7	9.0	11.7

electron donating and electron withdrawing substituents showed more negative V_{min} on the 6-membered ring than on the 5-membered ring. This feature suggests a preferable regioselective binding of a cation on the electron rich 6-membered ring. Rodgers and co-workers [Ruan *et al.* 2005] experimentally observed this kind of regioselective binding of the cations on indole systems. Compared to benzene, 6-membered ring of indole shows more negative V_{min} which can be attributed to the electron-donation from nitrogen lone-pair through the N-heterocycle whereas the magnitude of ΔV_{min} is smaller than that of a corresponding benzene derivative. V_{min} data indicate that 6-membered ring of indole is the most electron rich followed by benzene and naphthalene.

4.4.2 Relationship between V_{min} and Cation-π Interaction Energy

In Figure 4.3, optimized geometries of $C_6H_5X\cdots K^+$, $C_{10}H_7X\cdots K^+$, and $C_8H_6NX\cdots K^+$, (X = NH_2, CH_3, H, F, and CN) systems are shown along with the intermolecular distance, d_{M^+}, defined as the distance from centroid of the π-ring to M^+. Compared to d_{M^+} of an unsubstituted system, d_{M^+} of an electron donating substituted system is smaller while d_{M^+} of an electron withdrawing substituted system is larger for a majority of systems. For all the substituents, irrespective of the π-system, d_{M^+} follows the order $Li^+ < Na^+ < K^+ < NH_4^+$. The geometrical parameters indicate that the cation-π interaction depends on the substituent, nature of the π-system and the cation.

In Table 4.2, the cation-π interaction energy, E_{M^+} of $C_6H_5X\cdots M^+$, $C_{10}H_7X\cdots M^+$, and $C_8H_6NX\cdots M^+$ (M^+ = Li^+, Na^+, K^+, and NH_4^+) systems is reported. For all the cation-π complexes, higher interaction energy is observed for electron donating substituents and lower interaction energy is observed for electron withdrawing substituents. The trend observed for the substituent effect in the case of E_{M^+} is very similar to that of ΔV_{min} which is evident in the strong linear correlation obtained for ΔV_{min} and E_{M^+} given in Figure 4.4a for $C_6H_5X\cdots M^+$

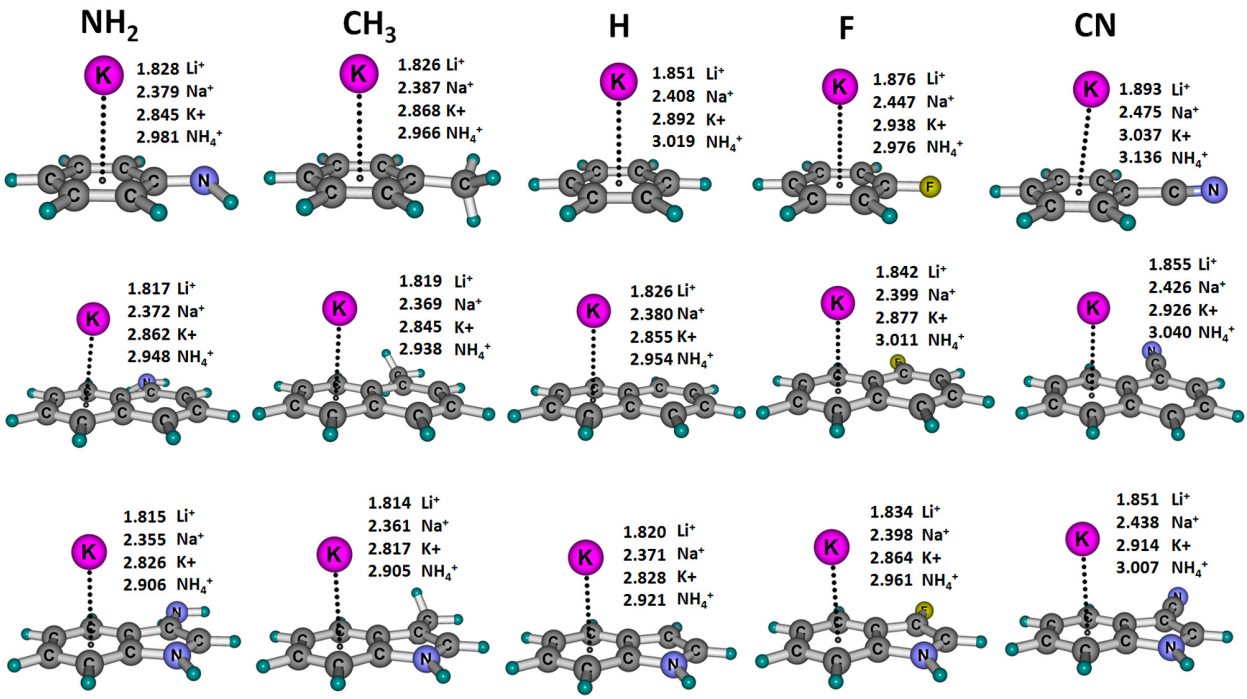

Figure 4.3 Optimized geometries of $C_6H_5X\cdots K^+$, $C_{10}H_7X\cdots K^+$, $C_8H_6NX\cdots K^+$, and (X = NH_2, CH_3, H, F, and CN) systems. The intermolecular distance, $d_{M}{}^{+}$ (in Å) is also given.

Table 4.2 $E_{M}{}^{+}$ values (in kcal/mol) of $C_6H_5X\cdots M^+$, $C_{10}H_7X\cdots M^+$, $C_8H_6NX\cdots M^+$ and (M^+ = Li^+, Na^+, K^+ and $NH_4{}^+$) systems.

	$C_6H_5X\cdots M^+$				$C_{10}H_7X\cdots M^+$				$C_8H_6NX\cdots M^+$			
X	$E_{Li}{}^{+}$	$E_{Na}{}^{+}$	$E_{K}{}^{+}$	$E_{NH4}{}^{+}$	$E_{Li}{}^{+}$	$E_{Na}{}^{+}$	$E_{K}{}^{+}$	$E_{NH4}{}^{+}$	$E_{Li}{}^{+}$	$E_{Na}{}^{+}$	$E_{K}{}^{+}$	$E_{NH4}{}^{+}$
$N(CH_3)_2$	-48.4	-31.1	-22.4	-22.3	-45.3	-29.4	-21.6	-21.5	-48.9	-32.2	-23.8	-23.8
NH_2	-44.8	-28.7	-20.8	-20.6	-44.1	-28.7	-21.2	-21.1	-48.5	-30.4	-24.0	-23.9
CH_3	-40.8	-25.1	-17.3	-17.0	-42.1	-26.6	-18.9	-18.8	-47.2	-30.5	-22.1	-22.0
OH	-38.4	-23.5	-16.3	-16.4	-42.3	-27.1	-19.4	-19.5	-46.6	-30.4	-22.3	-22.2
H	-37.8	-23.4	-15.8	-15.5	-40.5	-25.5	-18.0	-17.9	-45.7	-29.5	-21.3	-21.3
F	-31.8	-18.5	-12.1	-10.8	-36.9	-22.5	-15.5	-15.6	-41.2	-25.8	-18.2	-18.1
Cl	-32.6	-19.1	-12.7	-12.4	-37.2	-22.8	-15.8	-15.9	-41.7	-26.2	-18.5	-18.4
CN	-25.0	-13.0	-7.7	-7.5[a]	-32.1	-18.5	-12.0	-12.0	-35.5	-21.0	-14.0	-13.9
NO_2	-22.5	-10.9	-5.9[a]	-5.8[a]	-30.7	-17.3[a]	-10.8[a]	-10.7	-33.8	-19.8	-12.8	-12.8

[a] Cation is restricted to interact with the π-region as it prefers binding with the substituent.

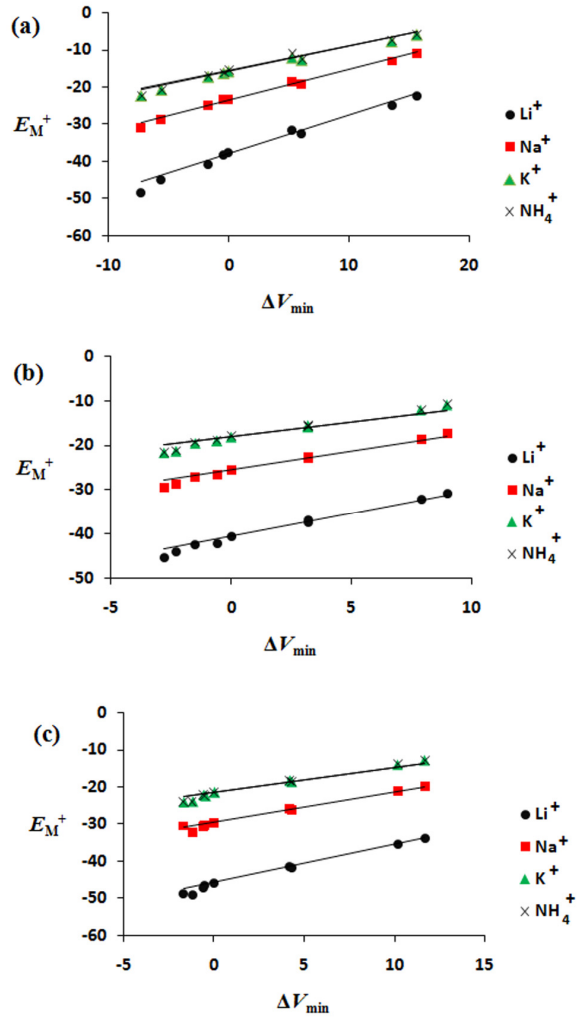

Figure 4.4 ΔV_{min} vs E_{M^+} correlations for (a) $C_6H_5X\cdots M^+$ (b) $C_{10}H_7X\cdots M^+$ (c) $C_8H_6NX\cdots M^+$ ($M^+ = Li^+$, Na^+, K^+, and NH_4^+).

complexes. To draw these correlation lines, the intercept is set equal to the interaction energy of unsubstituted benzene complex. This condition on the intercept is made because the value of the intercept of the best fit line was very close to the interaction energy of the $C_6H_6\cdots M^+$ complex. The correlation equations for $C_6H_5X\cdots M^+$ ($M^+ = Li^+$, Na^+, K^+ and NH_4^+) are shown in Table 4.3. The first term of these equations exclusively represents the contribution of the substituent effects on the cation-π interaction energy. An increase/decrease in the value of slope indicates stronger/weaker interaction of the cation on the π-system. On the basis of this interpretation, we can conclude that E_{M^+} of $C_6H_5X\cdots M^+$ follows the order $E_{Li^+} > E_{Na^+} > E_{K^+} \approx$

E_{NH4}^{+}. In Figure 4.4b and 4.4c, (ΔV_{min}, E_M^+) correlation line are shown for the $C_{10}H_7X\cdots M^+$ and $C_8H_6NX\cdots M^+$ systems, respectively. To derive these linear relationships, the intercept is fixed to the value of the interaction energy of the unsubstituted cation-π complex. Further, the slope of each line is assumed to be equal to the slope obtained for each cation using the benzene derivatives (Table 4.3). This assumption on the slope is valid due to the reason that substituent effect is largely transferable from one π-system to another. The correlation plots shown in Figure 4.4b and 4.4c obtained using these assumptions on slope and intercept is

Table 4.3 Linear relationship between E_M^+ and ΔV_{min} for various cation-π complexes. Mean absolute deviation (MAD) of the predicted E_M^+ from the calculated E_M^+ and correlation coefficient (r) of the best fit line are also given.

System	Linear equation	r	MAD
$C_6H_5X\cdots Li^+$	$E_{Li}^+ = 1.026\ \Delta V_{min} - 37.8$	0.986	0.27
$C_6H_5X\cdots Na^+$	$E_{Na}^+ = 0.819\ \Delta V_{min} - 23.4$	0.993	0.10
$C_6H_5X\cdots K^+$	$E_K^+ = 0.655\ \Delta V_{min} - 15.8$	0.985	0.14
$C_6H_5X\cdots NH_4^+$	$E_{NH4}^+ = 0.660\ \Delta V_{min} - 15.5$	0.979	0.26
$C_{10}H_7X\cdots Li^+$	$E_{Li}^+ = 1.026\ \Delta V_{min} - 40.5$	0.988	0.58
$C_{10}H_7X\cdots Na^+$	$E_{Na}^+ = 0.819\ \Delta V_{min} - 25.5$	0.988	0.60
$C_{10}H_7X\cdots K^+$	$E_K^+ = 0.655\ \Delta V_{min} - 18.0$	0.983	0.77
$C_{10}H_7X\cdots NH_4^+$	$E_{NH4}^+ = 0.655\ \Delta V_{min} - 17.9$	0.981	0.73
$C_8H_6NX\cdots Li^+$	$E_{Li}^+ = 1.026\ \Delta V_{min} - 45.7$	0.987	0.34
$C_8H_6NX\cdots Na^+$	$E_{Na}^+ = 0.819\ \Delta V_{min} - 29.5$	0.988	0.25
$C_8H_6NX\cdots K^+$	$E_K^+ = 0.655\ \Delta V_{min} - 21.3$	0.980	0.65
$C_8H_6NX\cdots NH_4^+$	$E_{NH4}^+ = 0.655\ \Delta V_{min} - 21.3$	0.982	0.66

found to be in good agreement with the best fit lines. The mean absolute deviation of the predicted E_M^+ value from that obtained from the best fit line is 0.19 kcal/mol. It is noteworthy that in all the complexes of K^+ and NH_4^+, E_K^+ is nearly identical to E_{NH4}^+. A similar observation has been previously noted by Sastry *et al*. [Reddy and Sastry 2005] and Mohajeri *et al*.[Mohajeri and Karimi 2006] in the case of cation-π complexes of unsubstituted benzene with K^+ and NH_4^+.

The set of equations shown in Table 4.3 can be expressed by the following general form,

$$E_M^+ = C_M^+(\Delta V_{min}) + E_M^{+'} \qquad \text{(Eq. 4.1)}$$

where C_M^+ is a characteristic constant for the interaction of M^+ with the π-system and $E_M^{+'}$ is the interaction energy of M^+ with the unsubstituted π-system. Eq. 4.1 is very similar to the Hammett equation,

$$\log(k_X) = \rho\sigma + \log(k_H) \qquad \text{(Eq. 4.2)}$$

where k_X, k_H, ρ and σ are rate constant of substituted molecule, rate constant of unsubstituted molecule, reaction constant and Hammett substituent constant, respectively. The ρ value varies with respect to the type of reaction, for example, $\rho = 1.000$ for ionization of substituted benzoic acids while $\rho = 0.466$ for ionization of substituted cinnamic acids. Similarly, in Eq. 4.1, C_M^+ acts as a reaction constant for the reaction between cation and π-system. For instance, C_M^+ is 1.026 for Li^+ and 0.819 for Na^+ which means that Li^+ binds more strongly to π-systems than Na^+. ΔV_{min} serves the role of σ, the substituent constant [Sayyed and Suresh 2009[b], Sayyed *et al*. 2010, Suresh and Gadre 2007].

4.4.3 Effect of Multiple Substituents on $C_6H_{6-n}X_n\cdots M^+$ (M^+ = Li^+, Na^+, K^+, and NH_4^+) Complexes

In order to understand the effect of multiple substituents in cation-π interactions, a comprehensive study on the substituted benzenes has been carried out. The optimized geometries of $C_6H_{6-n}X_n\cdots Na^+$ (X = NH_2, CH_3, F and CN; n = 1, 2, 3, and 6) complexes calculated at B3LYP/6-311+G(d,p) level are shown in Figure 4.5. The optimum intermolecular distance, $d_M{}^+$ is also shown in Figure 4.5. In the case of X = NH_2 as well as X = CH_3, a systematic decrease in $d_M{}^+$ value from mono to hexa-substitution is observed for all the cations. For instance, $d_M{}^+$ value (in Å) of $C_6H_{6-n}(NH_2)_n\cdots Li^+$ is 1.828 for n = 1, 1.813 for n = 2, 1.803 for n = 3 and 1.774 for n = 6. A similar trend for the $C_6H_{6-n}(NH_2)_n\cdots Na^+$, $C_6H_{6-n}(NH_2)_n\cdots K^+$ and $C_6H_{6-n}(NH_2)_n\cdots NH_4^+$ complexes is observed (Figure 4.5). On the other hand, F and CN substituted complexes show a systematic increment in $d_M{}^+$ value with respect to an increase in the substitution which may be attributed to the increase in the electron-deficient character of aromatic ring. For example, $d_M{}^+$ value (in Å) of $C_6H_{6-n}F_n\cdots Li^+$ is 1.876 for n = 1, 1.906 for n = 2, 1.944 for n = 3 and 2.047 for n = 6. A similar trend for the $C_6H_{6-n}F_n\cdots Na^+$, $C_6H_{6-n}F_n\cdots K^+$ and $C_6H_{6-n}F_n\cdots NH_4^+$ is also observed (Figure 4.5).

In Table 4.4, the $E_M{}^+$ values of the cation-π complexes of di-, tri- and hexa-substituted benzenes with M^+ = Li^+, Na^+, K^+, and NH_4^+ are presented. Among all the disubstituted complexes, $E_M{}^+$ is the highest for $C_6H_4(NH_2)_2\cdots M^+$ and the lowest for $C_6H_4(CN)_2\cdots M^+$. Compared to $C_6H_6\cdots M^+$, $E_M{}^+$ value of $C_6H_5NH_2\cdots M^+$ is 18.5% higher for Li^+ (-44.8 kcal/mol), 22.6% higher for Na^+ (-28.7 kcal/mol), 31.6% higher for K^+ (-20.8 kcal/mol) and 33.8% higher for NH_4^+ (-20.6 kcal/mol). With double NH_2 substitution ($C_6H_4(NH_2)_2\cdots M^+$), further increase in $E_M{}^+$ is observed, *viz.* 29.9% for Li^+, 38.9% for Na^+, 55.7% for K^+, and 59.1% for NH_4^+ and in each case the stabilization is roughly twice the stabilization in

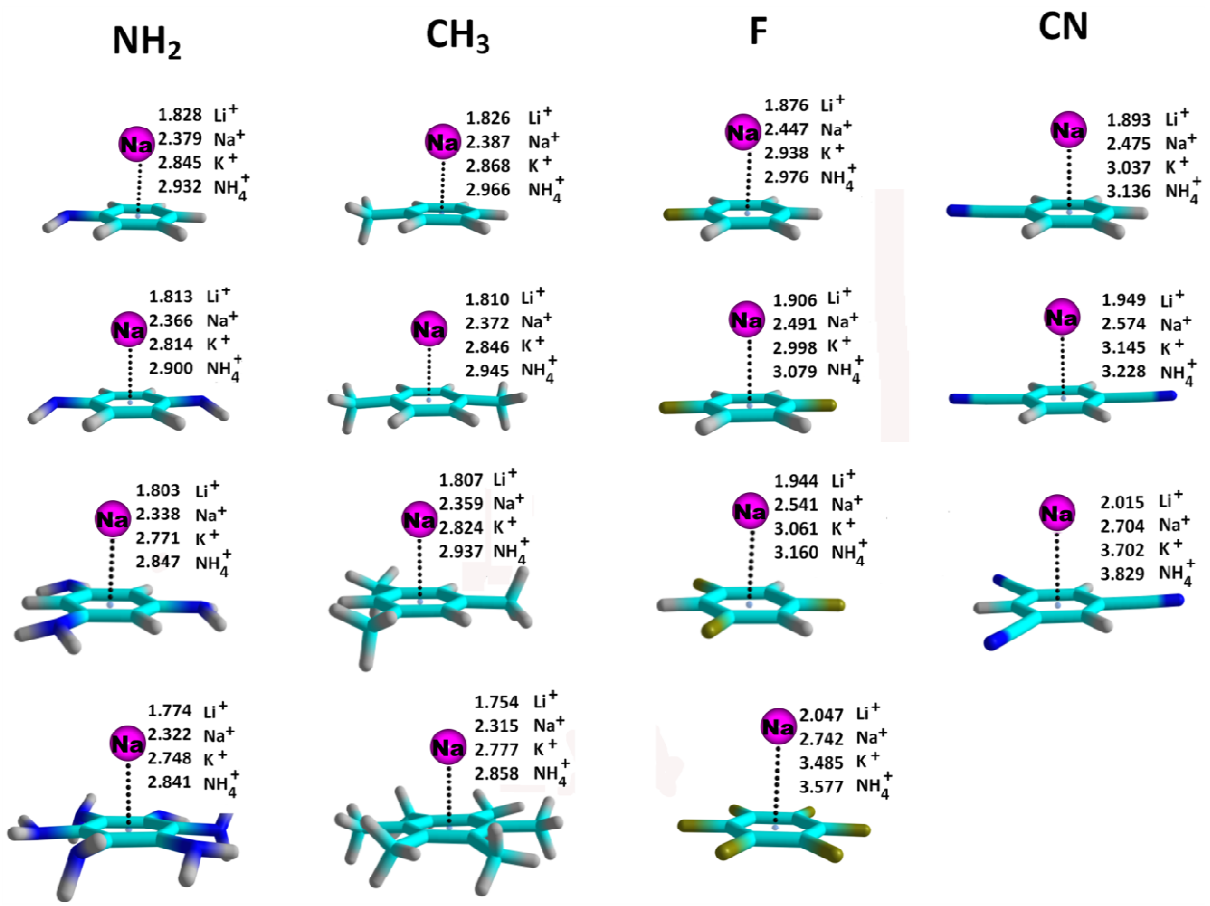

Figure 4.5 B3LYP/6-311+G(d,p) optimized geometries of $C_6H_{6-n}X_n\cdots Na^+$ (X = NH_2, CH_3, F and CN; n = 1, 2, 3, 6) complexes and intermolecular distance, d_{M^+} (in Å).

$C_6H_5NH_2\cdots M^+$. On the other hand, $C_6H_4(CN)_2\cdots M^+$ complexes are destabilized by 63.5% for Li^+, 82.1% for Na^+, 96.2% for K^+, and 96.8% for NH_4^+ compared to the corresponding $C_6H_6\cdots M^+$. Thus, the magnitude of stabilization caused by one NH_2 is significantly less than the magnitude of destabilization caused by one CN. This may be attributed to the fact that the through-space effect of CN is more dominant than the resonance effect of NH_2 [Sayyed and Suresh 2011[a]]. For instance, systems with one electron donating substituent and one electron withdrawing substituent show lower interaction energy than unsubstituted $C_6H_6\cdots M^+$. $C_6H_4(CH_3)_2\cdots M^+$ system show higher E_{M^+} than $C_6H_5(CH_3)\cdots M^+$ system by 6.1% for Li^+,

Table 4.4 Interaction energies (in kcal/mol), E_{M}^{+} (M^{+} = Li^{+}, Na^{+}, K^{+}, and NH_4^{+}) of multiple substituted cation-π complexes calculated at B3LYP/6-311+G(d,p) level.

Substituents	E_{Li}^{+}	E_{Na}^{+}	E_{K}^{+}	E_{NH4}^{+}
Disubstituted				
NH_2, NH_2	-49.1	-32.5	-24.6	-24.5
CH_3, CH_3	-43.4	-26.9	-18.6	-18.4
F, F	-25.8	-13.8	-8.5	-8.4
CN, CN	-13.8	-4.2	-0.6	-0.5
NH_2, CN	-31.9	-18.5	-12.3	-12.3[a]
CH_3, CN	-28.0	-15.0	-9.2	-9.0[a]
CH_3, F	-34.7	-20.4	-13.6	-13.5
NH_2, F	-38.2	-23.6	-16.8	-16.2
NH2, CH_3	-46.9	-30.1	-21.9	-21.7
F, CN	-19.3	-8.7	-4.7	-3.8[a]
Trisubstituted				
NH_2, NH_2, NH_2	-56.3	-38.7	-30.0	-30.8
CH_3, CH_3, CH_3	-45.6	-28.2	-19.6	-19.0
F, F, F	-20.4	-9.8	-5.4	-5.3
CN, CN, CN	-3.6	3.5	5.1	5.1
NH_2, CN, F	-27.0	-14.8	-9.6	-9.2[a]
NH_2, CN, CH_3	-34.9	-20.6	-14.0	-13.5[a]
F, CN, CH_3	-22.7	-11.0	-6.5	-5.9[a]
F, NH_2, CH_3	-41.6	-26.1	-18.7	-19.0
Hexasubstituted				
$(NH_2)_6$	-56.4	-37.2	-28.6	-28.8
$(CH_3)_6$	-50.4	-30.6	-21.2	-21.9
F_6	-5.4	1.3	3.0	3.1

[a] NH_4^{+} is restricted to interact with the π-region as it directly interacting with the CN.

4.7% for Na^+, 3.6% for K^+, 2.4% for NH_4^+ whereas the disubstituted fluorine systems show lower E_M^+ than the monosubstituted systems, the decrease being 19.0% for Li^+, 25.2% for Na^+, 29.8% for K^+, 22.3% for NH_4^+.

In all trisubstituted cation-π complexes, the highest interaction energy is observed for $C_6H_3(NH_2)_3\cdots M^+$ systems and the lowest for $C_6H_3(CN)_3\cdots M^+$. Among the tricyano Na^+, K^+, and NH_4^+ complexes, cation-π interaction is repulsive whereas Li^+ complexes show small amount of attractive interaction. Compared to $C_6H_6\cdots M^+$, the triamino substitution strengthens cation-π interaction by 48.8% for Li^+, 64.9% for Na^+, 89.5% for K^+ and 100.5% for NH_4^+. The enhancement in cation-π interaction due to trimethyl substitution is 20.5% for Li^+, 20.2% for Na^+, 23.8% for K^+, 23.6% for NH_4^+. On the other hand, destabilization due to trisubstitution of F is 46.2% for Li^+, 58.2% for Na^+, 65.9% for K^+, 65.3% for NH_4^+ and that for CN is 90.5% for Li^+, 115.0% for Na^+, 132.2% for K^+, 133.5% for NH_4^+. Among all the hexasubstituted systems, $C_6(NH_2)_6\cdots M^+$ systems showed the highest interaction energy. No bound structure for the cation with the π-ring of the $C_6(CN)_6$ is obtained. Only Li^+ showed a stabilizing interaction on the π-region of C_6F_6 and the interaction was repulsive for Na^+, K^+, and NH_4^+.

Interestingly, E_M^+ of $C_6(NH_2)_6\cdots M^+$ (-56.4 for Li^+, -37.2 for Na^+, -28.6 for K^+, -28.8, kcal/mol for NH_4^+) is almost equal or even slightly less than the corresponding E_M^+ values of $C_6H_3(NH_2)_3\cdots M^+$ (-56.3 for Li^+, -38.7 for Na^+, -30.0 for K^+, -30.8 kcal/mol for NH_4^+). This suggests that the total effect of the six NH_2 groups is comparable to that of the total effect of three NH_2 groups. A reason for this can be attributed to the geometric preferences of the NH_2 groups. In trisubstituted systems, all NH_2 groups are nearly in the plane of the aromatic ring, facilitating maximum resonance effect while in hexasubstituted systems, three NH_2 groups are nearly in the ring plane (they show slight pyramidal orientation at the N-centre) and the other three are largely twisted out from the ring plane (Figure 4.5). Therefore, a significant

reduction in the total resonance effect can be expected. Since 74.6% of the substituent effect of NH_2 is transmitted through resonance, a large reduction in the E_M^+ value from the expected additive effect may be observed [Sayyed and Suresh 2011[a]].

Additivity of substituent effect is defined as the total substituent effect of a multiple substituted system is equal to the sum of the individual substituent effect [Suresh *et al*. 2008]. The ΔE_M^+ values ($\Delta E_M^+ = \Delta E_M^+(X) - \Delta E_M^+(H)$) serve as the energy component of the substituent effect of X in the corresponding $C_6H_5X\cdots M^+$. Therefore, assuming additivity of substituent effect in cation-π interactions, a prediction on the total interaction energy of a multiple substituted complex (E_M^{+E}) can be made by adding ΔE_M^+ values of substituents to E_M^+ of $C_6H_6\cdots M^+$. E_M^{+E} of 84 cation-π complexes of multiple substituted benzenes (M^+ = Li^+, Na^+, K^+, and NH_4^+) are estimated and the values are reported in Table 4.5. In all the cases, except $C_6(NH_2)_6\cdots M^+$ system, E_M^{+E} showed a close agreement with E_M^+ as the mean absolute deviation (in kcal/mol) for all the complexes was 0.1 for Li^+, -0.6 for Na^+, -0.2 for K^+ and -0.8 for NH_4^+, indicating that substituent effect on cation-π interaction is additive. $C_6(NH_2)_6\cdots M^+$ system turned out to be an exception because hexa-substitution causes NH_2 group to undergo substantial change in its orientation with respect to the aromatic ring which significantly alters its electronic effect from the normally observed configuration in a monosubstituted system. In Figure 4.6, correlation plots showing relationship between E_M^+ and E_M^{+E} are shown for all the cations ($E_{Li}^+ = 0.975\ E_{Li}^{+E}$, $E_{Na}^+ = 0.981\ E_{Na}^{+E}$, $E_K^+ = 0.956\ E_K^{+E}$ and $E_{NH4}^+ = 0.949\ E_{NH4}^{+E}$) which clearly suggest that substituent effects on cation-π interactions are largely additive. These linear plots are drawn with intercept passing through zero to indicate the near perfect agreement between E_M^+ and E_M^{+E}.

Table 4.5 Predicted interaction energies, E_M^{+E} in kcal/mol of multiple substituted cation-π complexes predicted from the individual contributions of the interaction energies of mono substituted complexes. All values are in kcal/mol.

Substituents	E_{Li}^{+E}	E_{Na}^{+E}	E_K^{+E}	E_{NH4}^{+E}
di- substituted				
NH_2, NH_2	-51.8	-34.0	-25.8	-25.9
CH_3, CH_3	-43.7	-26.8	-18.8	-18.7
F,F	-25.8	-13.5	-8.4	-6.3
CN,CN	-12.2	-2.5	0.5	0.4
NH_2,CN	-32.0	-18.3	-12.7	-12.7
CH_3,CN	-28.0	-14.7	-9.2	-9.1
CH_3,F	-34.8	-20.2	-13.6	-12.5
NH_2,F	-38.8	-23.8	-17.1	-16.1
NH2, CH_3	-47.8	-30.4	-22.3	-22.3
F,CN	-19.0	-8.0	-4.0	-2.9
tri-substituted				
NH_2, NH_2, NH_2	-58.8	-39.4	-30.8	-31.2
CH_3, CH_3, CH_3	-46.7	-28.6	-20.3	-20.3
F, F, F	-19.8	-8.5	-4.7	-1.8
CN, CN, CN	0.6	7.9	8.6	8.3
NH_2,CN,F	-26.0	-13.3	-9.0	-8.2
NH_2,CN, CH_3	-35.0	-20.0	-14.2	-14.4
F,CN, CH_3	-22.0	-9.7	-5.5	-4.6
F, NH_2, CH_3	-41.8	-25.5	-18.6	-17.8
hexa-substituted				
$(NH_2)_6$	-79.7	-55.3	-45.8	-47.0
$(CH_3)_6$	-55.6	-33.7	-24.8	-25.3
F_6	-1.8	6.3	6.5	11.7

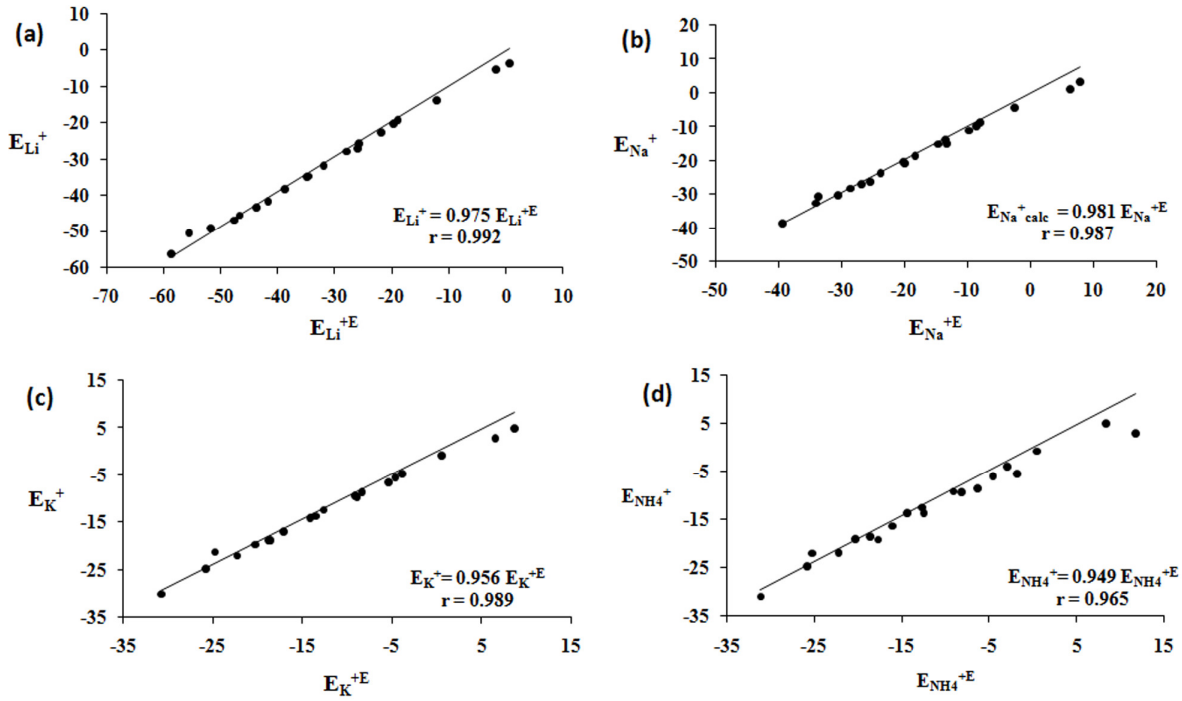

Figure 4.6. Correlation between calculated and predicted interaction energies (in kcal/mol) of multiple substituted cation-π complexes. (a) E_{Li}^{+} vs E_{Li}^{+E} (b) E_{Na}^{+} vs E_{Na}^{+E} (c) E_{K}^{+} vs E_{K}^{+E} (d) E_{NH4}^{+} vs E_{NH4}^{+E}.

4.4.4 Cation-π Interactions in a Diversified Set of Multiple Substituted π-Systems

To prove the reliability of ΔV_{min} approach given in Eq. 4.1 for the prediction of substituent effect on cation-π interactions, we have considered cation-π complexes of Li^{+} with a variety of different π-systems (Figure 4.7) which include the multiple substituted ethylene (**1**), acetylene (**2**), hexa-1,3,5-triene (**3**), benzene (**4**), naphthalene (**5**), indole (**6**), pyrrole (**7**), phenylalanine (**8**), tryptophan (**9**), tyrosine (**10**), azulene (**11**), pyrene (**12**), [6]-cyclacene (**13**) and corannulene (**14, 15**). In the case of **1-15** (except **8** and **9**), multiple substitution is considered in several cases to test the additivity of substituent effects.

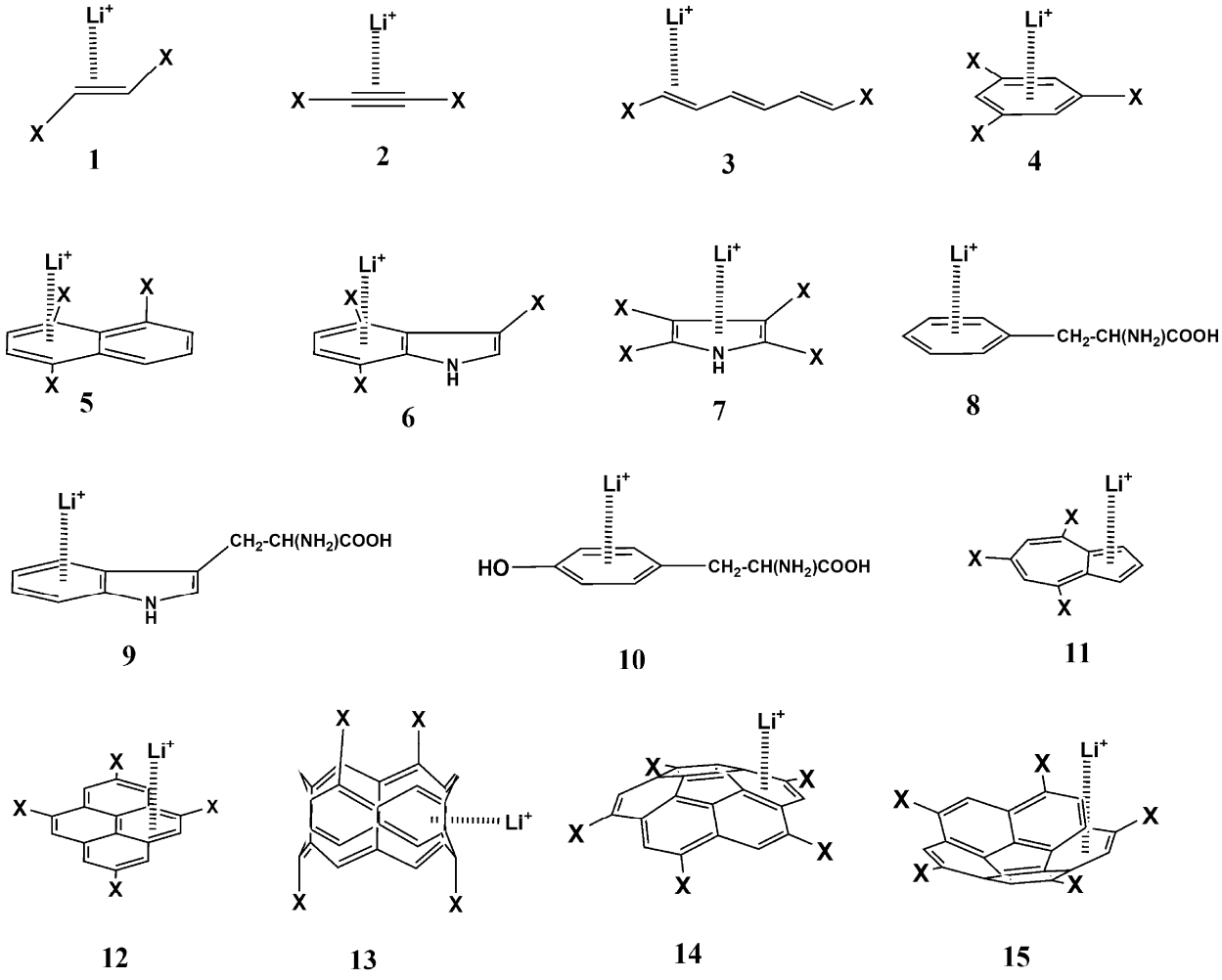

Figure 4.7 π-systems considered for testing the reliability of ΔV_{min} method for the quantification of cation-π interaction and also to test the additive effects.

According to the additivity rule, total substituent effect of a multiple substituted system is approximately equal to the sum of the individual substituent effect [Suresh *et al*. 2008]. Hence, Eq. 4.1 can be modified to a more general form, *viz*.

$$E_M^+ = C_M^+(\Sigma\Delta V_{min}) + E_M^{+\prime} \qquad \text{(Eq. 4.3)}$$

where $\Sigma\Delta V_{min}$ denotes the sum of ΔV_{min} [Sayyed and Suresh 2009[b], Suresh *et al*. 2008, Suresh and Gadre 1998]. The calculated E_M^+ and predicted E_M^+ using Eq. 4.3 along with $\Sigma\Delta V_{min}$ for all the cation-π complexes of Li^+ are reported in Table 4.6. Among all the systems (**1-15**), cation-π interaction energy of unsubstituted system is the highest for [6]-cyclacene (**13**) and

Table 4.6 Calculated and predicted E_M^+ of cation-π complexes between Li^+ and π-systems **1-15** and $\Sigma\Delta V_{min}$ of **1-15** systems. All values in kcal/mol.

π-system	X	$\Sigma\Delta V_{min}$	E_M^+	Predicted E_M^+	π-system	X	$\Sigma\Delta V_{min}$	E_M^+	Predicted E_M^+
1	NH_2	-18.1	-48.1	-40.0 [a]	**7**	NH_2	-7.8	-52.5	-49.2
	CH_3	-3.7	-26.9	-25.2		CH_3	-5.6	-50.8	-46.9
	H	0.0	-21.4	-21.4		H	0.0	-41.2	-41.2
	F	- [b]	- [a]	-		F	25.2	-17.2	-15.4
	CN	- [b]	- [a]	-		CN	- [b]	- [a]	-
2	NH_2	-23.1	-47.5	-44.9	**8**	Phe	-1.3	-42.7	-39.1
	CH_3	-8.9	-30.0	-30.3	**9**	Trp	-1.4	-45.2	-39.2
	H	0.0	-21.2	-21.2	**10**	Tyr	-1.7	-42.7	-39.5
	F	15.6	-9.9	-5.2	**11**	NH_2	-19.8	-65.4	-66.0
	CN	- [b]	0.4	-		CH_3	-5.3	-53.1	-51.1
3	NH_2	-17.7	-49.6	-50.0		H	0.0	-45.7	-45.7
	CH_3	-4.5	-37.4	-36.6		F	9.0	-37.2	-36.5
	H	0.0	-31.9	-31.9		CN	27.9	-21.8	-17.0
	F	9.2	-25.8	-22.4	**12**	NH_2	-9.2	-55.5	-51.2
	CN	20.5	-12.7	-10.9		CH_3	-2.9	-47.6	-44.7
4	NH_2	-16.5	-56.3	-54.7		H	0.0	-41.7	-41.7
	CH_3	-5.1	-46.0	-43.0		F	14.0	-27.6	-27.3
	H	0.0	-37.8	-37.8		CN	35.2	-10.5	-5.6
	F	15.9	-20.4	-21.5	**13**	NH_2	-16.3	-64.7	-70.3
	CN	40.8	-3.6	4.1		CH_3	-3.6	-58.4	-57.3
5	NH_2	-14.4	-53.7	-55.3		H	0.0	-53.6	-53.6
	CH_3	-4.2	-46.6	-44.8		F	7.8	-43.6	-45.6
	H	0.0	-40.5	-40.5		CN	14.8	-31.4	-38.4
	F	11.1	-27.4	-29.1	**14**	NH_2	-10.0	-59.5	-54.5

Table 4.6 (continued)

	CN	33.1	-11.4	-6.5		CH_3	-4.0	-50.2	-48.3
6	NH_2	-8.9	-55.1	-54.8		H	0.0	-44.2	-44.2
	CH_3	-2.3	-51.0	-48.1		F	15.0	-29.1	-28.8
	H	0.0	-45.7	-45.7		CN	35.8	-10.8	-7.5
	F	14.5	-30.8	-30.8	**15**	NH_2	-14.1	-59.8	-55.9
	CN	36.8	-14.7	-7.9		CH_3	-2.7	-48.0	-44.2
						H	0.0	-41.4	-41.4
						F	16.3	-24.7	-24.6
						CN	37.8	-6.2	-2.6

[a] Li^+ is directly interacting with the substituent and a cation-π complex is not formed. [b] V_{min} is not observed.

the lowest for acetylene (**2**). In general, the order of cation-π interaction is as follows; **13 > 6 ≈ 11 > 9 ≈ 14 > 8 ≈ 10 > 12 ≈ 15 > 7 > 5 > 4 > 3 > 1 > 2**. In all the cases, an electron donating substituent increases the strength of cation-π interaction while an electron withdrawing substituent decreases it. The mean absolute deviation of the predicted E_M^+ from the calculated E_M^+ is -0.07 kcal/mol. The good agreement between calculated and predicted E_M^+ is graphically represented in Figure 4.8 which indeed suggests that ΔV_{min} is a reliable descriptor for the quantification of substituent effects on cation-π interactions.

Recently, Cabaleiro-Lago and co-workers [Carrazana-García *et al.* 2011] have shown that in cation-π complexes of Li^+ and large curved π-systems such as coranullene and molecular bowls derived from fullerene, induction contribution dominates over the electrostatic contribution. In the test set, even for large aromatics, *viz.* pyrene (**12**), [6]-cyclacene (**13**) and corannulene (**14, 15**), predicted E_{Li}^+ values show good agreement with calculated E_M^+. It means that even if induction dominates, a prediction of the interaction energy is possible by adding the contribution due to substituent effect on the interaction

energy of unsubstituted system. In other words, in Eq. 4.3, dominating $E_M^{+\prime}$ term will take care of the contributions of various energy components while $C_M^+(\Sigma\Delta V_{min})$ term will give a good estimate of the contributions due to the substituent effect.

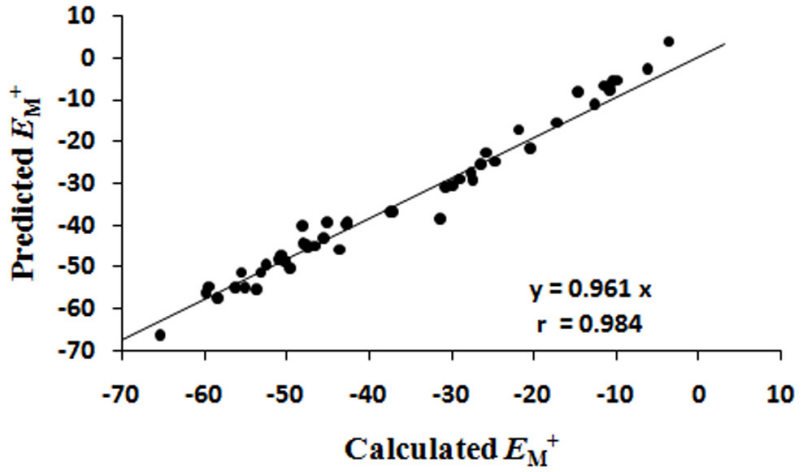

Figure 4.8 Correlation between calculated and predicted E_M^+ for cation-π complexes of Li^+ with π-systems **1-15**. All values are in kcal/mol.

4.4.5 Substituent Effects in Cationic Sandwich Benzene Complexes

The ΔV_{min} approach has been extended to study the substituent effects on the interaction energy of sandwich complexes of the type $C_6H_6\cdots M^+\cdots C_6H_5X$ (M^+ = Li^+, Na^+, K^+; X = NH_2, CH_3, H, F and CN) [Amicangelo and Armentrout 2000, Reddy *et al.* 2006]. The optimized geometries of $C_6H_6\cdots K^+\cdots C_6H_5X$ (X = NH_2, CH_3, H, F and CN) are shown in Figure 4.9 along with the distance of the cation from the centroid of the ring (d_M^+). d_M^+ values for other cations are also depicted in Figure 4.9. In general, a cation sits nearer to the C_6H_5X than C_6H_6 when X has electron donating character whereas it sits closer to C_6H_6 than C_6H_5X when X has electron withdrawing character.

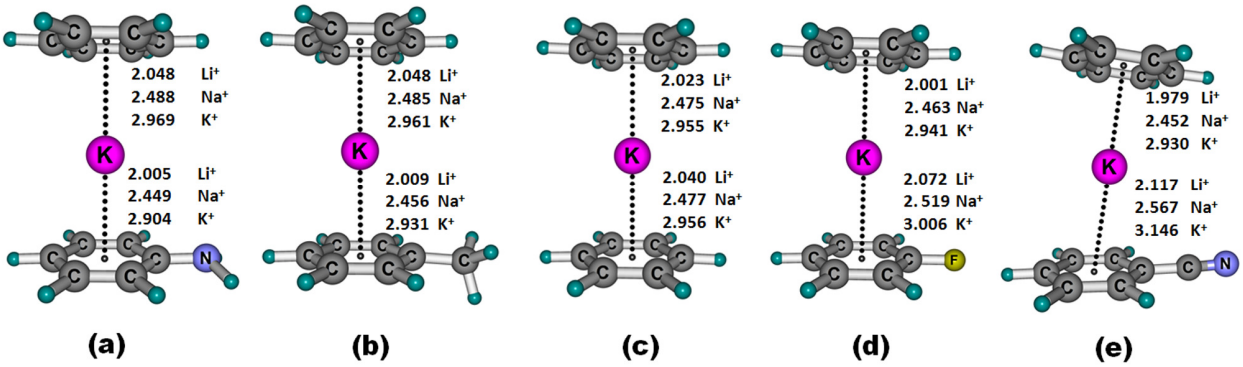

Figure 4.9 Optimized geometries of $C_6H_6\cdots K^+\cdots C_6H_5X$ (X = NH_2, CH_3, H, F and CN) systems. The distance from the centroid of the ring to the cation, d_{M^+} (in Å) is also given.

The total cation-π interaction energy, E_{M^+} is given in Table 4.7. The electron donating substituent enhances E_{M^+} while electron withdrawing substituent diminishes it. Compared to E_{M^+} of $C_6H_5X\cdots M^+$, substantial increase in E_{M^+} is observed for $C_6H_6\cdots M^+\cdots C_6H_5X$. For instance, E_{Li^+} of $C_6H_6\cdots Li^+$ is -37.8 kcal/mol and that of $(C_6H_6)_2\cdots Li^+$ is -59.0 kcal/mol

Table 4.7 Predicted and calculated cation-π interaction energies (E_{M^+}) of $C_6H_6\cdots M^+\cdots C_6H_5X$ complexes. All values are in kcal/mol.

	Li^+		Na^+		K^+	
X	E_{Li^+}	Predicted E_{Li^+}	E_{Na^+}	Predicted E_{Na^+}	E_{K^+}	Predicted E_{K^+}
NH_2	-64.3	-64.7	-45.4	-45.1	-32.8	-32.3
CH_3	-61.0	-60.7	-42.3	-42.1	-29.9	-29.7
H	-59.0	-	-40.8	-	-28.6	-
F	-54.8	-53.7	-36.9	-36.6	-25.3	-25.1
CN	-49.6	-44.4	-32.3	-29.5	-21.7[a]	-19.1

[a] Cation is restricted to interact with the π-region as the cation interacts directly with the substituent.

which also indicate that E_{Li}^{+} is not doubled by doubling the interacting π-system. E_{M}^{+} data of mono and bis-benzene complexes (Tables 4.2 and 4.7) clearly suggest that E_{M}^{+} is not additive with respect to the number of interacting π-systems. A similar observation has been reported earlier by Vollmer *et al*. [Vollmer *et al.* 2002]. Table 4.7 also depicts the predicted total cation-π interaction energy using Eq. 4.1. The linear plot given in Figure 4.10 shows that predicted E_{M}^{+} is 0.977 times calculated E_{M}^{+} and suggests that cation-π interaction energy of a substituted sandwich benzene complex can be predicted with ~97.7% accuracy using the ΔV_{min} method.

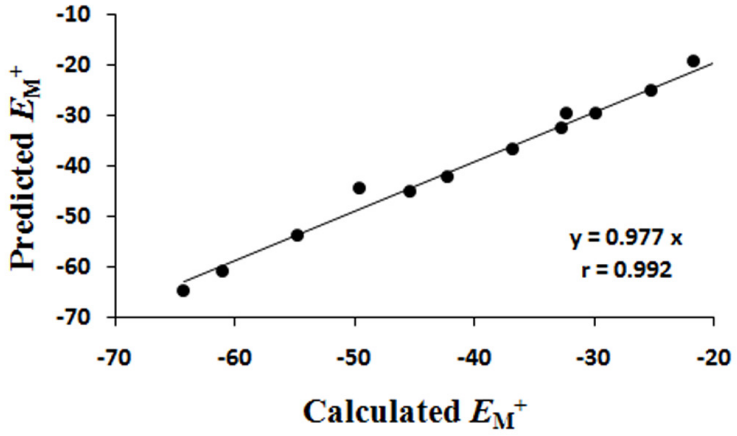

Figure 4.10 Correlation between calculated and predicted E_{M}^{+} of $C_6H_6\cdots M^+\cdots C_6H_5X$ systems (all values in kcal/mol).

4.4.6 Predicting E_{M}^{+} of a Large Variety of Cations with π-Systems

According to Eq. 4.1, for every cation, a unique C_{M}^{+} and $E_{M}^{+'}$ can be determined. Further, almost a perfect linear correlation (correlation coefficient, 0.995) exists between C_{M}^{+} and $E_{M}^{+'}$ (Eq. 4.4).

$$C_{M}^{+} = -0.016\, E_{M}^{+'} + 0.402 \qquad \text{(Eq. 4.4)}$$

It means that C_{M^+} of any M^+ can be predicted if the interaction energy of that cation with benzene is known. In order to validate this statement, we have considered 54 cation-π complexes of the type $C_6H_5X\cdots M^+$, $C_{10}H_7X\cdots M^+$, $C_8H_6NX\cdots M^+$ where M^+ is Mg^+ and Cu^+ and X is $N(CH_3)_2$, NH_2, CH_3, OH, H, F, Cl, CN, and NO_2. E_{M^+}' of $C_6H_6\cdots Mg^+$ is -30.1 kcal/mol and that of $C_6H_6\cdots Cu^+$ is -49.5 kcal/mol which upon substitution in Eq. 4.4 gives the corresponding C_{Mg^+} value 0.884 and C_{Cu^+} value 1.194. Since ΔV_{min} is known for all the substituents (Table 4.1), Eq. 4.4 can be used to predict the values of E_{Mg^+} and E_{Cu^+} and they are given in Table 4.8 for Mg^+ and Table 4.9 for Cu^+. The mean absolute deviation of the predicted E_{M^+} from the calculated E_{M^+} is 0.98 kcal/mol for Mg^+ and -0.73 kcal/mol for Cu^+, both agreeing to chemical accuracy [Neves *et al.* 2011].

Table 4.8 Calculated and predicted E_{Mg^+} (in kcal/mol) of $C_6H_5X\cdots Mg^+$, $C_{10}H_7X\cdots Mg^+$, and $C_8H_6NX\cdots Mg^+$ systems.

	$C_6H_5X\cdots Mg^+$		$C_{10}H_7X\cdots Mg^+$		$C_8H_6NX\cdots Mg^+$	
X	E_{Mg^+}	Predicted E_{Mg^+}	E_{Mg^+}	Predicted E_{Mg^+}	E_{Mg^+}	Predicted E_{Mg^+}
$N(CH_3)_2$	-42.1	-36.6	-38.3	-35.9	-42.5	-40.3
NH_2	-38.0	-35.1	-37.0	-35.4	-42.0	-40.7
CH_3	-33.3	-31.6	-35.0	-33.9	-40.7	-39.7
OH	-31.3	-30.5	-35.3	-34.7	-40.2	-39.6
H	-30.1	-30.1	-33.4	-33.4	-39.2	-39.2
F	-24.5	-25.4	-29.7	-30.6	-34.7	-35.5
Cl	-25.1	-24.7	-30.2	-30.6	-35.1	-35.4
CN	-17.5	-18.1	-24.7	-26.4	-28.9	-30.2
NO_2	-15.1	-16.2	-23.8[a]	-25.4	-27.4	-28.9

[a] Cation is restricted to interact with the π-region as the cation interacts directly with the substituent.

Table 4.9 Calculated and predicted E_{Cu}^{+} (in kcal/mol) of $C_6H_5X\cdots Cu^+$, $C_{10}H_7X\cdots Cu^+$, and $C_8H_6NX\cdots Cu^+$ systems.

	$C_6H_5X\cdots Cu^+$		$C_{10}H_7X\cdots Cu^+$		$C_8H_6NX\cdots Cu^+$	
X	E_{Cu}^{+}	Predicted E_{Cu}^{+}	E_{Cu}^{+}	Predicted E_{Cu}^{+}	E_{Cu}^{+}	Predicted E_{Cu}^{+}
$N(CH_3)_2$	-61.2	-58.2	-57.2	-56.6	-63.5	-61.0
NH_2	-59.8	-56.2	-56.1	-56.0	-63.2	-61.6
CH_3	-52.6	-51.5	-54.5	-54.0	-61.0	-60.3
OH	-52.0	-50.0	-56.9	-55.1	-61.8	-60.2
H	-49.5	-49.5	-53.3	-53.3	-59.6	-59.6
F	-45.6	-43.2	-51.7	-49.5	-56.6	-54.6
Cl	-45.4	-42.2	-52.2	-49.5	-57.0	-54.5
CN	-38.4	-33.3	-47.8	-43.9	-51.3	-47.4
NO_2	-36.3	-30.8	-44.5[a]	-42.6	-50.5	-45.6

[a] Cation is restricted to interact with the π-region to avoid the interaction of the cation with the substituent.

In order to further validate the generality of Eq. 4.4, we have also selected a total of 45 cation-π complexes randomly generated from a combination of (Φ, M^+, X) wherein Φ = C_6H_5X, $C_{10}H_7X$, C_8H_6NX; M^+ = Li^+, Na^+, K^+, $BeCl^+$, $MgCl^+$, $CaCl^+$, $TiCl_3^+$, $CrCl_2^+$, $NiCl^+$, Cu^+, $ZnCl^+$, NH_4^+, $CH_3NH_3^+$, $N(CH_3)_4^+$, $C(NH_2)_3^+$ and X = $N(CH_3)_2$, NH_2, OCH_3, CH_3, OH, H, SCH_3, SH, CCH, F, Cl, COOH, CHO, CF_3, CN, NO_2. For each Φ, fifteen cation-π complexes are considered. These cations include alkali metals, alkaline earth metal halides, 1st row transition metal derivatives and biologically significant cations such as NH_4^+, $CH_3NH_3^+$, $N(CH_3)_4^+$, and guanidinium ion ($C(NH_2)_3^+$). The E_M^{+}' value of all the systems and the corresponding C_M^+ value are given in Table 4.10. In Table 4.11, calculated E_M^+ and predicted E_M^+ using Eq. 4.1 are given. Figure 4.11 shows a good agreement between calculated and predicted E_M^+. The mean absolute deviation of predicted E_M^+ from calculated

E_{M^+} is 1.87 kcal/mol for $C_6H_5X\cdots M^+$, 0.59 kcal/mol for $C_{10}H_7X\cdots M^+$ and 1.14 kcal/mol for $C_8H_6NX\cdots M^+$.

Table 4.10 E_{M^+}' (in kcal/mol) and C_{M^+} of various cation-π complexes calculated at B3LYP/6-311+G(d,p) level.

	$C_6H_6\cdots M^+$ [a]	
M^+	E_{M^+}'	C_{M^+}
Li^+	-37.8	1.007
Na^+	-23.4	0.777
K^+	-15.8	0.655
$BeCl^+$	-87.5	1.802
$MgCl^+$	-55.7	1.294
$CaCl^+$	-35.4	0.968
$TiCl_3^+$	-51.7	1.229
$CrCl_2^+$ [b]	-58.7	1.341
$NiCl^+$	-76.7	1.630
Cu^+	-49.4	1.193
$ZnCl^+$	-64.1	1.428
NH_4^+	-15.4	0.648
$CH_3NH_3^+$	-13.5	0.617
$N(CH_3)_4^+$	-5.3	0.487
$C(NH_2)_3^+$	-9.8	0.559

[a] C_{M^+} is predicted using Eq. 4.4, [b] Spin multiplicity of Cr is 2.

Table 4.11 Calculated and predicted interaction energies (E_M^+). All values are in kcal/mol.

	$C_6H_5X\cdots M^+$			$C_{10}H_7X\cdots M^+$			$C_8H_6NX\cdots M^+$		
M^+	X	E_M^+	Predicted E_M^+	X	E_M^+	Predicted E_M^+	X	E_M^+	Predicted E_M^+
Li^+	OH	-38.4	-38.2	OH	-42.3	-42.1	CCH	-43.4	-42.4
Na^+	H	-23.4	-23.4	H	-25.5	-25.5	F	-25.8	-26.3
K^+	SCH_3	-17.9	-15.8	SCH_3	-20.0	-18.7	Cl	-18.5	-18.5
$BeCl^+$	SH	-88.8	-83.2	SH	-92.9	-91.5	COOH	-94.9	-90.9
$MgCl^+$	CCH	-54.5	-49.9	CHO	-57.0	-57.1	$N(CH_3)_2$	-72.2	-69.3
$CaCl^+$	F	-29.6	-29.9	CF_3	-34.7	-34.9	NH_2	-48.9	-48.0
$TiCl_3^+$	Cl	-46.4	-43.6	CN	-47.2	-47.6	OCH_3	-72.6	-64.1
$CrCl_2^+$	COOH	-51.3	-48.0	NO_2	-[a]	-53.2	CH_3	-73.9	-72.0
$NiCl^+$	CF_3	-70.0	-58.8	NH_2	-103.2	-98.6	CF_3	-87.9	-86.3
Cu^+	CN	-38.4	-32.1	OCH_3	-58.9	-56.5	CN	-51.3	-47.4
$ZnCl^+$	NO_2	-48.0	-40.1	CH_3	-72.6	-71.4	NO_2	-[a]	-62.1
NH_4^+	$N(CH_3)_2$	-22.3	-20.5	CCH	-17.7	-17.0	OH	-22.1	-21.6
$CH_3NH_3^+$	NH_2	-18.4	-17.1	F	-13.4	-13.6	H	-18.7	-18.7
$N(CH_3)_4^+$	OCH_3	-7.1	-6.3	Cl	-6.0	-5.5	SCH_3	-13.8	-7.1
$C(NH_2)_3^+$	CH_3	-10.9	-10.8	COOH	-[a]	-10.8	SH	-[a]	-14.1

[a]Cation directly interacting with the substituent.

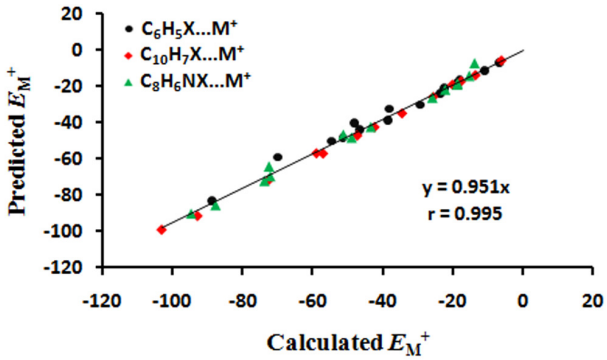

Figure 4.11 Correlation between calculated and predicted E_M^+ of cation-π complexes given in Table 4.11 (all values in kcal/mol).

4.5 Conclusions

The use of molecular electrostatic potential (MESP) topography for the quantification of substituent effects on cation-π interaction has been described for a large variety of cation-π complexes of the type Φ-X···M^+ where Φ, X and M^+ are the π-system, substituent and cation, respectively. The linear relationship, $E_{M^+} = C_{M^+}(\Sigma\Delta V_{min}) + E_{M^+}'$ is proposed as a good predictive model for the cation-π interaction energy where the first term exclusively represents the substituent contribution on the interaction energy. It means that to make a prediction on the cation-π interaction energy, one need to know only the interaction energy of the unsubstituted cation-π complex (E_{M^+}') and ΔV_{min} of the desired substituents. The linear correlation between C_{M^+} and E_{M^+}' facilitates the calculation of C_{M^+} for unknown cations. The agreement between calculated and predicted E_{M^+} strongly supports the additive effects of substituents as well as transferability of substituent effects on cation-π interactions. The use of ΔV_{min} as a global descriptor of substituent effect is evident in the good agreement obtained between calculated and predicted E_{M^+} for a large variety of cation-π systems and sandwich complexes. Further, the universal nature of the (E_{M^+}, ΔV_{min}) correlation is brought out by showing its resemblance to the Hammett equation.

List of publications

A) Articles in Journals

1. Quantification of substituent effects using molecular electrostatic potentials: additive nature and proximity effects**.** **Fareed Bhasha Sayyed** and Cherumuttathu H. Suresh, ***New. J. Chem.***, **2009**, 33, 2465.
2. An electrostatic scale of substituent resonance effect. **Fareed Bhasha Sayyed** and Cherumuttathu H. Suresh, ***Tetrahedron Lett.***, **2009**, 50, 7351.
3. Appraisal of Through-Bond and Through-Space Substituent Effects via Molecular Electrostatic Potential Topography. **Fareed Bhasha Sayyed**, Cherumuttathu H. Suresh and Shridhar R. Gadre, ***J. Phys. Chem. A***, **2010**, 114, 12330.
4. Analysis of structural water and CH···π interactions in HIV-1 protease and PTP1B complexes using a hydrogen bond prediction tool, HBPredicT. Yesudas, J. P.; **Fareed Bhasha Sayyed**, Cherumuttathu H. Suresh. ***J. Mol. Model*** , **2011**, 17, 401.
5. Substituent Effects in Cation-π Interactions: A Unified View from Inductive, Resonance, and Through-Space Effects. **Fareed Bhasha Sayyed** and Cherumuttathu H. Suresh. ***J. Phys. Chem. A***, **2011**, 115, 5660.
6. Quantitative Assessment of Substituent Effects on Cation-π Interactions Using Molecular Electrostatic Potential Topography. **Fareed Bhasha Sayyed** and Cherumuttathu H. Suresh. ***J. Phys. Chem. A***, **2011**, 115, 9300.
7. NMR characterization of substituent effects in cation–π interactions. **Fareed Bhasha Sayyed** and Cherumuttathu H. Suresh. ***Chem. Phys. Lett.***, **2012**, 523, 11.
8. Accurate Prediction of Cation-π Interaction Energy Using Substituent Effects. **Fareed Bhasha Sayyed** and Cherumuttathu H. Suresh. ***J. Phys. Chem. A***, **2012**, 116, 5723.

B) Published contributions to academic conferences

9. Presented a poster entitled “Molecular electrostatic potential as a unified descriptor for the studies of substituent effects” in the Theoretical chemistry symposium-2010, held at IIT-Kanpur, India during 08 –12 December 2010.

10. Presented a poster entitled “Quantification of Substituent Effects in Cation-π Interactions” in the international conference on “Applied theory on molecular systems"(Atoms-2011) held at IICT (CSIR), Hyderabad, India during 2–5 November 2011.

References

Adamo, C.; Barone, V. "Toward reliable density functional methods without adjustable parameters: The PBE0 model". *J. Chem. Phys. 110*, **1999**, 6158.

Allen, L. C.; Karo, A. M. "Basis Functions for Ab Initio Calculations". *Rev. Modern Phys. 32*, **1960**, 275.

Adcock, W.; Trout, N. A. "Nature of the Electronic Factor Governing Diastereofacial Selectivity in Some Reactions of Rigid Saturated Model Substrates". *Chem. Rev. 99*, **1999**, 1415.

Amicangelo, J. C.; Armentrout, P. B. "Absolute Binding Energies of Alkali-Metal Cation Complexes with Benzene Determined by Threshold Collision-Induced Dissociation Experiments and ab Initio Theory". *J. Phys. Chem. A 104*, **2000**, 11420.

Amunugama, R.; Rodgers, M. T. "Influence of Substituents on Cation-π Interactions. 1. Absolute Binding Energies of Alkali Metal Cation-Toluene Complexes Determined by Threshold Collision-Induced Dissociation and Theoretical Studies". *J. Phys. Chem. A 106*, **2002**[a], 5529.

Amunugama, R.; Rodgers, M. T. "Influence of Substituents on Cation-π Interactions. 2. Absolute Binding Energies of Alkali Metal Cation-Fluorobenzene Complexes Determined by Threshold Collision-Induced Dissociation and Theoretical Studies". *J. Phys. Chem. A 106*, **2002**[b], 9092.

Amunugama, R.; Rodgers, M. T. "The Influence of Substituents on Cation-π Interactions. 4. Absolute Binding Energies of Alkali Metal Cation-Phenol Complexes Determined by Threshold Collision-Induced Dissociation and Theoretical Studies". *J. Phys. Chem. A 106*, **2002**[c], 9718.

Amunugnama, R.; Rodgers, M. T. "Cation-π interactions with a model for an extended π-network Absolute binding energies of alkali metal cation–naphthalene complexes determined by threshold collision-induced dissociation and theoretical studies". *Int. J. Mass Spectrom. 227*, **2003**, 1.

Angelelli, J. M.; Brownlee, R. T. C.; Katritzky, A. R.; Topsom, R. D.; Yakhontov, L. "Infrared intensities as a quantitative measure of intramolecular interactions. IX. Aryl derivatives of metalloids". *J. Am. Chem. Soc. 91*, **1969**, 4500.

Bader, R. F. W. "A quantum theory of molecular structure and its applications". *Chem. Rev. 91*, **1991**, 893.

Bagno, A.; Saielli, G.; Scorrano, G. "DFT Calculation of Intermolecular Nuclear Spin-Spin Coupling in van derWaals Dimers". *Angew Chem., Int. Ed. 40*, **2001**, 2532.

Bagno, A.; Saielli, G.; Scorrano, G. "Through-Space Spin ± Spin Coupling in van derWaals Dimers and CH/π Interacting Systems. An Ab Initio and DFT Study". *Chem. Eur. J. 8*, **2002**, 2047.

Balanarayan, P.; Gadre, S. R. "Topography of molecular scalar fields. I. Algorithm and Poincaré-Hopf relation". *J. Chem. Phys. 119*, **2003**, 5037.

Balanarayan, P.; Kavathekar, R.; Gadre, S. R. "Electrostatic Potential Topography for Exploring Electronic Reorganizations in 1,3 Dipolar Cycloadditions". *J. Phys. Chem. A 111*, **2003**, 2733.

Becke, A. D. "Density-Functional Exchange-Energy Approximation with Correct Asymptotic Behavior". *Phys. Rev. A 38*, **1988**, 3098.

Becke, A. D. "Density-functional thermochemistry. III. The role of exact exchange". *J. Chem. Phys. 98*, **1993**, 5648.

Becke, A. D. "A new inhomogeneity parameter in density-functional theory". *J. Chem. Phys. 109*, **1998**, 2092.

Bohm, S.; Exner, O. "Steric inhibition of resonance: A revision and quantitative estimation on the basis of aromatic carboxylic acids". *Chem. Eur. J. 6*, **2000**, 3391.

Bohm, S.; Exner, O. "Steric effects and steric inhibition of resonance: Structure and ionization of 2-tert-butylbenzoic acid". *New. J. Chem. 25*, **2001**, 250.

Bohm, S.; Fiedler, P.; Exner, O. "Analysis of the ortho effect: Acidity of 2-substituted benzoic acids". *New. J. Chem. 28*, **2004**, 67.

Bohm, S.; Exner, O. "Inductive effects in radicals calculated from DFT energies; substituted bicyclo[2.2.2]octan-1-yloxy radicals". *J. Comput. Chem. 28*, **2007**, 1783.

Bonnaccorsi, R.; Scrocco, E.; Tomasi, J.; Pullman, A. "Ab initio molecular electrostatic potentials - Guanine compared to adenine". *Theor. Chim. Acta. 36*, **1975**, 339.

Born, M.; Oppenheimer, J., R. "Zur Quantentheorie der Molekeln". *Ann. Phys. 84*, **1927**, 457.

Bowden, K.; Grubbs, E. J. "Through-bond and through-space models for interpreting chemical reactivity in organic reactions". *Chem. Soc. Rev. 25*, **1996**, 171.

Boys, S., F. "Electronic Wave Functions. I. A General Method of Calculation for the Stationary States of Any Molecular System". *Proc. Roy. Soc. 200*, **1950**, 542.

Boys, S. F.; Bernardi, F. "The calculation of small molecular interactions by the differences of separate total energies. Some procedures with reduced errors". *Mol. Phys. 19*, **1970**, 553.

Brownlee, R. T. C.; Katritzky, A. R.; Topsom, R. D. "Direct infrared determination of the resonance interaction in monosubstituted benzenes". *J. Am. Chem. Soc. 87*, **1965**, 3260.

Brownlee, R. T. C.; Cameron, D. G.; Topsom, R. D.; Katritzky, A. R.; Pozharsky, A. F. "Infrared intensities as a quantitative measure of intramolecular interactions. Part XXV. Interactions between substituents in para-disubstituted benzenes". *J. Chem. Soc., Perkin Trans. 2 3*, **1974**, 282.

Busi, S.; Saxell, H.; Frohlich, R.; Rissanen, K. "The role of cation-π interactions in capsule formation: Co-crystals of resorcinarenes and alkyl ammonium salts". *Cryst. Eng. Comm. 10*, **2008**, 1803.

Campanelli, A. R.; Domenicano, A.; Piacente, G.; Ramondo, F. "Electronic Substituent Effects in Bicyclo[1.1.1]pentane and [n]Staffane Derivatives: A Quantum Chemical Study Based on Structural Variation". *J. Phys. Chem. A 114*, **2010**, 5162.

Carrazana-García, J. A.; Rodríguez-Otero, J.; Cabaleiro-Lago, E. M. "DFT Study of the Interaction between Alkaline Cations and Molecular Bowls Derived from Fullerene". *J. Phys. Chem. B 115*, **2011**, 2774.

Chai, J.-D.; Head-Gordon, M. "The M06 suite of density functionals for main group thermochemistry, thermochemical kinetics, noncovalent interactions, excited states, and transition elements: Two new functionals and systematic testing of four M06-class functionals and 12 other functionals". *Phys. Chem. Chem. Phys. 10*, **2008**, 6615.

Chałasiński, G.; Szczgsniak, M., M. "Origins of Structure and Energetics of van der Waals Clusters from ab Initio Calculations". *Chem. Rev. 94*, **1994**, 1723.

Charton, M. "Nature of the ortho effect. V. ortho-substituent constants". *J. Am. Chem. Soc. 91*, **1969**[a], 6649.

Charton, M. "The nature of the ortho effect. I. Electrophilic aromatic substitution". *J. Org. Chem. 34*, **1969**[b], 278.

Charton, M. "The nature of the ortho effect. VII. Nuclear magnetic resonance spectra". *J. Org. Chem. 36*, **1971**, 266.

Charton, M. "The nature of electrical effect transmission". *J. Phys. Org. Chem. 12*, **1999**, 275–282.

Charton, M.; Charton, B. I. "The nature of the ortho effect. VI. Polarographic half-wave potentials". *J. Org. Chem. 36*, **1971**, 260.

Cheng, J.; Zhu, W.; Tang, Y.; Xu, Y.; Li, Z.; Chen, K.; Jiang, H. "Effect of cation–π interaction on NMR: A theoretical investigation on complexes of Li^+, Na+, Be^{2+}, and Mg^{2+} with aromatics". *Chem. Phys. Lett. 422*, **2006**, 455.

Cubero, E.; Orozco, M.; Luque, F. J. "A Topological Analysis of Electron Density in Cation-π Complexes". *J. Phys. Chem. A 103*, **1999**, 315.

De Wall, S. L.; Meadows, E. S.; Barbour, L. J.; Gokel, G. W. "Solution- and solid-state evidence for alkali metal cation-π interactions with indole, the side chain of tryptophan". *J. Am. Chem. Soc. 121*, **1999**, 5613.

Dewar, M. J. S.; Thiel, W. "Ground-States of Molecules. 38. The MNDO Method: Approximations and Parameters," *J. Am. Chem. Soc.*, *99*, **1977**, 4899.

Ditchfield, R. "Self-consistent perturbation theory of diamagnetism I. A gauge-invariant LCAO method for N.M.R. chemical shifts". *Mol. Phys. 27*, **1974**, 789.

Ditchfield, R.; Hehre, W. J.; Pople, J. A. "Self-Consistent Molecular-Orbital Methods. IX. An Extended Gaussian-Type Basis for Molecular-Orbital Studies of Organic Molecules". *J. Chem. Phys. 54*, **1971**, 724.

Dougherty, D. A. "Cation-π interactions involving aromatic amino acids". *J. Nutr. 137*, **2007**, 1504S.

Dunbar, R. C. "Binding of Na ,Mg , and Al to the π Faces of Naphthalene and Indole: Ab Initio Mapping Study". *J. Phys. Chem. A 102*, **1998**, 8946.

Elango, M.; Parthasarathi, R.; Narayanan, G. K.; Sabeelullah, A. M.; Sarkar, U.; Venkatasubramaniyan, N. S.; Subramanian, V.; Chattaraj, P. K. "Relationship between electrophilicity index, Hammett constant and nucleus-independent chemical shift ". *Int. J. Mol. Sci. 117* **2005**, 61.

Engerer, L. K.; Hanusa, T. P. "Geometric effects in olefinic cation-π interactions with alkali metals: A computational study". *J. Org. Chem. 76*, **2011**, 42.

Exner, O. "The inductive effect: theory and quantitative assessment". *J. Phys. Org. Chem. 12*, **1999**, 265.

Exner, O.; Krygowski, T. M. "The nitro group as substituent". *Chem. Soc. Rev. 25*, **1996**, 71.

Exner, O.; Bohm, S. "Resonance energy in benzene and ethene derivatives in the gas phase as a measure of resonance ability of various functional groups". *J. Chem. Soc., Perkin Trans. 2*, **2000**, 1994.

Exner, O.; Böhm, S. "Background of the Hammett equation as observed for isolated molecules: Meta- and para-substituted benzoic acids ". *J. Org. Chem. 67*, **2002**, 6320.

Exner, O.; Bohm, S. "Inductive effect of uncharged groups: dependence on electronegativity". *J. Phys. Org. Chem. 19*, **2006**, 393.

Exner, O.; Bohm, S. "π-electron densities and resonance effects in benzene monoderivatives". *J. Mol. Struct. (THEOCHEM)*, **2002**, 103.

Exner, O.; Bohm, S. "Quantitative evaluation of resonance interaction:monosubstituted 1,3-butadienes". *J. Mol. Struct. (THEOCHEM)*, **2005**, 125.

Exner, O.; Böhm, S. "Theory of substituent effects: Recent advances ". *Current Organic Chemistry 10*, **2006**, 763.

Exner, O.; Böhm, S. "Revision of the dual substituent parameter treatment using the DFT-calculated reaction energies". *J. Phys. Org. Chem. 20*, **2007**, 454.

Fersner, A.; Karty, J. M.; Mo, Y. "Why are esters and amides weaker carbon acids than ketones and acid fluorides? Contributions by resonance and inductive effects". *J. Org. Chem. 74*, **2009**, 7245.

Fiedler, P.; Böhm, S.; Kulhánek, J.; Exner, O. "Acidity of ortho-substituted benzoic acids: An infrared and theoretical study of the intramolecular hydrogen bonds". *Org. Biomol. Chem. 4*, **2006**, 2003.

Fock, V. "Näherungsmethode zur Lösung des Quantenmechanischen Mehrkörper Problems". *Z. Phys. 61*, **1930**, 126.

Foresman, J. B.; Head-Gordon, M.; Pople, J. A.; Frisch, M. J. "Toward a Systematic Molecular Orbital Theory for Excited States," *J. Phys. Chem.*, *96*, **1992**, 135.

Fourré, I.; Gérard, H.; Silvi, B. "How the topological analysis of the electron localization function accounts for the inductive effect" *J. Mol. Struct. (THEOCHEM) 811*, **2007**, 69.

Frenking, G.; Frohlich, N. "The Nature of the Bonding in Transition-Metal Compounds". *Chem. Rev. 100*, **2000**, 717.

Frisch, M. J.; Trucks, G. W.; Schlegel, H. B.; Scuseria, G. E.; Robb, M. A.; Cheeseman, J. R.; Montgomery, J. A.; Vreven, J., T; Kudin, K. N.; Burant, J. C.; Millam, J. M.; Iyengar, S. S.; Tomasi, J.; Barone, V.; Mennucci, B.; Cossi, M.; Scalmani, G.; Rega, N.; Petersson, G. A.; Nakatsuji, H.; Hada, M.; Ehara, M.; Toyota, K.; Fukuda, R.; Hasegawa, J.; Ishida, M.; Nakajima, T.; Honda, Y.; Kitao, O.; Nakai, H.; Klene, M.; Li, X.; Knox, J. E.; Hratchian, H. P.; Cross, J. B.; Bakken, V.; Adamo, C.; Jaramillo, J.; Gomperts, R.; Stratmann, R. E.; Yazyev, O.; Austin, A. J.; Cammi, R.; Pomelli, C.; Ochterski, J. W.; Ayala, P. Y.; Morokuma, K.; Voth, G. A.; Salvador, P.; Dannenberg, J. J.; Zakrzewski, V. G.; Dapprich, S.; Daniels, A. D.; Strain, M. C.; Farkas, O.; Malick, D. K.; Rabuck, A. D.; Raghavachari, K.; Foresman, J. B.; Ortiz, J. V.; Cui, Q.; Baboul, A. G.; Clifford, S.; Cioslowski, J.; Stefanov, B. B.; Liu, G.; Liashenko, A.; Piskorz, P.; Komaromi, I.; Martin, R. L.; Fox, D. J.; Keith, T.; Al-Laham, M. A.; Peng, C. Y.; Nanayakkara, A.; Challacombe, M.; Gill, P. M. W.;

Johnson, B.; Chen, W.; Wong, M. W.; Gonzalez, C.; Pople, J. A. *Gaussian 03*, Revision E.01; Gaussian Inc. Wallingford CT 2004.

Gadre, S. R.; Suresh, C. H. "Electronic Perturbations of the Aromatic Nucleus: Hammett Constants and Electrostatic Potential Topography". *J. Org. Chem. 62*, **1997**, 2625.

Gadre, S. R.; Pundlik, S. S. "Complementary electrostatics for the study of DNA base-pair interactions". *J. Phys. Chem. B 101*, **1997**, 3298.

Gadre, S. R.; Shirsat, R. N. *Electrostatics of Atoms and Molecules*; Universities Press: Hyderabad, 2000.

Gadre, S. R.; Kulkarni, S. A.; Suresh, C. H.; Shrivastava, I. H. "Basis set dependence of the molecular electrostatic potential topography. A case study of substituted benzenes". *Chem. Phys. Lett. 239*, **1995**, 273.

Galabov, B.; Ilieva, S.; Schaefer III, H. F. "An Efficient Computational Approach for the Evaluation of Substituent Constants". *J. Org. Chem. 71*, **2006**, 6382.

Galabov, B.; Nikolova, V.; Wilke, J. J.; Schaefer III, H. F.; Allen, W. D. "Origin of the SN2 benzylic effect". *J. Am. Chem. Soc. 130*, **2008**, 9887.

Galkin, V. I. "Inductive substituent effects". *J. Phys. Org. Chem. 12*, **1999**, 283.

Gallivan, J. P.; Dougherty, D. A. "Cation-π interactions in structural biology". *Proc. Natl. Acad. Sci. U. S. A. 96*, **1999**, 9459.

Gieleciak, R.; Polanski, J. "Modeling robust QSAR. 2. Iterative variable elimination schemes for CoMSA: Application for modeling benzoic acid pKa values". *J. Chem. Inf. Model. 47*, **2007**, 547.

Girones, X.; Carbo-Dorca, R.; Ponec, R. "Molecular Basis of LFER. Modeling of the Electronic Substituent Effect Using Fragment Quantum Self-Similarity Measures". *J. Chem. Inf. Model. 43*, **2003**, 2033.

Gokel, G. W.; De Wall, S. L.; Meadows, E. S. "Experimental evidence for alkali metal cation-π interactions". *Eur. J. Org. Chem.*, **2000**, 2967.

Grimme, S. "Semiempirical GGA-type density functional constructed with a long-range dispersion correction". *J. Comput. Chem. 27*, **2006**, 1787.

Gross, K. C.; Seybold, P. G.; Peralta-Inga, Z.; Murray, J. S.; Politzer, P. "Comparison of quantum chemical parameters and Hammett constants in correlating pK_a values of substituted anilines". *J. Org. Chem. 66*, **2001**, 6919.

Gutowski, M.; Chałasiński, G. "Critical evaluation of some computational approaches to the problem of basis set superposition error". *J. Chem. Phys. 98*, **1993**, 5540.

Haeberlein, M.; Brinck, T. "Computational Analysis of Substituent Effects in Para-Substituted Phenoxide Ions". *J. Phys. Chem. 100*, **1996**, 10116.

Hall, G. G. "The Molecular Orbital Theory of Chemical Valency. VIII. A Method of Calculating Ionization Potentials". *Proc. Roy. Soc.* (London) *A205*, 1951, 541.

Hallowita, N.; Udonkang, E.; Ruan, C.; Frieler, C., E; Rodgers, M., T. "Inductive effects on cation-π interactions: Structures and bond dissociation energies of alkali metal cation–halobenzene complexes". *Int. J. Mass Spectrom. 283*, **2009**, 35.

Hamada, F.; Higuchi, Y.; Kondo, Y.; Kabuto, C.; Iki, N. "Supramolecular assembly based on π-π stacking and π-cation interactions between thiacalix[6]arene and DMF". *Tetrahedron Lett. 47*, **2006**, 5591.

Hammett, L. P. "The Effect of Structure upon the Reactions of Organic Compounds. Benzene Derivatives". *J. Am. Chem. Soc. 59*, **1937**, 96.

Hansch, C.; Leo, A.; Taft, R. W. "A Survey of Hammett Substituent Constants and Resonance and Field Parameters". *Chem. Rev. 91*, **1991**, 165.

Hartree, R. R. "The Wave Mechanics of an Atom with a Non-Coulomb Central Field. Part I. Theory and Methods". *Proc. Cambridge Phil. Soc. 24*, **1928**, 89.

Hay, P. J.; Wadt, W. R. "Ab Initio Effective Core Potentials for Molecular Calculations. Potentials for the Transition Metal Atoms Sc to Hg". *J. Chem. Phys. 82*, **1985**, 270.

He, L.; Cheng, J.; Wang, T.; Li, C.; Gong, Z.; Liu, H.; Zeng, B.-B.; Jiang, H.; Zhu, W. "Cation–p complexes formed between cyclooctatetraene and alkaline earth metals: Predicted and recorded NMR features". *Chem. Phys. Lett. 462*, **2008**, 45.

Hehre, W. J.; Stewart, R. F.; Pople, J. A. "Self-Consistent Molecular-Orbital Methods. I. Use of Gaussian Expansions of Slater-Type Atomic Orbitals". *J. Chem. Phys. 51*, **1969**, 2657.

Helgaker, T.; Jaszuński, M.; Ruud, K. "Ab initio methods for the calculation of NMR shielding and indirect spin-spin coupling constants". *Chem. Rev. 99*, **1999**, 293.

Hollingsworth, C. A.; Seybold, P. G.; Hadad, C. M. "Explicitly correlated SCF study of anharmonic vibrations in $(H_2O)_2$ ". *Int. J. Quantum. Chem. 90*, **2002**, 1414.

Hoefnagel, A. J.; Wepster, B. M. "Substituent Effects. **IV."3** A Reexamination of σ^n**,** $\Delta\sigma_R^+$**,** and σ_R^n Values; Arylacetic Acids, and Other Insulated Systems". *J .Am.Chem.Soc. 95*, **1973**, 5357.

Hohenberg, P.; Kohn, W. "Inhomogeneous Electron Gas". *Phys. Rev. 136*, **1964**, B864.

Holtz, H. D.; Stock, L. M. "Dissociation constants for 4-substituted bicyclo[2.2.2]octane-1-carboxylic acids. Empirical and theoretical analysis". *J. Am. Chem. Soc. 86*, **1964**, 5188.

Hunter, C. A.; Low, C. M. R.; Rotger, C.; Vinter, J. G.; Zonta, C. "Substituent effects on cation-π interactions: A quantitative study". *Proc. Natl. Acad. Sci. U. S. A. 99*, **2002**, 4873.

Jaffé, H. H. "Correlation of hammett's σ-values with electron densities calculated by molecular orbital theory". *J. Chem. Phys. 20*, **1952**, 279.

Jaffé, H. H. "A reëxamination of the hammett equation". *Chem. Rev. 53*, **1953**, 191.

Jones, B.; Robinson, J. "Additive effects of substituents". *Nature 165*, **1950**, 453.

Katritzky, A. R.; Topsom, R. D. "The σ- and π-inductive effects". *J. Chem. Educ. 48*, **1971**, 427.

Katritzky, A. R.; Topsom, R. D. "Infrared intensities: A guide to intramolecular interactions in conjugated system". *Chem. Rev. 77*, **1977**, 639.

Keiluweit, M.; kleber, M. "Molecular-Level Interactions in Soils and Sediments: The Role of Aromatic π-Systems". *Environ. Sci. Technol. 43*, **2009**, 3421.

Keith, T. A.; Bader, R. F. W. "Calculation of magnetic response properties using atoms in molecules". *Chem. Phys. Lett. 194*, **1992**, 1.

Kim, D.; Lee, E. C.; Kim, K. S.; Tarakeshwar, P. "Cation-π-anion interaction: A theoretical investigation of the role of induction energies". *J. Phys. Chem. A 111*, **2007**, 7980.

Kim, D.; Hu, S.; Tarakeshwar, P.; Kim, K. S.; Lisy, J. M. "Cation-π interactions: A theoretical investigation of the interaction of metallic and organic cations with alkenes, arenes, and heteroarenes". *J. Phys. Chem. A 107*, **2003**, 1228.

Klein, E.; Lukeš, V. "Study of gas-phase O-H bond dissociation enthalpies and ionization potentials of substituted phenols - Applicability of ab initio and DFT/B3LYP methods". *Chem. Phys. 330* **2006**, 515.

Klein, E.; Lukes, V. "DFT/B3LYP study of the substituent effect on the reaction enthalpies of the individual steps of sequential proton loss electron transfer mechanism of phenols antioxidant action: Correlation with phenolic C-O bond length". *J. Mol. Struct. (THEOCHEM) 805*, **2007**, 153.

Kulhanek, J.; Bohm, S.; Palat Jr., K.; Exner, O. " Steric inhibition of resonance: revision of the principle on the electronic spectra of methyl-substituted acetophenones". *J. Phys. Org. Chem. 17*, **2004**, 686.

Krygowski, T. M.; Stepien, B. T. "Sigma- and Pi-Electron Delocalization: Focus on Substituent Effects". *Chem. Rev. 105*, **2005**, 3482.

Krygowski, T. M.; Zachara-Horeglad, J. E. "Resonance-assisted hydrogen bonding in terms of substituent effect". *Tetrahedron 65*, **2009**, 2010.

Krygowski, T. M.; Stępień, B. T.; Cyrański, M. K.; Ejsmont, K. "Relation between resonance energy and substituent resonance effect in P-phenols". *J. Phys. Org. Chem. 18*, **2005**, 886.

Krygowski, T. M.; Ejsmont, K.; Stepień, B. T.; Cyrański, M. K.; Poater, J.; Solà, M. "Relation between the Substituent Effect and Aromaticity". *J. Org. Chem. 69*, **2004**, 6634.

Kulhanek, J.; Bohm, S.; Palat Jr., K.; Exner, O. " Steric inhibition of resonance: Revision of the principle on the electronic spectra of methyl-substituted acetophenones ". *J. Phys. Org. Chem. 17*, **2004**, 686.

Kushwaha, P. S.; Mishra, P. C. "Molecular electrostatic potential maps of the anti-cancer drugs daunomycin and adriamycin: An ab initio theoretical study". *J. Mol. Struct. (THEOCHEM) 636*, **2006**, 149.

Lee, C.; Yang, W.; Parr, R. G. "Development of the Colle-Salvetti correlation-energy formula into a functional of the electron density ". *Phys.Rev B 37* **1988**, 785.

Liu, T.; Gu, J.; Tan, X.-J.; Zhu, W.-L.; Luo, X.-M.; Jiang, H.-L.; Ji, R.-Y.; Chen, K., -X; Silman, I.; Sussman, J., L. "Theoretical insight into the interactions of TMA-benzene and TMA-pyrrole with B3LYP Density-Functional Theory (DFT) and ab initio second order Møller-Plesset perturbation theory (MP2) calculations". *J. Phys. Chem. A 105*, **2001**, 5431.

Liu, T.; Zhu, W.; Gu, J.; Shen, J.; Luo, X.; Chen, G.; Puah, C. M.; Silman, I.; Chen, K.; Sussman, J. L.; Jiang, H. "Additivity of cation-π interactions: An ab initio

computational study on π- Cation-π sandwich complexes". *J. Phys. Chem. A 108*, **2004**, 9400.

Liu, T., Li, H.; Huang, M.-B.; Duan, Y.; Wang, Z.-X. "Two-way effects between hydrogen bond and intramolecular resonance effect: An ab initio study on complexes of formamide and its derivatives with water". *J. Phys. Chem A 112*, **2008**, 5436.

Lucas, X.; Quiñonero, D.; Frontera, A.; Deyà, P. M. "Counterintuitive Substituent Effect of the Ethynyl Group in Ion π Interactions". *J. Phys. Chem. A 113*, **2009**, 10367.

Ma, J. C.; Dougherty, D. A. "The Cation-π Interaction". *Chem. Rev. 97*, **1997**, 1303.

Marshall, M. S.; Steele, R. P.; Thanthiriwatte, K. S.; Sherrill, C. D. "Potential Energy Curves for Cation-π Interactions: Off-Axis Configurations Are Also Attractive". *J. Phys. Chem. A 113*, **2009**, 13628.

Martin, N. H.; Main, K. L.; Pyles, A. K. "Computation of through-space NMR shielding effects by aromatic ring-cation complexes: Substantial synergistic effect of complexation". *J. Mol.Graphics Model. 25*, **2008**, 806.

Martin, N. H.; Brown, J. D.; Nance, K. H.; Schaefer III, H. F.; Schleyer, P. v. R.; Wang, Z.-X.; Woodcock, H. L. "Analysis of the Origin of Through-Space Proton NMR Deshielding by Selected Organic Functional Groups". *Org. Lett. 3*, **2001**, 3823.

Mathew, J.; Suresh, C. H. "Use of molecular electrostatic potential at the carbene carbon as a simple and efficient electronic parameter of N-heterocyclic carbenes". *Inorg. Chem. 49*, **2010**, 4665.

Mathew, J.; Thomas, T.; Suresh, C. H. "Quantitative assessment of the stereoelectronic profile of phosphine ligands". *Inorg. Chem. 46*, **2007**, 10800.

Matsumura, H.; Yamamoto, T.; Leow, T. C.; Mori, T.; Salleh, A. B.; Basri, M.; Inoue, T.; Kai, Y.; Rahman, R. N. Z. R. A. "Novel cation-π interaction revealed by crystal structure of thermoalkalophilic lipase". *Proteins 70*, **2008**, 592.

McDaniel, D. H.; Brown, H. C. "An extended table of Hammett substituent constants based on the lonization of substituted benzoic acids". *J. Org. Chem. 23* **1958**, 420.

McLean, A. D.; Chandler, G. S. “Contracted Gaussian-basis sets for molecular calculations. 1. 2nd row atoms, Z=11-18”. *J. Chem. Phys.*, *72*, **1980,** 5639.

McWeeny, R.; Dierksen, D. “Self-consistent perturbation theory. 2. Extension to open shells,” *J. Chem. Phys.*, *49*, **1968**, 4852.

Meadows, E. S.; De Wall, S. L.; Barbour, L. J.; Gokel, G. W. "Alkali metal cation-π Interactions observed by using a lariat ether model system". *J. Am. Chem. Soc. 123*, **2001**, 3092.

Mecozzi, S.; West Jr., A. P.; Dougherty, D. A. "Cation-π interactions in simple aromatics: Electrostatics provide a predictive tool". *J. Am. Chem. Soc. 118*, **1996** [a], 2307.

Mecozzi, S.; West, A. P., Jr; Dougherty, D. A. "Cation-π interactions in aromatics of biological and medicinal interest: Electrostatic potential surfaces as a useful qualitative guide". *Proc. Natl. Acad. Sci. U. S. A. 93*, **1996**[b], 10566.

Meyer, E. A.; Castellano, R. K.; Diederich, F. "Interactions with Aromatic Rings in Chemical and Biological Recognition". *Angew Chem., Int. Ed. 42*, **2003**, 1210.

Mo, G. C. H.; Yip, C. M. "Supported lipid bilayer templated J-aggregate growth: Role of stabilizing cation-π interactions and headgroup packing". *Langmuir 25*, **2009**, 10719.

Mohajeri, A.; Karimi, E. "AIM and NBO analyses of cation-π interaction". *J. Mol. Struct. (Theochem) 774*, **2006**, 71.

Møller, C.; Plesset, M. S. "Note on an approximation treatment for many-electron systems". *Phys. Rev. 46* **1934**, 618.

Murray, J. S.; Politzer, P. "Molecular surfaces, van der Waals Radii and electrostatic potentials in relation to noncovalent interactions". *Croat. Chem. Acta 82*, **2009**, 267.

Murray, J. S.; Politzer, P. "The electrostatic potential". *WIREs Comput. Mol. Sci. 1*, **2011**, 153.

Naray-Szabo, G.; Ferenczy, G. G. "Molecular electrostatics". *Chem. Rev. 95*, **1995**, 829.

Neves, A. R.; Fernandes, P. A.; Ramos, M. J. "The accuracy of density functional theory in the description of cation-π and π-hydrogen bond interactions". *J. Chem. Theory Comput. 7*, **2011**, 2059.

Niwa, J. " The Ab Initio Modeling of Hammett-Type Correlations. The Separation of Inductive Effects from Mesomeric Effects in Aromatic Systems". *Bull. Chem. Soc. Jpn*. *62*, **1989**, 226.

Nolan, E., M; Linck, R., G. "Charge Variationsin Substituted Alkanes:Evidence for a Through-Space Effect". *J. Am. Chem. Soc. 122*, **2000**, 11497.

Orner, B. P.; Salvatella, X.; Sánchez-Quesada, J.; De Mendoza, J.; Giralt, E.; Hamilton, A. D. "De novo protein surface design: Use of cation-π interactions to enhance binding between an α-helical peptide and a cationic molecule in 50% aqueous solution". *Angew Chem., Int. Ed. 41*, **2002**, 117.

Ott, H.; Pieper, U.; Leusser, D.; Flierler, U.; Henn, J.; Stalke, D. "Carbanion or Amide? First Charge Density Study of Parent 2-Picolyllithium". *Angew. Chem. Int. Ed. 48*, **2009**, 2978.

Palat Jr, K.; Waisser, K.; Exner, O. "Infrared intensities of benzene derivatives as a measure of the substituent resonance effects". *J. Phys. Org. Chem. 14*, **2001**, 677.

Platts, J. A.; Gkionis, K. "NMR shielding as a probe of intermolecular interactions: ab initio and density functional theory studies". *Phys. Chem. Chem. Phys. 11*, **2009**, 10331.

Perdew, J. P. "Density-Functional Approximation for the Correlation Energy of the Inhomogeneous Electron Gas". *Phys. Rev. B 33*, **1986**, 8822.

Perdew, J. P.; Chevary, J. A.; Vosko, S. H.; Jackson, K. A.; Pederson, M. R.; Singh, D. J.; Fiolhais, J. C. "Atoms, Molecules, Solids, and Surfaces: Applications of the Generalized Gradient Approximation for Exchange and Correlation". *Phys. Rev. B 46*, **1992**, 6671.

Pinjari, R. V.; Gejji.S. P. "Electronic Structure, Molecular Electrostatic Potential and NMR Chemical Shifts in Cucurbit[n]urils (n=5-8), Ferrocene and their Complexes". *J. Phy. Chem. A. 112*, **2008**, 12679.

Ponec, R.; Van Damme, S. "Molecular basis of LFER: theoretical study of polar substituent effect in aliphatic series". *J. Phys. Org. Chem. 20*, **2007**, 662.

Politzer, P.; Murray, J. S. "The fundamental nature and role of the electrostatic potential in atoms and molecules". *Theor. Chem. Acc. 108*, **2002**, 134.

Pople, J. A.; Nesbet, R. K. "Self-Consistent Orbitals for Radicals," *J. Chem. Phys.*, *22*, **1954**, 571.

Price, C. C. "Substitution and orientation in the benzene ring". *Chem. Rev. 29*, **1940**, 37.

Pytela, O. "Chemometric analysis of substituent effects. IX. Alternative interpretation of substituent effects (AISE) -orthogonal model". *Collect. Czech. Chem. Commun. 61*, **1996**, 704.

Raju, R. K.; Bloom, J. W. G.; An, Y.; Wheeler, S. E. "Substituent effects on non-covalent interactions with aromatic rings: Insights from computational chemistry". *Chemphyschem 12*, **2011**, 3116.

Reddy, A. S.; Sastry, G. N. "Cation [M = H^+, Li^+, Na^+, K^+, Ca^{2+}, Mg^{2+}, NH_4^+, and NMe_4^+] Interactions with the Aromatic Motifs of Naturally Occurring Amino Acids: A Theoretical Study". *J. Phys. Chem. A 109*, **2005**, 8893.

Reddy, A. S.; Vijay, D.; Sastry, G. M.; Sastry, G. N. "From Subtle to Substantial: Role of Metal Ions on π-π Interactions". *J. Phys. Chem. B 110*, **2006**, 2479.

Ribelin, T.; Katz, C. E.; English, D. G.; Smith, S.; Manukyan, A. K.; Day, V. W.; Neuenswander, B.; Poutsma, J. L.; Aubé, J. "Highly stereoselective ring expansion reactions mediated by attractive cation-n interactions". *Angew Chem., Int. Ed. 47*, **2008**, 6233.

Roberts, J. D.; Moreland, W. T. "Electrical Effects of Substituent Groups in Saturated Systems. Reactivities of 4-Substituted Bicyclo [2.2.2]octane-1-carboxylic Acids". *J. Am. Chem. Soc. 75*, **1953**, 2167.

Roothaan, C. C. J. "New Developments in Molecular Orbital Theory". *Rev. Mod. Phys. 23*, **1951**, 69.

Ruan, C.; Yang, Z.; Rodgers, M. T. "Influence of the d orbital occupation on the nature and strength of copper cation–π interactions: threshold collision-induced dissociation and theoretical studies". *Phys. Chem. Chem. Phys. 9*, **2007**, 5902.

Ruan, C.; Yang, Z.; Hallowita, N.; Rodgers, M. T. "Cation-π Interactions with a Model for the Side Chain of Tryptophan: Structures and Absolute Binding Energies of Alkali Metal Cation Indole Complexes". *J. Phys. Chem. A 109*, **2005**, 11539.

Ruzziconi, R.; Spizzichino, S.; Lunazzi, L.; Mazzanti, A.; Schlosser, M. "B values as a sensitive measure of steric effects". *Chem. Eur. J. 15*, **2009**, 2645.

Sakakura, K.; Ishihara, K. "Asymmetric Cu(II) catalyses for cycloaddition reactions based on π cation or n–cation interactions". *Chem. Soc. Rev. 40*, **2011**, 163.

Salonen, L. M.; Bucher, C.; Banner, D. W.; Haap, W.; Mary, J.-L.; Benz, J.; Kuster, O.; Seiler, P.; Schweizer, W. B.; Diederich, F. "Cation-π interactions at the active site of factor Xa: Dramatic enhancement upon stepwise N-alkylation of ammonium ions". *Angew Chem., Int. Ed. 48*, **2009**, 811.

Sayyed, F. B.; Suresh, C. H. "An electrostatic scale of resonance substituent effect". *Tetrahedron Lett. 50*, **2009**[a], 7351.

Sayyed, F. B.; Suresh, C. H. "Quantification of substituent effects using molecular electrostatic potentials: additive nature and proximity pffects". *New. J. Chem. 33*, **2009** [b], 2465.

Sayyed, F. B.; Suresh, C. H. "Substituent effects in cation-π interactions: A unified explanation from Inductive, resonance and through-space effects". *J. Phys. Chem. A 115*, **2011**[a], 5660.

Sayyed, F. B.; Suresh, C. H. "Quantitative assessment of substituent effects on cation-π interactions using molecular electrostatic potential topography". *J. Phys. Chem. A 115*, **2011**[b], 9300.

Sayyed, F. B.; Suresh, C. H.; Gadre, S. R. "Appraisal of Through-Bond and Through-Space Substituent Effects via Molecular Electrostatic Potential Topography". *J. Phys. Chem. A 114*, **2010**, 12330.

Schindler, M., Kutzelnigg, W. "Theory of magnetic susceptibilities and NMR chemical shifts in terms of localized quantities. II. Application to some simple molecules". *J. Chem. Phys.* 76, **1982**, 1919.

Segurado, M. A. P.; Reis, J. C. R.; De Oliveira, J. D. G.; Kabilan, S.; Shanthi, M. "Chlorination of 2-phenoxypropanoic acid with NCP in aqueous acetic acid: Using a novel ortho-para relationship and the para/meta ratio of substituent effects for mechanism elucidation". *J. Org. Chem. 72*, **2007**, 5327.

Shorter, J. "Values of om and op based on the ionization of substituted benzoic acids in water at 25°C ". *Pure Appl. Chem. 66*, **1994**, 2451.

Shorter, J. "Compilation and critical evaluation of structure-reactivity parameters and equations: part 2". *Pure Appl. Chem. 69*, **1997**, 2497.

Shorter, J.; Stubbs, F. J. "The additive effect of substituents on the strength of benzoic acid". *J. Chem. Soc.*, **1949**, 1180.

Slater, J., C. "Note on Hartree's Method". *Phys. Rev. 35*, **1930**, 210.

Silva, P. J. "Inductive and resonance effects on the acidities of phenol, enols, and carbonyl α-hydrogens". *J. Org. Chem. 74*, **2009**, 914.

Smith, A., P; McKercher, A., E; Mawhinney, R., C. "Inductive Effect: A Quantum Theory of Atoms in Molecules Perspective". *J. Phys. Chem. A 115*, **2011**, 12544.

Soteras, L.; Orozco, M.; Luque, F. J. "Induction effects in metal cation–benzene complexes". *Phys. Chem. Chem. Phys. 10*, **2008**, 2616.

Stewart, R. F. "On the mapping of electrostatic properties from Bragg diffraction data". *Chem. Phys. Lett. 65*, **1979**, 335.

Stewart, J. J. P. "Optimization of parameters for semiempirical methods. I. Method," *J. Comp. Chem. **10***, **1989**, 209.

Stewart, J. J. P. "Optimization of parameters for semiempirical methods. V. Modification of NDDO approximations and application to 70 elements," *J. Mol. Model. 13*, **2007**, 1173.

Sullivan, J. J.; Jones, A. D.; Tanji, K. K. "QSAR treatment of electronic substituent effects using frontier orbital theory and topological parameters". *J. Chem. Inf. Model. 40*, **2000**, 1113.

Suresh, C. H.; Gadre, S. R. "A Novel Electrostatic Approach to Substituent Constants: Doubly Substituted Benzenes". *J. Am. Chem. Soc. 120*, **1998**, 7049.

Suresh, C. H.; Gadre, S. R. "Electrostatic potential minimum of the aromatic ring as a measure of substituent constant". *J. Phys. Chem. A 111*, **2007**, 710.

Suresh, C. H.; Alexander, P.; Vijayalakshmi, K. P.; Sajith, P. K.; Gadre, S. R. "Use of molecular electrostatic potential for quantitative assessment of inductive effect". *Phys. Chem. Chem. Phys. 10*, **2008**, 6492.

Taft, R. W. "The General Nature of the Proportionality of Polar Effects of Substituent Groups in organic chemistry". *J. Am. Chem. Soc. 75*, **1953**, 4231.

Taft, R. W. "Sigma values from reactivities". *J. Phys. Chem. 64*, **1960**, 1805.

Taft, R. W.; Lewis, C. R. "Evaluation of resonance effects on reactivity by application of the linear inductive energy relationship. V. Concerning a σ_R scale of resonance effects". *J. Am. Chem. Soc. 81*, **1959**, 5343.

Taft, R. W.; Price, E.; Fox, I. R.; Lewis, I. C.; Anderson, K. K.; Davis, G. T. "Fluorine nuclear magnetic resonance shielding in p-substituted fluorobenzenes. The influence of structure and solvent on resonance effects". *J. Am. Chem. Soc. 85*, **1963**, 3146.

Takahata, Y.; Chong, D. P. "Estimation of Hammett sigma constants of substituted benzenes through accurate density-functional calculation of core-electron binding energy shifts". *Int. J. Quantum. Chem. 103*, **2005**, 509.

Torrent-Sucarrat, M.; Liu, S.; Proft, F. D. "Steric Effect: Partitioning in Atomic and Functional Group Contributions". *J. Phys. Chem. A 113*, **2009**, 3698.

Tiwari, S.; Shukla, P. K.; Mishra, P. C. "Improved electrostatic properties using combined Mulliken and hybridization-displaced charges for radicals". *J. Mol. Model. 14*, **2008**, 631.

Tsuzuki, S.; Uchimaru, T.; Mikami, M. "Is the Cation-π Interaction in Alkaline-Earth-Metal Dication/Benzene Complexes a Covalent Interaction?". *J. Phys. Chem. A 107*, **2003**, 10414.

Vaara, J. "Theory and computation of nuclear magnetic resonance parameters". *Phys. Chem. Chem. Phys. 9*, **2007**, 5399.

Van Bekkum, H.; Verkade, P. E.; Wepster, B. M. "A simple re-evaluation of the Hammett σ relation". *Recl. Trav. Chim. 78*, **1959**, 815.

Vollmer, J. M.; Kandalam, A. K.; Curtiss, L. A. "Lithium Benzene Sandwich Compounds: A Quantum Chemical Study". *J. Phys. Chem. A 106*, **2002**, 9533.

Vosko, S., H; Wilk, L.; Nusair, M. "Accurate spin-dependent electron liquid correlation energies for local spin density calculations: a critical analysis". *Can. J. Phys. 58*, **1980**, 1200.

Watt, M.; Hwang, J.; Cormier, K. W.; Lewis, M. "Preference for Na^+-π binding over Na^+-dipole binding in Na^+-arene interactions". *J. Phys. Chem. A 113*, **2009**, 6192.

Wells, P. R. "Linear free energy relationships". *Chem. Rev. 63*, **1963**, 171.

Wheeler, S. E.; Houk, K. N. "Substituent effects in the benzene dimer are due to direct interactions of the substituents with the unsubstituted benzene". *J. Am. Chem. Soc. 130*, **2008**, 10854.

Wheeler, S. E.; Houk, K. N. "Substituent effects in cation/π interactions and electrostatic potentials above the centers of substituted benzenes are due primarily to through-space effects of the substituents". *J. Am. Chem. Soc. 131*, **2009[a]**, 3126.

Wheeler, S. E.; Houk, K. N. "Through-Space Effects of Substituents Dominate Molecular Electrostatic Potentials of Substituted Arenes". *J. Chem. Theory Comput. 5*, **2009[b]**, 2301.

Wiberg, K. B. "Substituent effects on the acidity of weak acids. 1. Bicyclo[2.2.2]octane-1-carboxylic Acids and Bicyclo[1.1.1]pentane-1-carboxylic Acids". *J. Org. Chem. 67*, **2002[a]**, 1613.

Wiberg, K. B. “Substituent effects on the acidity of weak acids. 2. Calculated gas-phase acidities of substituted benzoic acids". *J. Org. Chem. 67*, **2002[b]**, 4787

Wiberg, K. B. " Substituent effects on the acidity of weak acids. 3. Phenols and benzyl alcohols". *J. Org. Chem 68*, **2003**, 875.

Willans, M., J; Schurko, R., W. "A Solid-State NMR and ab Initio Study of Sodium Metallocenes". *J. Phys. Chem. B 107*, **2003**, 5144.

Wong, A.; Whitehead, R. D.; Gan, Z.; Wu, G. "A Solid-State NMR and Computational Study of Sodium and Potassium Tetraphenylborates: 23Na and 39K NMR Signatures for Systems Containing Cation-ð Interactions". *J. Phys. Chem. A 108*, **2004**, 10551.

Wu, G.; Terskikh, V. "A Multinuclear Solid-State NMR Study of Alkali Metal Ions in Tetraphenylborate Salts, M[BPh_4] (M) Na, K, Rb and Cs): What Is the NMR Signature of Cation-π Interactions?". *J. Phys. Chem. A 112*, **2008**, 10359.

Wu, R.; McMahon, T. B. "Investigation of cation-π interactions in biological systems". *J. Am. Chem. Soc. 130*, **2008**, 12554.

Xiu, X.; Puskar, N. L.; Shanata, J. A. P.; Lester, H. A.; Dougherty, D. A. "Nicotine binding to brain receptors requires a strong cation–p interaction". *Nature 458*, **2009**, 534.

Yamada, S. "Intramolecular cation-π interaction in organic synthesis". *Org. Biomol. Chem. 5*, **2007**, 2903.

Yamada, S.; Tokugawa, Y. "Cation-φ controlled solid-state photodimerization of 4-azachalcones". *J. Am. Chem. Soc. 131*, **2009**, 2098.

Yamada, S.; Uematsu, N.; Yamashita, K. "Role of cation- π interactions in the photodimerization of trans-4-styrylpyridines". *J. Am. Chem. Soc. 129*, **2007**, 12100.

Yamada, S.; Nojiri, Y.; Sugawara, M. "[2+2] Photodimerization of (Z)-4-styrylpyridine through a cation-π interaction: formation of cis-cis-trans dimers". *Tetrahedron Lett. 51*, **2010**, 2533.

Yamada, S.; Fossey, J. S. "Nitrogen cation–π interactions in asymmetric organocatalytic synthesis". *Org. Biomol. Chem. 9*, **2011**, 7275.

Yanai, T.; Tew, D. P.; Handy, N. C. "A new hybrid exchange-correlation functional using the Coulomb-attenuating method (CAM-B3LYP)". *Chem. Phys. Lett. 393*, **2004**, 51.

Yeole, S. D.; Gadre, S. R. "Topography of Scalar Fields: Molecular Clusters and π-Conjugated Systems". *J. Phys. Chem. A 115*, **2011**, 12769.

Yi, H.-B.; Lee, H. M.; Kim, K. S. "Interaction of Benzene with Transition Metal Cations: Theoretical Study of Structures, Energies, and IR Spectra". *J. Chem. Theory Comput. 5*, **2009**, 1709.

Zhao, Y.; Truhlar, D. G. "The M06 suite of density functionals for main group thermochemistry, thermochemical kinetics, noncovalent interactions, excited states, and transition elements: Two new functionals and systematic testing of four M06-class functionals and 12 other functionals". *Theor. Chem. Acc. 120*, **2008**, 215.

Zhong, W.; Gallivan, J. P.; Zhang, Y.; Li, L.; Lester, H. A.; Dougherty, D. A. "From ab initio quantum mechanics to molecular neurobiology: A cation-π binding site in the nicotinic receptor". *Proc. Natl. Acad. Sci. U. S. A. 95*, **1998**, 12088.

Zhu, W.-L.; Tan, X.-J.; Shen, J.; Luo, X.-M.; Cheng, F.; Mok, P., c; Ji, R.-Y.; Chen, K.-X.; Jiang, H.-L. "Differentiation of Cation-π Bonding from Cation-π Intermolecular Interactions: A Quantum Chemistry Study Using Density-Functional Theory and Morokuma Decomposition Methods". *J. Phys. Chem. A 107*, **2003**, 2296.